A STUDY OF VELOCITY FIELDS IN THE Hα CHROMOSPHERE BY MEANS OF TIME-LAPSE DOPPLER MOVIES

Thesis by

Alan Morton Title

In Partial Fulfillment of the Requirements

For the Degree of

Doctor of Philosophy

California Institute of Technology

Pasadena, California

1966

(Submitted March 29, 1966)

ACKNOWLEDGMENTS

It is a pleasure to thank my research advisor, Professor R.B. Leighton, for his aid and many helpful suggestions. Especially valuable were the odds that he offered on the possibility that various components of the camera system would actually function. These odds made many of the hours spent in design and in the machine shop at least seem shorter.

Also I wish to thank Dr. Jack Evans for his generous loan of the series of Hα spectra studied in this thesis, and for his permission to use the Sacramento Peak Observatory (SPO) digitizing microphotometer and computer facilities. I am also grateful to Dr. George Simon for his aid in the operation of the SPO computer facilities, and the use of his computer programs.

Special thanks are due to Messrs. Jim Aries and Ken Nordsieck for accompanying me to Mount Wilson at 4 am to aid in the observations; thanks are also due for their aid in much tedious data reduction. I am grateful to Mr. Nordsieck for writing most of the computer programs.

Financial and other aid from the California Institute of Technology, the United States Office of Naval Research, and the Mount Wilson and Palomar Observatories is gratefully acknowledged.

ABSTRACT

The technique of Leighton for making Doppler spectroheliograms has been extended to movies. Doppler movies made in Hα .7 Å from the core show a class of upgoing features with a 113 ± 3.4 second mean lifetime and a definite velocity history. The velocity reaches its maximum in less than 30 seconds, then declines for the next 90 seconds. In the case of 27 percent of these features a similar upflow event occurred soon after the first had died away. The average lifetime of these "double" events is 236 ± 8 seconds, approximately twice the lifetime of a single event. No region has been observed to repeat more than twice in the time a region could be followed (about 15 m), nor has any showed a tendency to repeat after a lapse of more than 60 seconds. Moreover, the region on the sun where an upflow event has occurred tends to show no downflow for at least fifteen minutes afterward.

The prominent upgoing features occur in the rosette structure seen in the Hα wings. Further, they are often visible as absorbing features in the red as well as the violet wing. This suggests that their profiles are broadened with respect to the mean profile. A statistical study of a time series of high dispersion Hα spectra has shown that there is a positive correlation between the average speed of upgoing features and their profile width. The measured increase in width is sufficient to cause features with speeds greater than 1.5 km/second to appear in absorption on both sides of the line.

Lifetimes of upflow features have been measured using the time series of spectra and the Doppler movies. The results of these

measurements are consistent with there being a single predominate form of upflow that is visible in the Hα wings further than .4 Å from the core with an average lifetime of a few minutes.

The mean lifetime of downflow regions is six to nine minutes. However, about 20 percent of the downflow regions are observed to persist for fifteen minutes or more. A few downflow regions have lasted the entire length of a Doppler movie, which is about forty minutes.

Downflow typically occurs in the central regions of rosettes. As with upflow features, downflow features often are visible as absorbing features in both wings of Hα. However, the statistical study of spectra has shown that although the average profile width increases with average speed for downflow features, approximately 50 percent of the downflow features have profiles that do not tend to increase with feature speed.

Individual upflow or downflow features did not have a periodic nature on a time scale longer than a few minutes. However, plots of the total upflow or total downflow areas as a function of time in regions 30×10^3 km square did show systematic variations. The auto-correlation functions made from the plots of up and downflow area versus time had secondary peaks spaced by about 550 seconds thus indicating a periodicity in both the total upflow and total down-flow with a period of 550 seconds. Cross-correlation of the plots of upflow and downflow areas for six different regions indicated that the phase relation between upflow and downflow is random.

TABLE OF CONTENTS

INTRODUCTION

The principal observations upon which this thesis is based were taken with a newly designed spectroheliograph camera, during the summer of 1964 at the Mount Wilson Observatory 60 foot solar tower.

This camera together with a semiautomatic cancellation machine makes possible the production of Doppler and Zeeman movies. The techniquesused for the production of the movies are an extension to film of the techniques originally developed by R.B. Leighton for the production of Doppler and Zeeman plates.

The advantages of the camera system over the previous techniques using plates are discussed in Part I. Design considerations and instruction manuals for the various elements of the camera system are contained in the appendices.

The main body of the thesis is concerned with the properties of the flow regions seen in the Hα Doppler movies. Prominent characteristics of the movies are discussed in Part II. Lifetime measurements of velocity features and absorbing features seen in the violet and red wings are reported in Part III. Autocorrelation studies of the area covered by upflow and downflow regions are discussed in Part IV.

Part V is a study of the relationship between Doppler shift and profile width on a series of high resolution Hα spectra. These spectra were taken at Sacramento Peak Observatory in 1961 by J. Evans.

The results of Parts II through V are summarized and correlated in Part VI. Part VI also contains comments on some recent observa-

tions, and some suggestion for future usage of the camera system.

PART I CAMERA SYSTEM

A. INTRODUCTION

In 1958, R.B. Leighton developed a technique for creating Zeeman spectroheliograms[1]. On these plates the density was directly related to the Zeeman splitting in the observed line. This method was soon extended to produce Doppler spectroheliograms on which the density was directly related to the doppler shifts in the observed line[2].

Both techniques utilize a pair of photographic plates taken simultaneously in the same spectral line, but under slightly different circumstances. The two Zeeman plates are taken at the same wavelength, but differ in that one plate has the right circularized component of the light missing, while the other has the left circularized component missing. Doppler plates are taken in two slightly different wavelengths; one at plus $\Delta\lambda$ from the core of the line, and the other at minus $\Delta\lambda$ from the core.

Zeeman and Doppler spectroheliograms are made from the pairs of original plates by overlaying a unit gamma contact copy of one member of the pair on the other such that corresponding image points are in contact. The overlaying procedure is called cancellation.

Zeeman and Doppler spectroheliograms have proved to be an excellent research tool. By means of them the five minute oscillation period of the upper photosphere and the lower chromosphere[2,3,4], the "large cell" convection pattern[2,3,5,6], spatial properties of the solar magnetic field[1,3,5,6,7], and correlations between the magnetic field

and structures visible in various wavelengths have been discovered[1,3,5,6,7]. However, since glass plates were used, it was difficult to study short lifetime characteristics of small scale features (< 10000 km), except statistically. In the summer of 1963 the author started to develop a system to produce either Zeeman or Doppler time lapse movie sequences so as to be able to study lifetimes of smaller features and to obviate some of the technical problems associated with glass plates.

The motion picture system developed required essentially no modification of the equipment at the 60 foot tower telescope used to take the pairs of simultaneous plates. Thus, the set-up procedures for taking a plate and a movie are the same. But for a movie the dual camera instead of the plateholder is placed in the plateholder assembly. The details of the spectroheliograph, the set up procedures, and the methods for making a cancelled plate are discussed in detail on pages 3 through 18 of R.W. Noyes thesis (1963). The design consideration and instruction manuals for the components of the camera system form Appendices I through V of this thesis.

B. ADVANTAGES OF THE CAMERA SYSTEM

The advantages of the camera system over glass plates fall into four general areas, movies, data acquisition, contact printing, and cancellation.

1. Movies

The advantage of a true Doppler movie over a series of plates for studying how regions develop in time is obvious, i.e., with a time lapse movie one can actually watch the time development of

velocity fields. Another advantage of the movies, which has not been utilized in the work reported in this thesis, is the possibility of creating a "lateral displacement" movie by subtracting (canceling) one of the original movies with itself, but offset in time. That is, subtracting a movie from itself such that frame i overlays frame i + s. A lateral displacement movie would yield information on the velocity field perpendicular to the line of sight. However, before lateral displacement movies can be produced the guiding system of the 60 foot tower telescope will have to be improved.

2. Data Acquisition

The primary advantage of the camera system for data acquisition is the increased amount of data that can be obtained in a given time. In a normal morning's run the camera operated for one or two hours and took between 130 and 200 frames. A similar number of images of the same size would require one to two dozen glass plates. Also since the camera advance and spectroheliograph (referred to hereafter as SHG) reversal are automatic. Those operator errors associated with shifting the plate holder assembly and reversing the SHG are eliminated. Eliminated also are the dust streaks caused by dust raised by the opening and closing of the plate holder dark slide. Further the time between frames is more accurately known, since the automatic reversal is controlled by a synchronous timer.

The distance from the film plane in the camera to the top of the slit is 2 mm - a reduction of 1 mm from the plate to slit top distance. The effect of the gap reduction is to reduce by one-third the image spread caused by the gap. The width of the image spread is

$$2\delta = bA/S + a, \quad 4)$$

where b is the gap distance, a is the width of the exit slit, and S/A is the focal ratio = 60. For the normal exit slit width of 0.08 mm, 2δ = 0.13 mm for plates and 2δ = 0.113 for film.

A final advantage is that the automatic operation of the camera allows the operators to go to breakfast. Previously in periods of good seeing, breakfast was missed, or at best, eaten cold.

3. Contact Printing

The production of the unity gamma contact print of an original movie necessary for the cancellation procedure is semi-automatic, and a contact print can be made in ten minutes when the equipment is set up. (The method and apparatus for making the contact print are described in Appendix IV.) This is necessary, of course, if there is to be any advantage to the increased amount of data acquired. Also since the original film and the contact print are aligned with respect to the sprocket holes on the films, the frames on the original and contact print are in the same registration with respect to the sprocket holes. The original movies and the contacts are on Estar (Mylar) base film which has exceptional dimensional stability. The distance between consecutive sprocket holes varies by less than ± .0002 inches, and the distance between one hundred consecutive frames varies by less than ± .005 inches. In the contact printing procedure the sprocket holes are realigned each time the films are advanced-every twenty four sprocket holes.

By means of a specially developed reel system the contact

prints can be developed uniformly. Even if exact unit gamma is not achieved, the entire contact will have the same gamma. This is a considerable advantage over plates where it is almost impossible to insure that the gamma of the contacts does not vary between plates.

4. Cancellation

The cancellation machine automatically aligns the contact and original films with respect to their sprocket holes. (The method and apparatus for producing cancelled films is discussed in Appendix V.) The relative alignment of the contact and the original is the same, within the errors of the sprocket holes, from frame to frame. The fact that the cancellation is performed in exactly the same manner on all frames is a significant advantage over the hand alignment of glass plates. With glass plates it is impossible to be certain that the cancellation of one plate is the same as the next. The reasons for the difficulties are that the quality of focus varies across the two images, and is not the same at corresponding points[4].

Small changes in the placement of the contact on the original cause significant changes in the cancelled plate or film. But in the case of the movie, frame to frame changes in the cancelled film are due to changes on the sun, (whereas one cannot be certain of changes that occur from plate to plate.) For this reason it is advantageous to use the dual camera system for studying time changes even when the time between individual exposures is so long that cine viewing would not be practical.

C. DISADVANTAGES

The principle disadvantage of the camera is the loss of image

with respect to plates. The useful width of 70 mm film is 2.375 inches, while the beam splitter images are 3.5 inches wide. Since the plates are capable of recording the entire width, the use of film results in a thirty five percent loss in image. This is somewhat mitigated by the fact that sections of the image lost are the parts in the worst focus.

With the plate holder system regions of the spectrum requiring differing photographic emulsions can be studied just as rapidly as the spectroheliograph can be set up in a line. All that is required is that a holder had been previously loaded with the proper emulsion plate. The camera requires between five to seven minutes to insert a new film. However, it is possible to take plates while the camera is being reloaded.

PART II OBSERVATIONS OF DOPPLER MOVIES

A. INTRODUCTION

During the summer of 1964 the dual camera was used to take a series of 70 mm movies in a number of different spectral lines. Most of the movies, however, were taken in the violet and red wings of Hα at 0.7 $\mathring{A}$ from the core with a bandpass of 0.14 $\mathring{A}$. Although the time between frames varied during a run, the average time between 1.9 cm frames was 27.5 seconds, when the offset was 0.7 $\mathring{A}$ and the bandpass 0.14 $\mathring{A}$. Other Hα movies were taken at offsets from the core ranging between 0.4 $\mathring{A}$ and 0.8 $\mathring{A}$ with bandpasses between 0.07 $\mathring{A}$ and 0.14 $\mathring{A}$. On one occasion a step-scan movie was made. In the step-scan movie the offset from the core was changed between each frame. The offset cycle was 0.7 $\mathring{A}$, 0.56 $\mathring{A}$, 0.42 $\mathring{A}$, 0.00 $\mathring{A}$, 0.42 $\mathring{A}$, 0.56 $\mathring{A}$.

Using the cancellation machine described in Appendix V a 35 mm Doppler movie was produced from a pair of 70 mm wing movies. The cancellation machine was also used to produce 35 mm copies of the original wing movies. Thus one obtained three 35 mm sequences from a single day's observations. These three movie sequences were spliced together so that the Doppler movie was followed by the violet and red movies from which it was made. A master movie was then produced by splicing together all of the sets of daily observations.

To make cinematic study more convenient the master movie was reduced to 16 mm by Pathé Film Laboratories. On the doppler sections of the final 16 mm movie downward flow regions appeared darker than average and upward flow regions appeared lighter than average; in the

wing sections absorbing regions appeared lighter than average. Pathé also produced a contact print of the 16 mm master. The purpose of having both a negative and positive copy was to minimize the possibility of studying the psychological effects of dark or light spots on a grey background.

All the movie observations discussed in this thesis were made using one or more L-W Photo Model 224-A projectors.

The 224-A can be run forward and in reverse at frame rates of 1,2,4,6,8,12,16, 24 frames per second without flicker. Also it can be advanced frame by frame.

B. RESULTS

The 0.7 $\overset{o}{A}$ Hα doppler movies showed four prominent characteristics (see Figs. 1, 2, and 3).

1. Most of the velocity activity occurred on the boundary of regions roughly 20 to 30 x 10^3 km in diameter.

2. Upward velocity regions tended to surround downward velocity regions.

3. Individual upward velocity regions appeared to have a lifetime of a few minutes.

4. The total downflow area in regions of the order of 10 to 20 x 10^3 km long fluctuated in time with an apparent period of about ten minutes.

Characteristic (1) strongly suggested that the majority of velocity activity occurred in the network regions seen in the Hα wings. To verify this, composite drawings of the velocity field seen in a number of doppler frames were compared with the network structure seen in corresponding wing frames. The composite drawings were

Figure 1:

Figure 1 shows seven consecutive violet and red wing movie frames. These were taken from the movie of August 25, 1964. Also shown of Fig. 1 are the cancelled frames made from the violet and red wing frames.

On the violet and red wing frames the darker than average areas correspond to absorbing regions on the sun. On the cancelled frames, lighter than average areas correspond to upward moving features.

On violet and red frames number 4 is a pair of black fiducial marks. Note that on the cancelled frame number 4 these marks are barely distinguishable.

The gradual variations in mean density visible on the frames of Fig. 1 are not present on the original movies. They were introduced in the production of Fig. 1.

The times the frames were taken are:

1	6:37:01 a.m. P S T
2	6:37:31
3	6:38:01
4	6:38:31
5	6:39:01
6	6:39:31
7	6:40:01

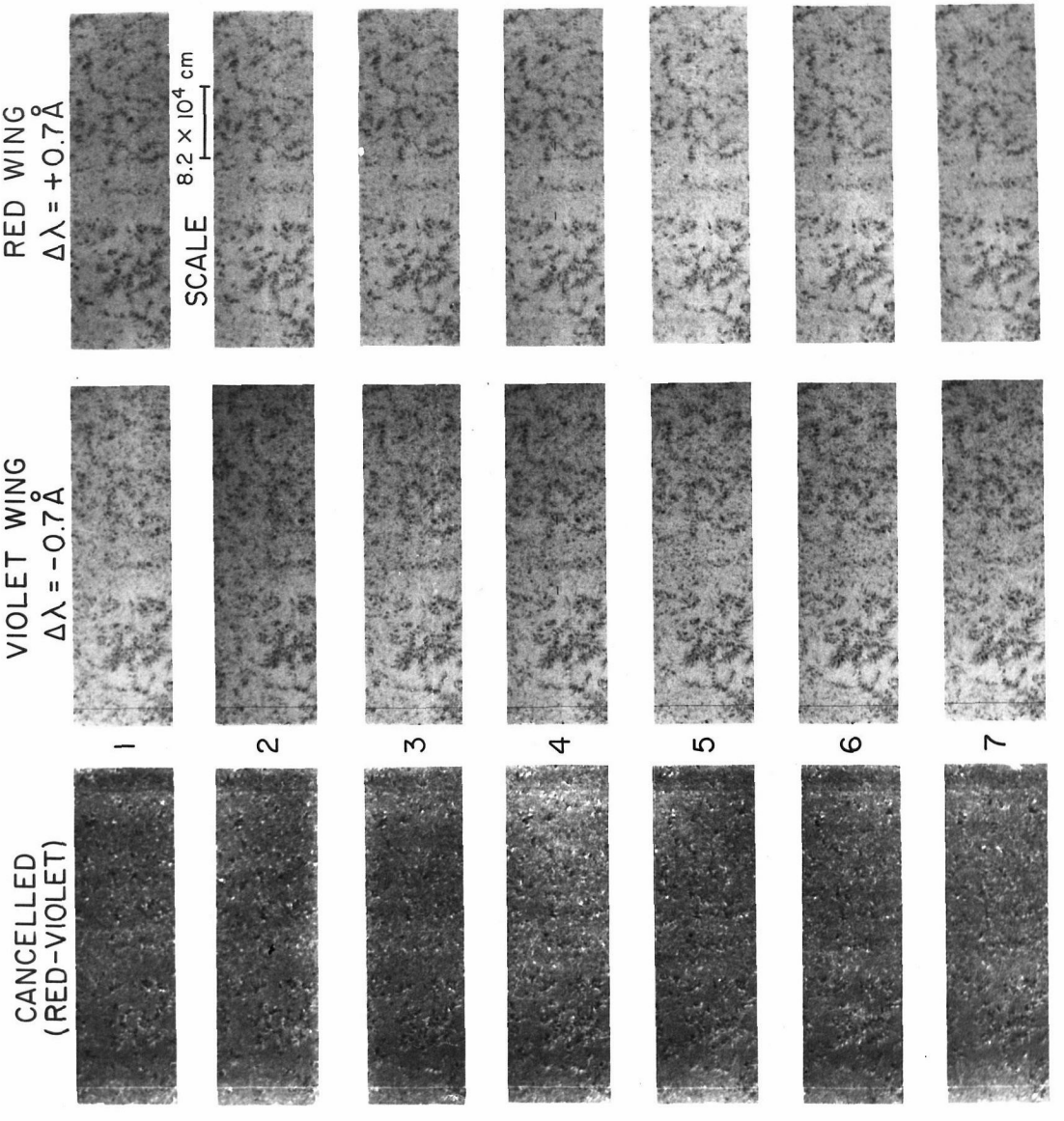
RED WING
Δλ = +0.7Å
SCALE 8.2 × 10⁴ cm
VIOLET WING
Δλ = -0.7Å
CANCELLED
(RED-VIOLET)
1
2
3
4
5
6
7

Figure 1

Figure 2:

Figure 2 shows two consecutive frames of a violet ($\Delta\lambda$ = - 0.7 Å) wing movie taken August 21, 1964. The movie was taken near the limb of the sun.

An idea of the scale can be obtained from the fiducial marks. The length of a fiducial mark corresponds to 10.6×10^3 km on the sun.

Darker than average areas on the frames correspond to absorbing features on the sun.

The upper frame was taken at 6:16:40 a.m. PST, the lower at 6:17:55 a.m. PST.

Figure 3:

This figure shows two consecutive red ($\Delta\lambda$ = + 0.7 Å) wing frames taken simultaneously with the violet wing frames in Fig. 2.

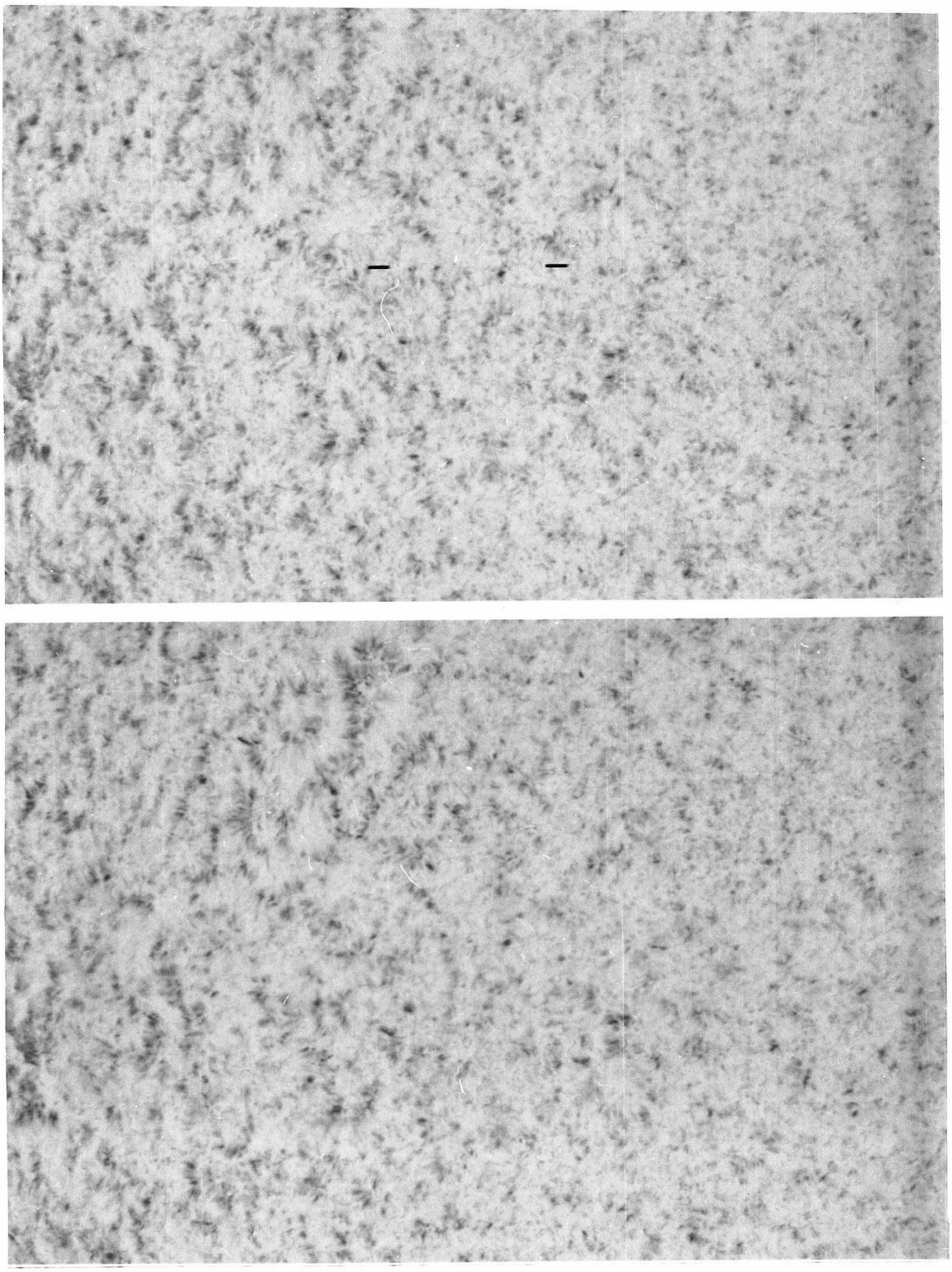

Figure 2

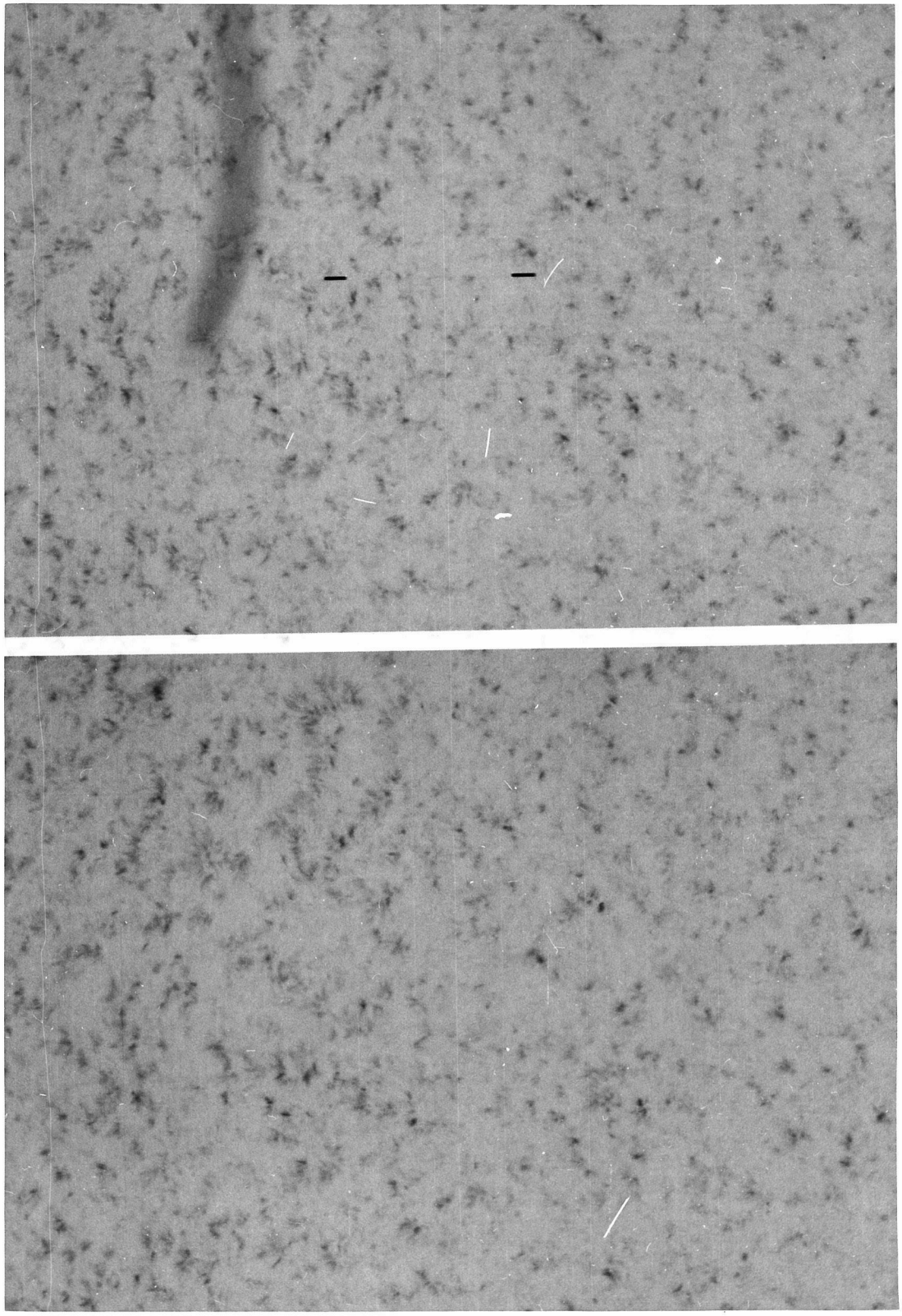

Figure 3

produced by copying the velocity field seen on a doppler frame onto a sheet of paper taped to the projection screen, then advancing the projector and copying the next Doppler frame on the same sheet of paper. The projector was advanced and the copying procedure was repeated until a composite of six to ten Doppler frames was produced. The comparison was performed by advancing the projector to the wing movie immediately following the Doppler movie and noting whether the network and the drawing coincided. Composite drawings were made for the velocity field seen in six different Doppler sequences. In each case the network seen in the wings coincided with the high velocity-density regions on the drawings.

Characteristic (2) suggested that the upflow was occurring in the elongated mottles of the "rosette" structure described by Beckers[8]. Rosettes, which consist of a series of fine absorbing features about 2×10^3 km wide and 2 to 10×10^3 km long that are often arranged radially about a center-like the petals of a flower, are the predominant structures in the Hα wing network. The rosettes are seen in both wings, but in the red wing the most absorbing features are closer to the center of the rosette than the most absorbing features seen in the violet wing. Near the limb the rosettes become "bushes" and the elongated absorbing petals point toward the limb[9]. To investigate the relation between rosettes and the features seen on the Doppler frames a projection system was arranged, so that an Hα wing frame and the corresponding Doppler frame could be viewed either simultaneously or consecutively.

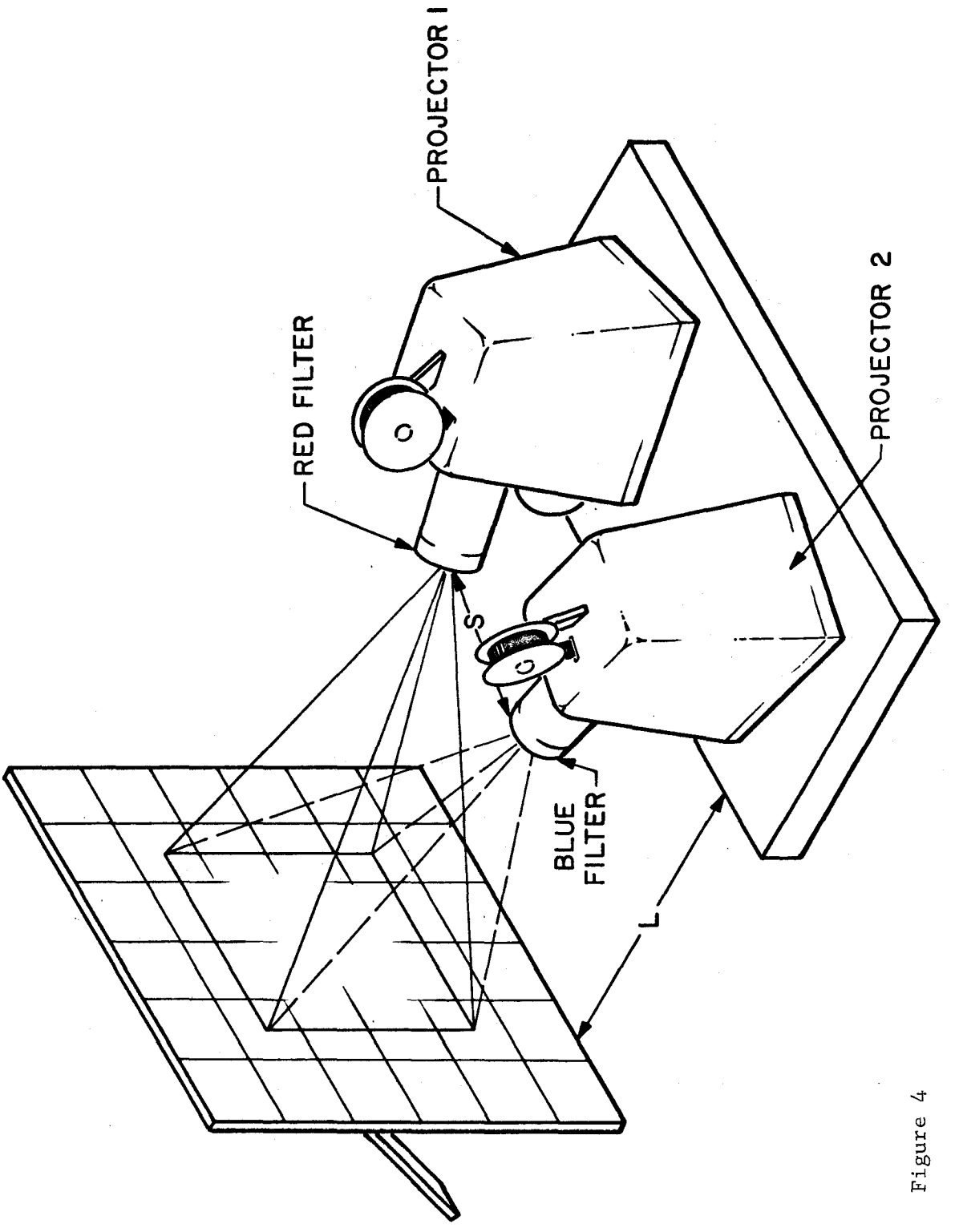

Figure 4

Figure 4 shows the two projector system. In Fig. 4 the projectors are shown much closer to the screen than they are normally. In practice, L is much greater than S so that the parallax between the two images is small. Since the two images were projected in different colors, regions common to both could often be recognized when the two frames were viewed simultaneously. (As mentioned earlier, the wing movies are lighter than average in absorbing regions, thus projected absorbing regions appeared in a markedly more saturated color than the rather muddy background.) By alternately occulting the beams of projector one and two it was possible to blink the two images and thus compare in detail the spatial relations between features on the two different frames.

Comparison of the Doppler and violet frame pairs showed that the upward motion occurred predominately in outer sections in the elongated petals of the rosettes. Similar comparisons of Doppler and red frame pairs showed that the downward flow tended to occur near the center of the rosettes. Simultaneous comparison of violet and red frames quite strikingly exhibited the absorbing regions on the violet frames surrounding the absorbing regions on the red frame. In all cases the velocity regions in the Doppler frames coincided with the absorbing regions seen in the wings.

A recent paper by R. Bhavilai[10] also reports that absorbing regions seen in the violet wing tend to surround the absorbing features seen in the red wing. Bhavilai compared sets of Hα wing filtergrams taken consecutively at $\pm$ 0.5 Å and $\pm$ 0.75 Å.

While comparing violet and Doppler frames it was noted that often a prominent absorbing feature on the violet wing would coincide with a downflow region on the Doppler frame. When this occurred comparison of the corresponding red frame with the Doppler frame always showed an even more strongly absorbing feature at the same location on the red frame. A similar comparison of red and Doppler frames often showed a prominent absorbing feature on the red frame occurring at a point where an upward velocity was indicated on the Doppler frame. Again when the corresponding violet frame was compared with the Doppler frame a stronger absorbing feature occurred on the violet frame at that point. Thus, features recognized as either upward or downward moving on the Doppler frames often appeared as absorbing features on both the red and violet wing simultaneously, thereby indicating that some moving features have considerably broadened absorption profiles. However, the broadened downward moving features tended to be more strongly absorbing on the violet wing than the upward moving features on the red wing.

The above suggested a relationship between velocity and profile width. This was studied statistically on a series of high resolution Hα profiles. Part V is devoted to the methodology and results of this study.

Characteristics three and four are discussed in detail in Parts III and IV.

PART III LIFETIMES

A. INTRODUCTION

The prominent upflow features seen on the Hα Doppler movies have been measured by following individual events on successive frames. The mean lifetime of these events is 113 ± 3.4 seconds. For twenty upflow events the regions in which the upflow occurred have been followed for fifteen minutes. After a few minutes the downflow that occurs in such regions shows no systematic change with time.

The lifetimes of upflow and downflow features on Doppler movies and lifetimes of absorbing regions on violet and red movies have been measured by the method of comparison with a key photograph. The key photograph method yields lifetimes of two to three minutes and six to nine minutes, respectively, for upflow and downflow features; and a lifetime of about ten minutes for absorbing features seen in the violet and red wings 0.5 Å from the core.

Comparison of successive Doppler frames indicated that about twenty percent of the downflow features last at least fifteen minutes. Comparison of successive red wing frames also showed that about twenty percent of the absorbing features also last fifteen minutes or more.

B. RESULTS

a. Maps of Individual Features.

The prominent upflow features were those that appeared much brighter than average on Doppler movies. To measure the lifetime of these prominent features a movie frame was projected and the position

of a prominent feature was marked. The projector was then run backward until no feature appeared at the marked point for several frames. The projector was then advanced until the upgoing feature appeared at the marked position. A piece of graph paper was taped over the point and the feature drawn. The projector was then advanced a single frame, the graph paper was moved up slightly, and the feature drawn again. This process was repeated until there was a distinct lapse of activity at the marked point.

The seventy five prominent upflow events measured fell with one exception into two groups. One group consisted of features that lasted about four frames (the time between frames was 27.5 seconds), "single" events, the other consisted of events that lasted nine frames, "double" events. Single events characteristically showed a very strong Doppler signal on the first or second frame they appeared on. When the Doppler signal was strong on the second frame the Doppler signal on the first frame was weak, thus suggesting that the risetime of the single events is somewhat less than the time between frames. The velocity life history of an average single event was a rise to peak velocity in less than thirty seconds and then a decay in velocity for the next ninety seconds. Double events were merely two single events that occurred sequentially. They are worth mentioning only because double events were the only manner in which multiple single events occurred. In the entire set of measurements no single events occurred in the same region more than twice in a ten minute interval nor did a single event ever repeat after more than two frames after a previous single event.

The drawings of the upflow features were made from Doppler movies taken on 8/25/64, 8/28/64, 9/2/64, 9/12/64. The mean lifetime for the single events was 113. ± 3.4 seconds with 66 percent of the event's lifetimes falling within 26 seconds of the mean. For the double events the mean lifetime was 236.0 ± 8.5 seconds with 66 percent of the double event's lifetimes falling within 38 seconds of the mean. Twenty seven percent of the events were doubles. A histogram of the number of events versus the number of frames an event was visible is shown in Figure 5a.

Measurements of the size of the upflow features were also made. The mean area was $7.10 \pm .13 \times 10^6$ km^2 with 66 percent of the events falling within 1.2×10^6 km of the mean. The features usually appeared elongated. The mean length was $3.12 \pm .10 \times 10^3$ km with 66 percent of the events within 0.94×10^3 km of the mean; the mean width was $2.10 \pm 0.08 \times 10^3$ km with 66 percent of the events within 0.78×10^3 km of the mean. The above dimensions should be taken as a lower limit on the size, since they were the result of a visual judgement.

In the process of measuring the lifetime of the upflow features it was noticed that downflow seemed to avoid regions in which upflow had occurred. To check this observation the maximum extent of upflow features was drawn on the screen, and the fractional overlap of these regions by either upflow or downflow was recorded for the next forty frames. The average of twenty such measurements is shown in Figure 5b. In Figure 5c is shown the average of twenty similar measurements in which the regions were drawn from downflow features. From Fig. 5 b it

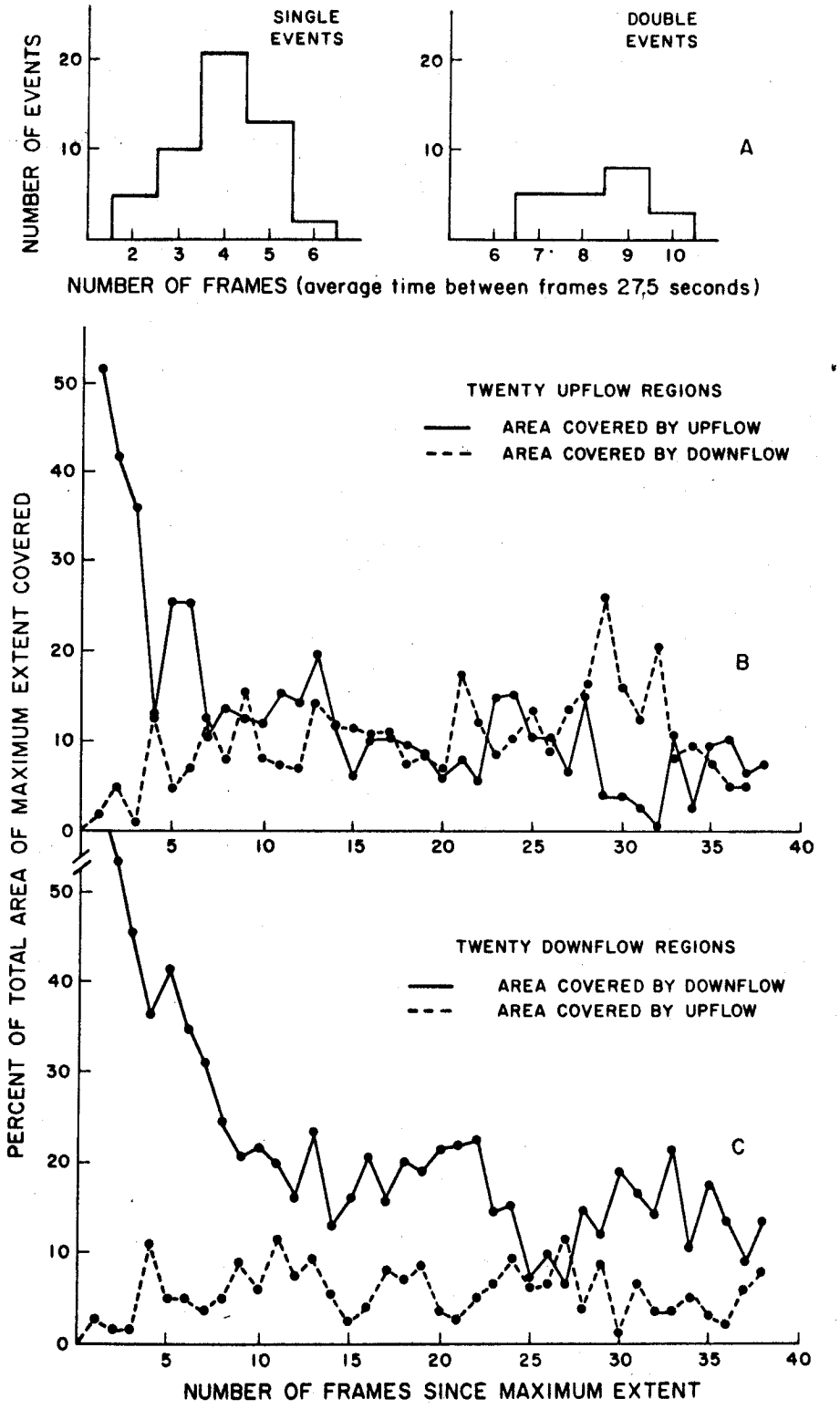
SINGLE EVENTS
DOUBLE EVENTS
NUMBER OF EVENTS
A
NUMBER OF FRAMES (average time between frames 27,5 seconds)
TWENTY UPFLOW REGIONS
AREA COVERED BY UPFLOW
AREA COVERED BY DOWNFLOW
B
TWENTY DOWNFLOW REGIONS
AREA COVERED BY DOWNFLOW
AREA COVERED BY UPFLOW
C
PERCENT OF TOTAL AREA OF MAXIMUM EXTENT COVERED
NUMBER OF FRAMES SINCE MAXIMUM EXTENT

Figure 5

is clear that downflow in regions that originally contained upflow features does not markedly change with time after a few minutes. The fluctuations of the downflow (dashed curve of Fig. 5b) are not any larger than one would expect from fluctuations in seeing and guiding. Figure 5c clearly demonstrates that upflow does not tend to increase in regions in which downflow has occurred. The higher average level on the downflow curve in Fig. 5c merely reflects the fact that about twenty percent of the downflow regions persist for fifteen minutes or more.

Beckers has reported that 30 to 100 percent of the fine features seen in violet wing filtergrams are characterized by rising and then falling twelve minutes later[8]. This result was based on a movie twenty minutes in length taken through a 1/8 $\mathring{A}$ bandpass tuneable Hα filter. Alternate frames of the movie were taken at plus and minus 0.5 $\mathring{A}$ from the core. Beckers compared contact prints of the individual movie frames. In his comparison procedure a red wing filtergram near the middle of the movie was compared with all the other frames of the movies. However, Beckers did not require features on the chosen key red filtergram to be coincident features seen in earlier and later frames.

Figures 5a and 5b do not show the phenomena described by Beckers. To attempt to duplicate Beckers' procedure a series of transparencies was made from corresponding thirty minute segments of a pair of simultaneous Hα wing movies taken at 0.5 $\mathring{A}$ from the core. The average time between frames was 125 seconds. Each transparency included not only the movie's frame, but also the image of the ad-

jacent sprocket holes. Hence, it was possible to align pairs of transparencies by means of the sprocket hole images.

Forty features were marked on a red wing transparency near the middle of the series. This key transparency was compared with all the other members of the series. Beckers' effect was not observed.

I have not seen Beckers' photographs. Perhaps the quality of the images and the alignment from frame to frame is superior to that obtained at Mount Wilson, although the movie used for my comparison procedure was the best Hα movie so far obtained. However, on the basis of my results I believe it is safe to say that most of the upflow features do not rise then fall for at least fifteen minutes.

The velocity lifetimes described above depend on the choice of the zero level of velocity. R. Noyes' thesis (1963) contains a discussion of the velocity sensitivity of the Doppler cancellation method. Noyes' analysis indicates that a velocity of 0.2 km/second should be clearly visible. Therefore, the velocity lifetime should be interpreted as lifetimes above 0.2 km/second.

b. Measurements by the Key Photograph Method.

To measure the lifetimes of features by the key photograph method a frame was projected on the screen and a number of features were outlined. Then earlier and later frames were compared at the outlined locations. Features visible in the outlined regions of the screen were given a visibility score of one to four. Four was given if a distinct feature filled 90 percent or more of an outlined region, three if a distinct feature filled 60 percent of more on an outlined region, two if a feature was visible in 30 percent or more of an

outlined region, and one if any feature could be identified in an outlined region. A score of zero was given if no feature was visible in an outlined region.

Figures 6a and 6b show, respectively, plots of the visibility versus number of frames from the key for fifty upflow and fifty downflow features. A score of one on the visibility scale represents a rather marginal recognition of a feature in an outlined region. Therefore, a reasonable estimate from Fig. 6a of the lifetime for upflow features is two or three minutes. The shape and width of Figure 6a are not inconsistent with the 113 second lifetime events being the predominant form of upflow that is visible 0.7 $\mathring{A}$ from the core. The leveling of the downflow visibility curve is an indication of the fact that about twenty percent of the downflow features persist for fifteen minutes or more. The lifetime of the downflow is made somewhat ambiguous by the persistant component, but comparison of figures of 6a and 6b indicates that the downflow lifetime is two to three times that of the upflow or six to nine minutes.

Figures 7a and 7b are, respectively, plots of visibility against time for sixty five features in the violet wing and sixty five features visible in the red wing. These show that features seen in the wings at .5 $\mathring{A}$ have lifetimes of about 10 minutes. Again the flattening of the visibility graph for the red wing features indicated the presence of downflow features with lifetimes of longer than fifteen minutes. Unfortunately, after twelve minutes the sun has rotated 1.4×10^3 km, which is about half the scale size of the feature followed, and therefore identification of individual features becomes

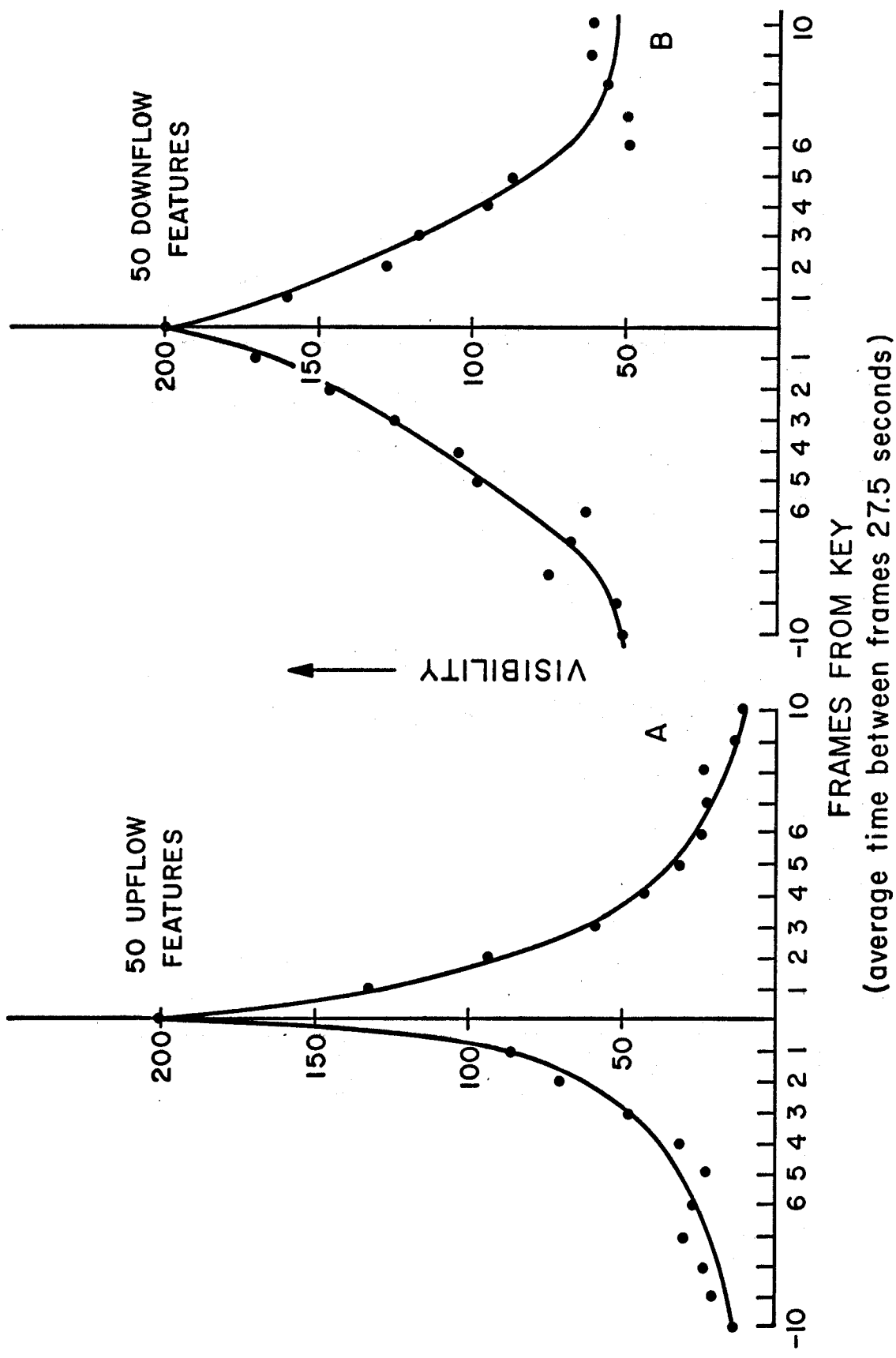
50 UPFLOW FEATURES
50 DOWNFLOW FEATURES
200
150
100
50
A
B
VISIBILITY
-10 6 5 4 3 2 1 1 2 3 4 5 6 10
FRAMES FROM KEY
(average time between frames 27.5 seconds)

Figure 6

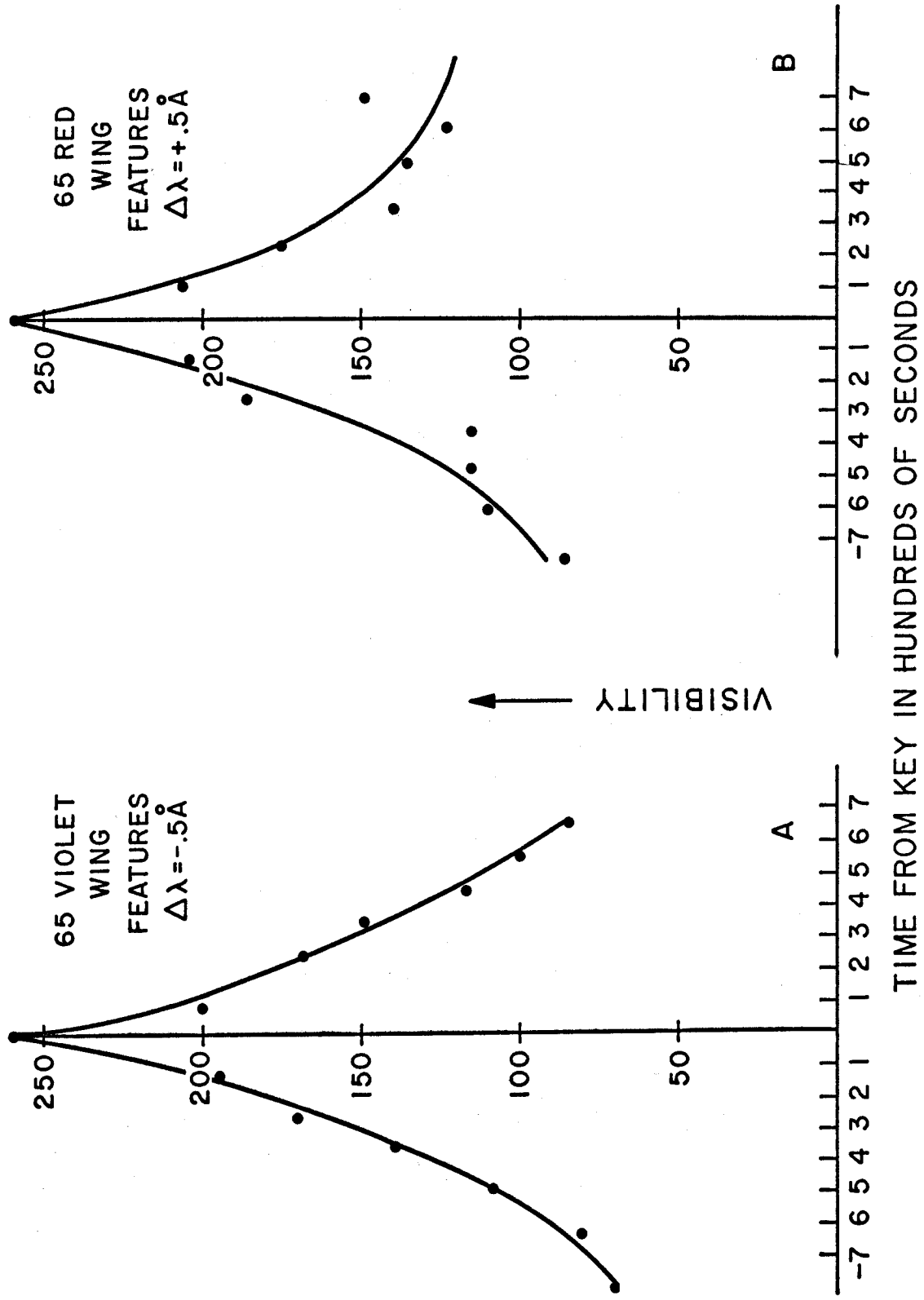
65 VIOLET WING FEATURES Δλ=-.5Å
65 RED WING FEATURES Δλ=+.5Å
250
200
150
100
50
VISIBILITY
A
B
-7 6 5 4 3 2 1
1 2 3 4 5 6 7
TIME FROM KEY IN HUNDREDS OF SECONDS

Figure 7

difficult. However, a few persistent downflow and red wing features have been followed for forty minutes, that is, the entire length of a movie.

The ten minute lifetime for the fine features seen in the Hα wings at .5 $\mathring{A}$ is in agreement with the lifetimes measured by Beckers[8] for the same features. Also it is the same as the lifetime measured by Howard and Harvey[11] for features seen in the core of Hα.

PART IV AUTOCORRELATION STUDIES

A. INTRODUCTION

In Part II it was stated that one of the characteristic features of the Doppler movies was that in areas about 10000 km long on the boundaries of large cells, the downward flow fluctuated with an apparent period of nine to ten minutes. To investigate this phenomenon the total area covered by downflow features in regions 31.2×10^3 km square was measured as a function of time. The same thing was also done for the upflow features in the same regions. The resulting plots of the area covered by downflow and upflow versus time were analyzed for periodicity by autocorrelation and Fourier transform techniques.

The power spectra of the area versus time graphs for both upflow and downflow had peaks at 550 ± 25 second. Application of standard mathematical tests for confidence level indicated that the 550 second peaks were real at the 99.9 percent confidence level for both the upflow and downflow area versus time plots.

The methods for creating the area versus time plots, and the autocorrelation and Fourier transform techniques used to analyze them are discussed at some length below.

B. PLOTS

The down or upflow area versus frame number (time) plots were made by measuring down or upflow areas on a series of drawings of the velocity field in a region of the sun. To make the velocity field

in a region of the sun. To make the velocity field drawings, the stop motion projector was set up to project Doppler frames on the ruled screen. The set-up was similar to that shown in Fig. 4 , but with only one projector. A region of the screen was chosen at random, and the portion of the projected Doppler frame in that region was drawn on a sheet of graph paper overlayed on the screen. The projector was then advanced one frame, and the velocity field in the chosen region of the screen was drawn on another section of the graph paper. Care was taken that the drawings were indexed with respect to the graph paper.

The screen region was always 1.2 inches square, corresponding to a region 31.2×10^3 km square on the sun. A series of drawings was usually eighty frames long, and the average time between frames was 27.5 seconds.

Each of the drawings of a series was subdivided by a grid having a 0.3 inch mesh. The grid was aligned with each of the drawings in the same manner. Area versus frame number plots were then constructed by measuring the area covered by, say, downflow in corresponding squares of the grid for all the drawings of the series. In this manner a set of thirty two graphs of area versus frame number was obtained. Sixteen were of the area of downflow in 7.8×10^3 km square sub-regions; the other sixteen were the area of upflow in the same sub-regions.

The purpose of subdividing the original 1.2 inch square regions into sixteen 0.3 inch square sub-regions was to attempt to discover on what scale organized behavior started. The area versus frame number

graphs for the 7.8 km square regions showed no repetitive character. The next larger areas studied were the half regions formed by bisecting the original regions through the midpoints of a pair of opposite sides. The graphs for the half regions were obtained by adding the proper set of graphs for the sub-regions of which it was composed. Similarly, graphs were constructed for the entire region by adding the proper sixteen graphs.

In making the velocity field drawings it was necessary to make a judgement of the extent of each flow region. Essentially, this judgement consisted of choosing a cut-off level of intensity for both the darker than average downflow regions and the lighter than average upflow regions. Once the cut-off levels were decided upon, an observer could draw a section of a Doppler frame, and then at some later time make another drawing of the same region that would agree with the first. The effect of changing the cut-off intensity levels was investigated by making two series of drawings of a region using different sets of cut-offs. Aside from a scale factor due to the fact that one set of drawings had systematically larger flow regions than the other, the area versus frame number graphs for the two series were similar. The entire procedure of making two series of drawings was repeated for another region, and again the graphs were quite similar.

In all, eight series of drawings and graphs were made, six of them on different regions of the sun. Series one, two, three and four were made on four different regions on the movie taken on

September 2, 1964. Series five and six were made on two different regions on the movie of August 25, 1964. Ideally, each of the series of drawings would have been made on a different movie. However, this was not possible because of the lack of movies with nearly uniform good seeing that persisted for at least eighty frames, or about forty minutes. Both movies used were taken in the center of the disk at 0.7 $\overset{o}{A}$ from the core.

C. AUTOCORRELATION AND FOURIER TRANSFORM TECHNIQUES

Autocorrelation functions of the area versus frame number graphs were formed to study the systematic character of the graphs. An autocorrelation function of a function f(x) is defined as

$$C(s) = \lim_{L\to\infty} 1/L \int_{-L/2}^{L/2} f(x)\ f(x+s)\ ds.$$

In practice where f(x) is an experimentally measured quantity the range over which f(x) is known is finite. In that case, C(s) is approximated by

$$\bar{C}(s) = 1/(L-s) \int_{-L/2}^{L/2} f(x)\ f(x+s)\ ds,$$

where $f(x) = 0$ for $x < -L/2$, $x > L/2$.

In the case one does not have a continuous function, but a series of equally spaced measurements f_i, the analog of $\bar{C}(s)$ is

$$C_s = 1/(L-s) \sum_{i=1}^{L} f_i f_{i+s},$$

where $f_i = 0$ for $i < 1$, $i > L$.

In this paper it will be more convenient to use a normalized autocorrelation function

$$C_s = \frac{1/(L-s)\sum_{i=1}^{L} f_i f_{i+s}}{\sum_{i=1}^{L} f_i f_i} \quad . \tag{1}$$

In a similar manner, a cross-correlation function of functions $f_1(x)$ and $f_2(x)$ is defined as

$$C_{12}(s) = \lim_{L\to\infty} \frac{1}{L} \int_{-L/2}^{L/2} f_1(x)\ f_2(x+s)\ ds.$$

The analogous expression for the normalized finite discrete cross correlation function is

$$C_{12s} = \frac{1/(L-s)\sum_{i=1}^{L} f_{1i} f_{2(i+s)}}{\left(\sum_{i=1}^{L} f_{1i} f_{1i}\right)^{1/2} \left(\sum_{i=1}^{L} f_{2i} f_{2i}\right)^{1/2}} \quad . \tag{2}$$

Autocorrelations of the area versus frame number graphs were performed using expression (1), and cross-correlations of the up and downflow area versus frame number plots were performed using expression (2). (Hereafter autocorrelation and cross-correlation will be abbreviated by AC and CC, respectively.) The AC and CC functions were calculated and plotted by the Caltech IBM 7094.

It can be easily shown that the Fourier transform of the AC function of a function $f(x)$ is the power spectrum of $f(x)$. Hence, the power spectrum of the area versus frame number plots should be

obtainable by Fourier transforming their AC functions. However, some complications are introduced because the graphs are of finite length. It is not sufficient or correct to Fourier transform a function known on a region of length L as if it were a periodic function on L. Rather, one must assume that one has a section of a function that could have been measured forever. That is, one should assume that one has measured a function f(x) where

$$f(x) = g(x)\ h(x)$$

where $g(x) = 1$ for $0 \leq x \leq L$

$= 0$ for $x < 0;\ x > L,$

and that h(x) is a function that goes on forever, The function f(x) as defined by expression (7) should be transformed by a Fourier integral transform. The transform of f(x) can be written as

$$F(k) = \int_{-\infty}^{\infty} f(x)\ \exp(-ikx)dx$$

$$= \int_{0}^{L} h(x)\ \exp(-ikx)dx.$$

Similarly, one can denote the Fourier transforms of g(x) and h(x) by G(k) and H(k). Then by the convolution theorem

$$F(k) = \int_{-\infty}^{\infty} G(k - s)\ H(s)ds. \qquad (3)$$

The function G(k) is the diffraction pattern of a window of length L.

$$G(k) = \frac{\sin (Lk/2)}{Lk/2} \quad . \qquad (4)$$

The first secondary peak of G(k) is twenty percent of the primary peak.

From expression (3) one sees that Fourier transforming a function of finite length results in a convolution of the function of interest, that is, h(x), and a diffraction pattern of a window of length L. Expressions (3) and (4) make clear what one knew beforehand, namely that one gets no information on periods on the order of or longer than the length of the original record. However, expressions (3) and (4) also demonstrate that peaks may appear in F(k) where none exists in H(k) because of the secondary peaks of G(k).

The secondary peaks caused by the window function g(x) are important in the case of Fourier transforming the AC functions and the area versus frame number graphs. This is because seeing normally deteriorates with time. The deterioration in seeing causes the movie frames to decrease in contrast with time, and therefore causes the total flow area measured to decrease with time. Thus, the Fourier transforms of the AC functions and the area versus frame number graphs tend to have a low frequency seeing peak.

Fortunately, it is possible to minimize the secondary peaks caused by the finite length of the original function by pre-multiplying the original function by a proper "window"[12]. If before Fourier transforming, f(x) is multiplied by

$$g^*(x) = .5\ (1 - \cos(2\pi x/L))\ \text{for}\ 0 \leq x \leq L/2$$

$$= .5\ (1 + \cos(2\pi(x - L/2)))\ \text{for}\ L/2 < x \leq L$$

$$= 0 \quad \text{for} \quad x < 0;\ x > L,$$

multiplying by $g^*(x)$ is called hanning, the secondary peaks are reduced. The first secondary peak of $G^*(k)$ is a tenth that of the rectangular window $G(k)$. Figure 9c shows a plot of $G^*(k)$, the hanning window, and $G(k)$, the rectangular window.

In all the Fourier transforms discussed in this part, the transformed function has had its average subtracted to make the zero frequency Fourier component zero, and has been premultiplied by a hanning window to minimize secondary peaks.

D. RESULTS

As stated earlier in this part the area versus frame number plots for the 7.8×10^3 km square sub-regions showed no periodicity. However, the area versus frame number plots for the $15.6 \times 31.2 \times 10^3$ km half regions and the 31.2×10^3 km square full regions often seemed to have a periodic structure. (For the rest of this part the downflow and upflow versus frame number plots will be abbreviated as DAF and UAF, respectively.)

The AC functions of both the DAF and UAF plots of six of the twelve half regions had two or more secondary spaced approximately 550 seconds apart. These half regions were parts of full regions, one, two, four, five, and six. Both region two's half regions yielded AC functions with secondary peaks, while neither of region

three's half regions had AC functions with other than the primary peak. All of the six half regions that did not yield AC functions with secondary peaks were drawn from sections of the sun in which little velocity activity occurred. In Part II it was demonstrated that most velocity activity occurred on the boundary of large cells, and since the regions drawn were chosen at random, it is not surprising that some of the half regions did not contain a significant amount of network.

In Fig. 8a, is shown the sum of the six AC functions formed from the UAF graphs of the six half-regions which yield AC functions with secondary peaks. In Fig. 8b is shown the sum of the AC functions formed from the DAF plots of the same set of half-regions. For comparison purposes, the right half of Fig. 8c shows the sum of four AC functions formed from random functions, generated by a random number table. On the left half of Fig. 8c is shown the sum of four CC functions formed from random functions.

Five of the six full region's AC functions had secondary peaks that were as high or less than as high as the secondary peaks of AC functions of the half-regions in which the majority of the velocity activity occurred. In the case of region two, the full region's AC functions had secondary peaks about 20 percent higher than the secondary peaks of the AC functions formed from its composite half-regions. Region two contained a U shaped section of network.

The summed AC functions shown in Figs. 8a and 8b were Fourier transformed so as to obtain the power spectra of the UAF and DAF plots. The solid curves in Figs. 9a and 9b are the power spectra of the UAF and DAF plots. The dashed curves in 9a and 9b are the

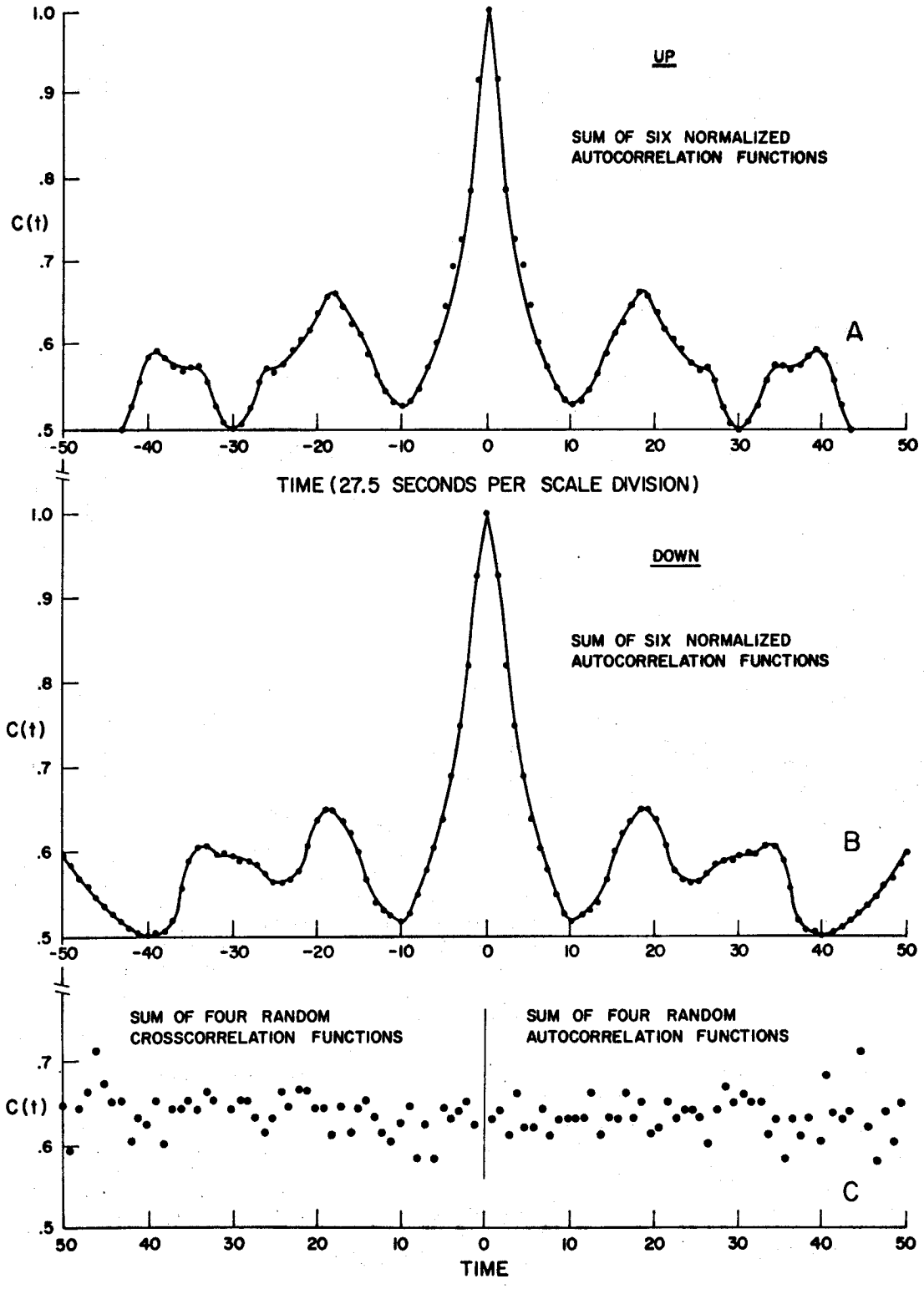
UP
SUM OF SIX NORMALIZED
AUTOCORRELATION FUNCTIONS
C(t)
A
TIME (27.5 SECONDS PER SCALE DIVISION)
DOWN
SUM OF SIX NORMALIZED
AUTOCORRELATION FUNCTIONS
B
SUM OF FOUR RANDOM
CROSSCORRELATION FUNCTIONS
SUM OF FOUR RANDOM
AUTOCORRELATION FUNCTIONS
C
TIME

Figure 8

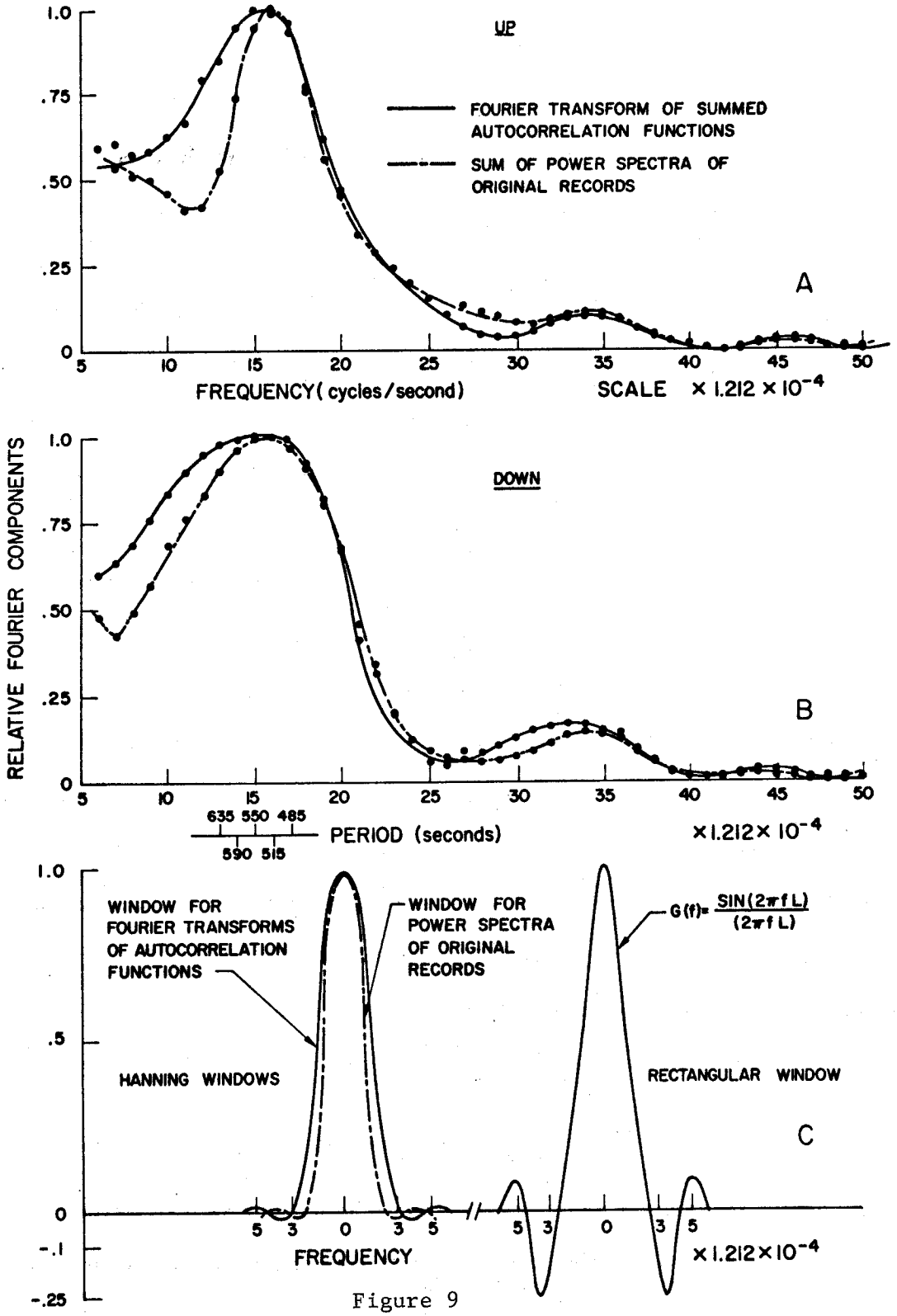
UP
FOURIER TRANSFORM OF SUMMED AUTOCORRELATION FUNCTIONS
SUM OF POWER SPECTRA OF ORIGINAL RECORDS
A
FREQUENCY(cycles/second)
SCALE × 1.212 × 10⁻⁴
RELATIVE FOURIER COMPONENTS
DOWN
B
635 550 485
590 515
PERIOD (seconds)
×1.212× 10⁻⁴
WINDOW FOR FOURIER TRANSFORMS OF AUTOCORRELATION FUNCTIONS
WINDOW FOR POWER SPECTRA OF ORIGINAL RECORDS
G(f)= SIN(2πfL) / (2πfL)
HANNING WINDOWS
RECTANGULAR WINDOW
C
FREQUENCY
×1.212×10⁻⁴

Figure 9

power spectra of the UAF and DAF plots obtained by Fourier transforming the UAF and DAF plots directly and then summing the squares of the Fourier transforms. Figure 9c shows the resolution widths of Figs. 9a and 9b. The resolution width for the power spectra which was obtained directly from the DAF and UAF graphs is slightly narrower than the AC function obtained power spectra obtained from the AC functions because the window of the DAF and UAF plots was slightly larger than the window of the AC functions. The dashed and solid curves agree rather well. This is very satisfying since they were obtained by quite different methods, and thus demonstrate that the peaks in the power spectra are, at least, not a property of a computer program.

Application of standard mathematical tests[12] for the reality of a peak in a power spectra obtained from an AC function shows that the 550 second peak in Figs. 9a and 9b is real at the 99.9 percent confidence level.

CC functions formed from UAF and DAF plots also tended to have peaks spaced by 550 seconds. However, this is only to be expected, since the AC functions of DAF and UAF plots have already shown that a 550 second period is present. That is, the AC functions have shown that the UAF and DAF records are approximately of the form

$$f(t,\theta) = \text{Noise}(t) + A\cos(2\pi t/550 + \theta),$$

where Noise (t) is a random function, and A is a constant. The amplitude A can be chosen so that AC functions made from $f(t,\theta)$ are similar to the AC function made from the UAF and DAF plots. It is

clear that the CC of $f(t,\theta_1)$ and $f(t,\theta_2)$ where θ_1 and θ_2 are chosen at random, will yield a CC function with peaks spaced at 550 second intervals. However, the position of the peaks will vary as the phase difference $(\theta_1 - \theta_2)$ varies.

The CC functions of UAF and DAF graphs have peaks, but the location of the peaks vary from region to region. The behavior of the CC functions implies that the phase relation between upflow and downflow is random.

It has been suggested that the rosettes are loops seen from the top[10]. That material flows up the petals, then over, where the material is not seen, and then down the center of the rosette. It is hard, if not impossible, to reconcile a loop mechanism with the facts that both upflow and downflow in a region containing many rosettes are periodic, and the phase relation between upflow and downflow is random.

E. PHYSICAL ORIGIN

In the sections above several interesting questions have not been answered. One of the most interesting is, on what scale do the observed fluctuations stop? The fact that the half-regions tend to yield AC functions with higher secondary peaks than full regions' AC functions suggests that the fluctuations may stop at the level of large cells. However, this is just a surmise and is by no means demonstrated. To learn at what scale the fluctuations stop it will be necessary to carry out a program similar to that described above for larger regions. Unfortunately large cells are about 30×10^3 km in diameter which means regions of the sun of at least 60×10^3 km

square will have to be mapped. The six maps used for the studies described above took three people three months of extremely tedious work to draw and reduce.

Also unanswered is the question of what causes the observed fluctuations. The low frequency of the fluctuations may suggest that the origin is the photosphere or lower, but at present, the origin of the fluctuations is unknown.

F. ERRORS

The fact that the upflow and downflow do not fluctuate in phase is a strong argument that the observed effects do not originate in the telescope or photographic processing. The computer processing of the DAF and UAF graphs has been checked both by hand and by using input data whose AC and Fourier transforms are known.

PART V STATISTICAL STUDY OF Hα SPECTRA

A. INTRODUCTION

Since simultaneous viewing of Doppler and violet or red movie frames, by the two-projector method described in Part II, demonstrated that at least some of the high speed features seen in the Doppler frames had broader than average profiles, simultaneous measurement of both the offset and width of features on Hα spectra also ought to show that some of the high offset features have larger than average widths. Besides being an independent method of confirming the movie observations, the measurement of spectra offers the chance to discover a correlation between feature speed (offset) and feature width if a correlation exists. A correlation is easier to discover on spectra than by comparison of Doppler and wing frames, since features with broad profiles but low speed do not yield strong signals on the Doppler frames. Further, studies of a time sequence of spectra offer the possibility learning how a speed-width correlation might vary with time.

Sacramento Peak Observatory (SPO) was kind enough to lend me a time series of Hα spectra. However, it then became necessary to develop a method of measuring both width and offset of features on the spectra. Difficulties arose because of the large amount of input and output data that is involved. To obtain the offset information a minimum of two points must be measured on each feature of interest; to obtain both the width and the offset at least three points must be measured on each feature. Each spectrum contains approximately 10^3

features, and there were twenty spectra in the time series. Thus the minimum amount of input data was approximately 6×10^4 numbers. In the program actually used, four points were measured on each spectrum so that an idea of the error in the measurement procedure could be obtained. The amount of output data was the same as the input, since the width, offset, central intensity, and error were calculated for each of the 2×10^4 features of the spectra.

The spectra, the data reduction methods, and the format of the data output are discussed in the section devoted to them.

B. DATA

The SPO spectra were taken September 24, 1961 using the observatory's coelostat system on 70 mm 103-Hα film. The slit of the spectrograph was aligned along the solar central meridian and extended from approximately 16 3/4° North to 2 3/4° South latitude on the sun. The slit width used was 100 microns-543 km on the sun; the slit length was 5.1 cm - 2.77×10^5 km on the sun. A spectrum took four seconds to expose, and the time between exposures was thirty seconds. To compensate for solar rotation the slit of the spectrograph was moved 50 microns every three minutes. The original series consisted of twenty six spectra and four step wedges. The spectrum frames were numbered from 88 through 113; the step wedges were numbered from 114 through 117. When the series was received at Caltech, frames 88, 92, 93, 100, 108, and 113 were missing or unusable because of flaws.

C. DATA REDUCTION METHODS

The method for obtaining the maximum amount of information on the relationship between profile width and line of sight velocity would be to make a series of microphotometer tracings (on each frame) along the dispersion direction, then to measure on each of the tracings the width and shift of the profile center. However, the spectral features of interest are on the order of 0.1 mm wide on the frame and each frame was about 50 mm wide. Therefore about one thousand tracings would have to be made on each spectrum of the series. Since each microphotometer trace would take about three minutes, the entire microphotometering project would require about eight weeks.

To lessen the amount of data taken and to have it in a form more convenient for computing equipment, it was decided to make the tracings at a series of fixed wavelengths. A computer could fit a curve to the measurements at a set of fixed wavelengths, and calculate the curve's width and offset. To determine the type of curve to be fitted and the best wavelength at which to make the measurements forty five traces were made along the dispersion direction on frame 89. In the region between .3 $\mathring{A}$ and .6 $\mathring{A}$ on both sides of the line center, these tracings were well fitted by gaussians. The wavelengths chosen for the measurements were $\pm$ .4 $\mathring{A}$ and $\pm$ .6 $\mathring{A}$ from the mean center of Hα. Since the measurements were to be made at a series of fixed wavelengths, it was decided to make the microphotometer traces perpendicular to the dispersion direction. This method reduces the total number of tracings necessary to forty. Another advantage of this method is that if the original tracings are digitized, the alignment of all the

tracings and the gaussian fitting procedure can be done by computer.

Sacramento Peak Observatory very kindly allowed me to use their digitizing microphotometer and computer facilities to carry out the procedure outlined above. The digitizer system was set up to record and punch a value of the frame density each 50 microns on the film - 272 km on the sun. Since the density on a photograph is not directly proportional to incident intensity, it was necessary to convert the density-punch cards to intensity-punch cards before the fitting procedure could be performed. The SPO IBM 1620 II was used to produce a set of intensity-punch cards from the original density-punch cards and the density relation obtained from step wedge data. The intensity-punch cards were then plotted by a Cal Computer 565. On Fig. 10 is shown the location on the microphotometer traces on spectrum 102 and the intensity corrected microphotometer traces for the spectrum.

When the spectra were taken a fiducial line was imposed on each spectrum by means of a wire placed across the focal plane of the spectrograph. Hence, each frame of the series had a line across it at the same position relative to the exit slit. When the microphotometer slit crossed the fiducial line a sharp peak was recorded. A computer program was written to recognize this peak on the punch cards, and renumber all the data points in a tracing with respect to a predetermined number for the peak. The fiducial line was not exactly perpendicular to the slit direction so that the fiducial mark number was different for tracings at different wavelengths. However, for all tracing at the same wavelength the fiducial mark had the same number.

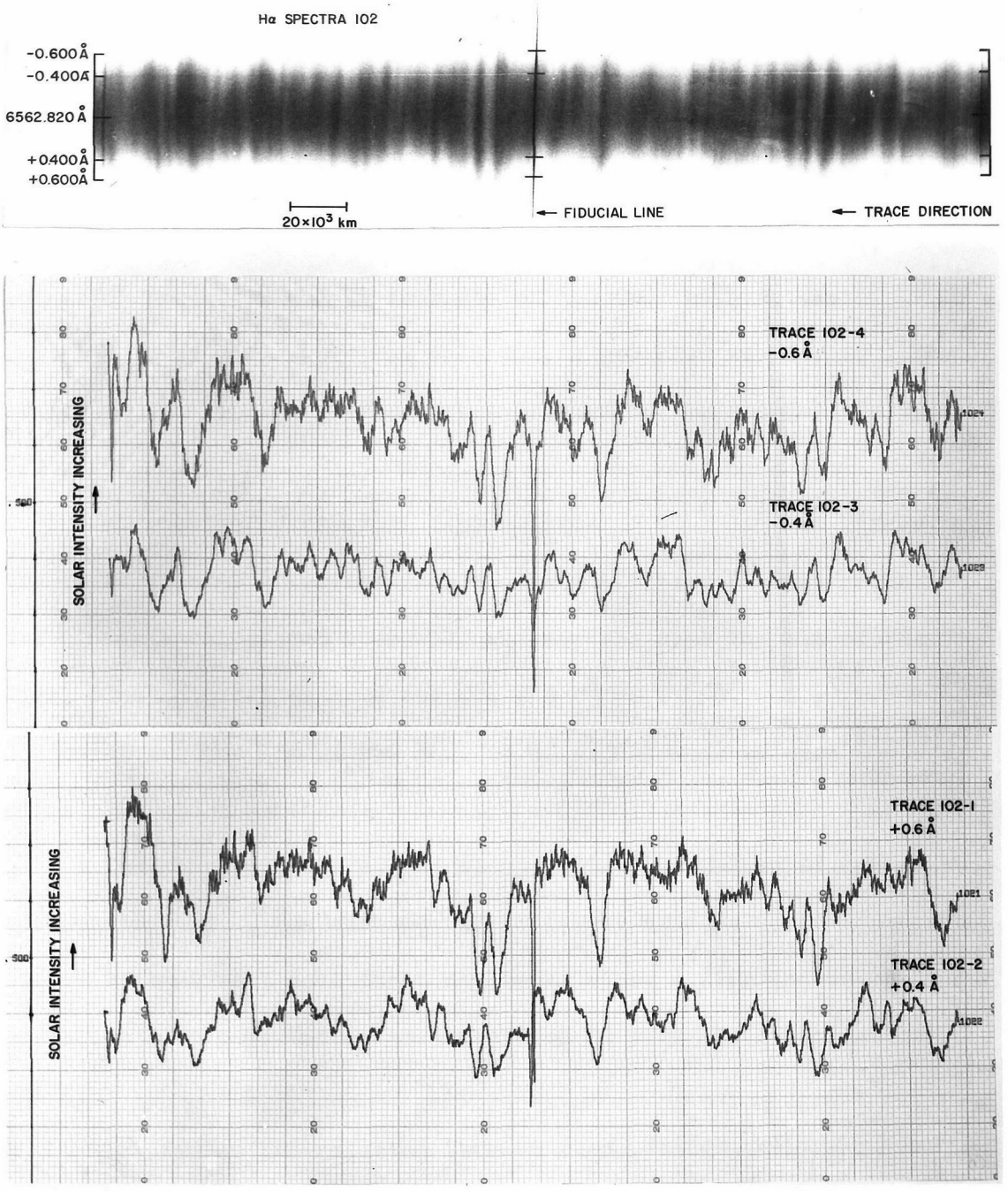
Hα SPECTRA 102
-0.600 Å
-0.400 Å
6562.820 Å
+0.400 Å
+0.600 Å
20×10³ km
FIDUCIAL LINE
TRACE DIRECTION
TRACE 102-4
-0.6 Å
TRACE 102-3
-0.4 Å
SOLAR INTENSITY INCREASING
TRACE 102-1
+0.6 Å
TRACE 102-2
+0.4 Å
SOLAR INTENSITY INCREASING

Figure 10

After the tracings were aligned with respect to the fiducial mark, each tracing consisted of 1081 data points. Each point was the value of the solar intensity at some fixed wavelength. The point number indicated at what point along the slit the point had been recorded. Thus, each data point had a number like 3-89-256. The three indicated that it was from a tracing at - .4 $\mathring{A}$; the 89 that the tracing was made on frame 89; the 256 that it was taken at point 256 on the slit. To each set of the four points, say, 1-89-256, 2-89-256, 3-89-256, 4-89-256, a gaussian was fitted. The alignment and fitting programs were carried out on the Caltech IBM 7094.

A gaussian of the form $I(\lambda) = I_c - Ie^{-\frac{1}{2}\left(\frac{\lambda - \lambda_s}{\sigma}\right)^2}$ was fitted by the least squares method to each of the 21620 sets of data points. The I_c was a calculated constant, and was the same for all of the fits. The computer printed out λ_s, $V = \frac{\lambda_s c}{\lambda(H\alpha)}$, I_c, σ, and an error. The error was the sum of the squares of differences between I calculated and I measured.

The computer printed out along a line the values of one of the parameters, say σ, for each of the 20 frames at some point along the slit. To examine a data sheet one looks along a line to see the variation of the parameter as a function of time for a particular point.

To display the relation between sigma (half width) and velocity, the CIT IBM 7094 was used to plot a "three-dimensional" histogram. Sigma was plotted on the x-axis of the histogram in steps .01 $\mathring{A}$ from .375 $\mathring{A}$ to .655 $\mathring{A}$; velocity was plotted on the y axis

in steps of 0.1 km from 3.45 km/sec to-3.45 km/sec. (The sign convention used here denoted upward velocities with a minus sigma, and downward velocities with a plus sigma.) This division of the x and y axis defined an array of 1960 (28 x 70) bins. The histogram was formed by sorting the 21620 sigma-velocity pairs into the .01 Å by 0.1 km/sec bins. In each bin was printed out the number of pairs with sigma and velocity in the bin's range. Besides the histogram the averages and sum's of each row and column of the histogram was calculated. In the case of the columns, sums and averages were also calculated for both positive and negative velocities. For example, the sum of the row labeled, say, 3.1 km/sec was the total number of fitted gaussians that had a shift corresponding to a downward velocity of between 3.05 km/sec and 3.15 km/sec; the average of the row was the average sigma for elements with a downward velocity between 3.05 and 3.15 km/sec. A similar set of sums and averages for a velocity-intensity histogram was also calculated.

D. RESULTS

The three-dimensional histogram shows that on the average higher speed features have wider than average profiles, and that for features with speeds greater than 1.2 km/sec the average profile width is linear in the speed. Further, for features with speeds greater than 1.5 km/second the increase in profile width is sufficient to cause such features to appear as absorbing on both sides of the line on wing pictures taken at ± .7 Å from the Hα core.

A slight modification on the method for creating the three-

dimensional histograms yields time correlation histograms. These show that the correlation between velocity and width for upward moving features decays in about 120 seconds. This suggests that the 113 second velocity lifetime features discussed in Part II are the predominant form of upward velocity features.

Detailed arguments and the calculations that yielded the results mentioned above are contained in the sections that follow.

The three-dimensional histogram and the various sums and averages over its row and columns form a large body of statistical information on the spectral features. Many of these statistical results are tabulated and discussed in the following sections.

1. Velocity Distributions.

Using the data obtained with the three-dimensional histogram, a histogram of a number of features with a velocity v versus velocity was constructed. In the region between - 0.85 km/second and 1.65 km/second the graph is excellently fitted by a gaussian

$$N = 945 \exp\left(- 1/2((v - .384)/.805)^2\right).$$

Figure 11 shows the histogram and gaussian.

Since it seemed physically reasonable that small velocities should be symmetrically distributed about zero, .384 km/second was subtracted from each of the measured velocities and a new zero shifted histogram was constructed. A check of the difference between merely subtracting .384 km/second and recalculating each velocity on the basis of a shift in the original scan positions showed a less than 0.1 percent difference in the two methods.

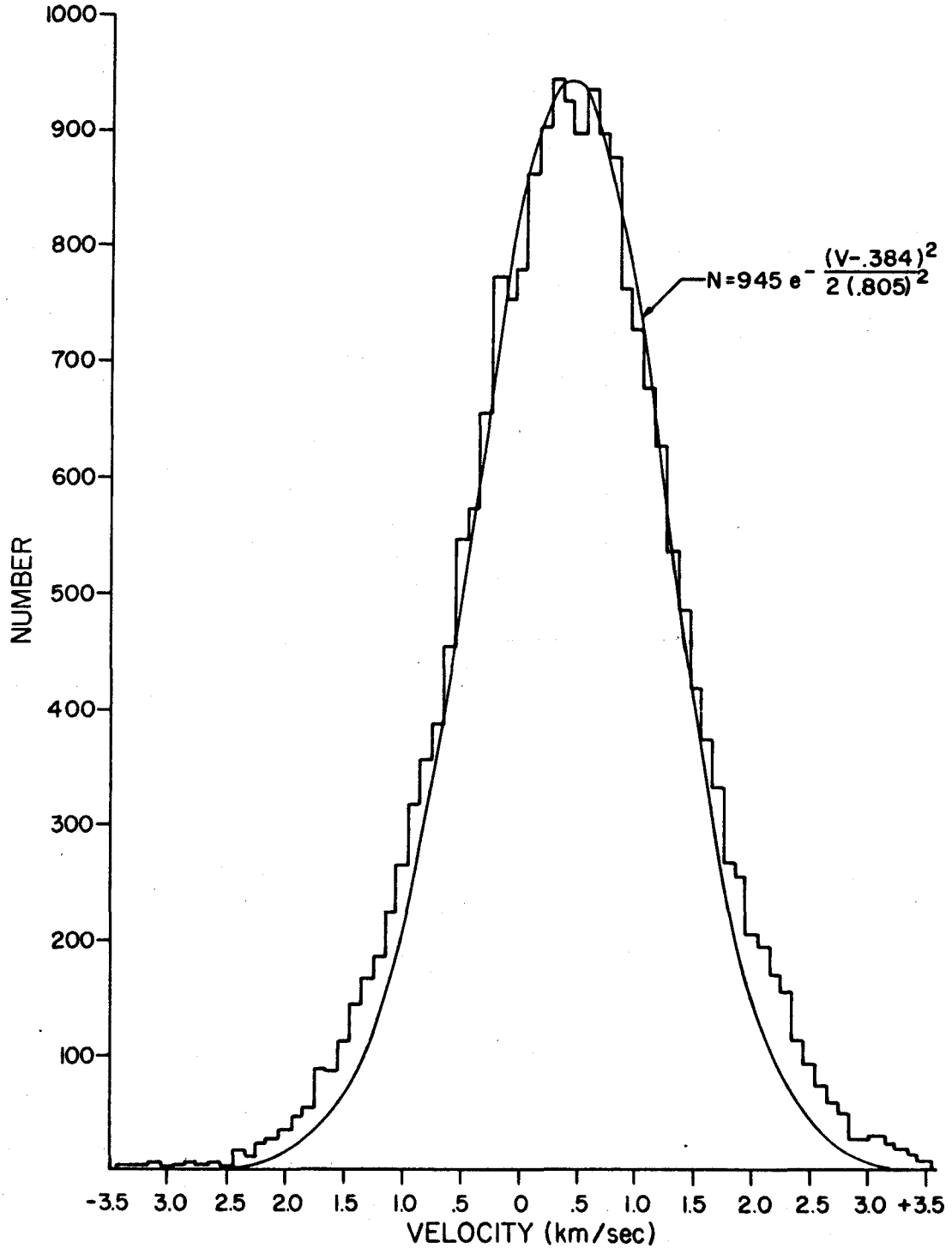
1000
900
800
700
600
500
400
300
200
100
NUMBER
N=945 e^- (V-.384)^2 / 2 (.805)^2
-3.5 3.0 2.5 2.0 1.5 1.0 .5 0 .5 1.0 1.5 2.0 2.5 3.0 +3.5
VELOCITY (km/sec)

Figure 11

The shift of the zero point of velocity affects only the sigma averages that depend on the sign of the velocity. None of the basic characteristics of the three-dimensional histogram is affected, and the original and shifted histograms agree when placed upon each other with the proper offset.

A gaussian $N = 945 \exp(-1/2(v/.805)^2)$ fits the number versus velocity histogram obtained from the zero shifted three-dimensional histogram. The total area under the gaussian and number-velocity plot agree to within 0.01 percent between ± 1.25 km/second. However, for speeds with magnitudes greater than 1.25 km/second the fitted gaussian drops below the histogram. The area under the gaussian from 1.25 km/second to infinity is equivalent to 1143 points. The area under the corresponding down section of the histogram is 1867 points - a 62 percent excess; the area under the corresponding up section of the histogram is 1776 points - a 54 percent excess.

2. Sigma Distribution.

Using the data of the zero shifted three-dimensional histogram, histograms of number versus sigma were constructed for up and down velocities. These are shown in Fig. 12. Note that the sigma-up distribution can be fitted by two straight lines, while the sigma-down distribution must be fitted by three straight lines.

The slopes of the fitted lines are summarized in Table 1.

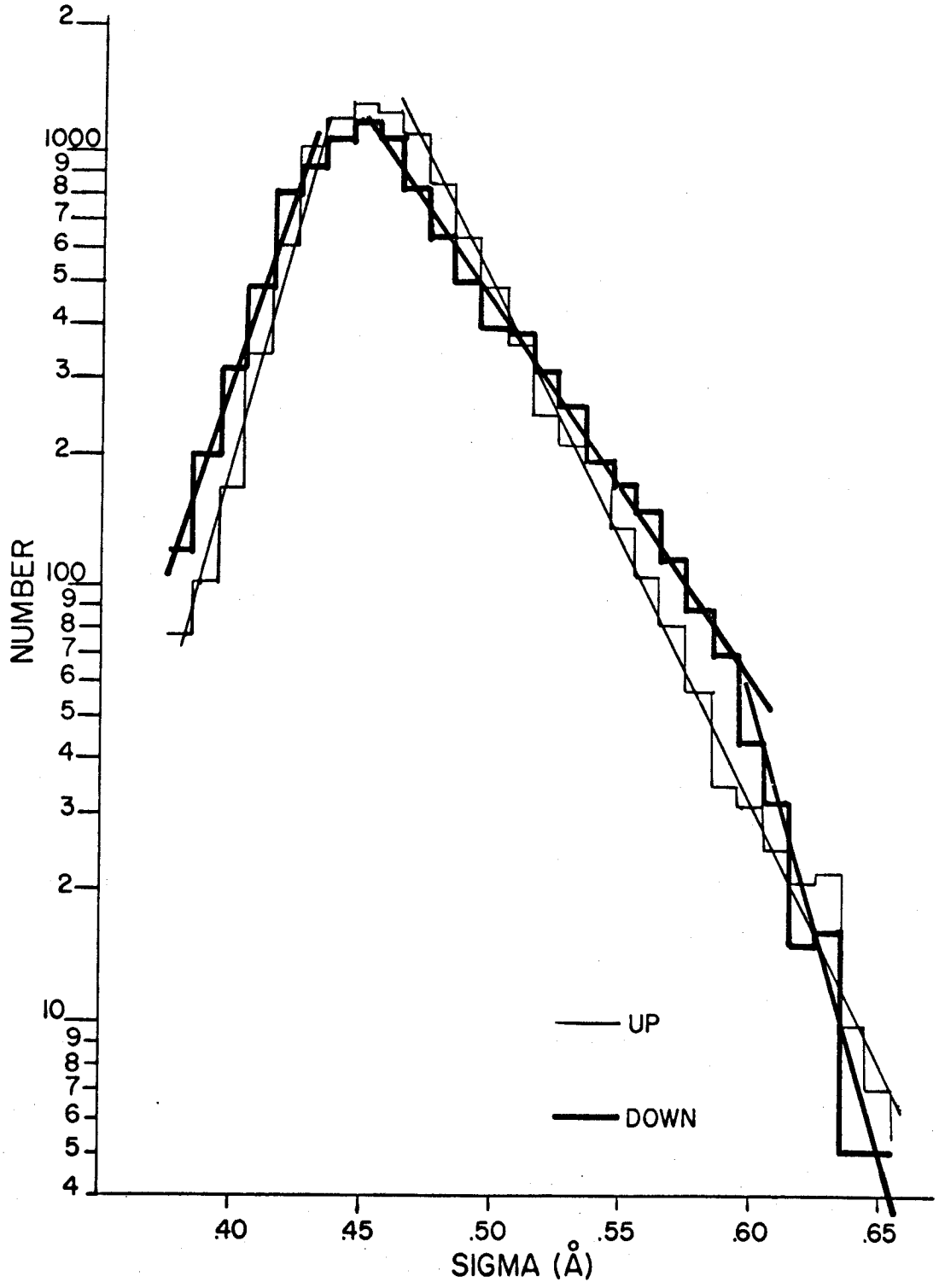
NUMBER
SIGMA (Å)
UP
DOWN
2
1000
9
8
7
6
5
4
3
2
100
9
8
7
6
5
4
3
2
10
9
8
7
6
5
4
.40
.45
.50
.55
.60
.65

Figure 12

Table 1

Range	Slope Total	Up	Down	
.38 - .45 Å	20	22	19	$C = C_0 10^{S\sigma}$
.47 - .57 Å	-10	-12	-8.5	
.59 - .65 Å	-15.5	-12	-18	

3. Three-Dimensional Histograms.

Unfortunately, it is impossible to reduce the three-dimensional histogram to a 6" by 9" thesis format and still have the numbers readable. However, a drawing of the histograms average sigma versus velocity, average velocity up versus sigma, average velocity down versus sigma, and modal sigma versus velocity curves on the histogram format rather succinctly represent the three-dimensional histogram. Figure 13 is such a "schematic" histogram. The modal sigma versus velocity curves are not shown on Fig. 13 unless they differ significantly from the average sigma versus velocity curve. To further aid in the visualization of the three-dimensional histogram a contour map of the histogram has been drawn. This is shown in Fig. 14.

The average sigma versus velocity curve on Fig. 13 demonstrates that on the average, the higher speed features have wider profiles. For speeds greater than 1.2 km/second the average sigma at velocity V, σ_V, is linear in speed.

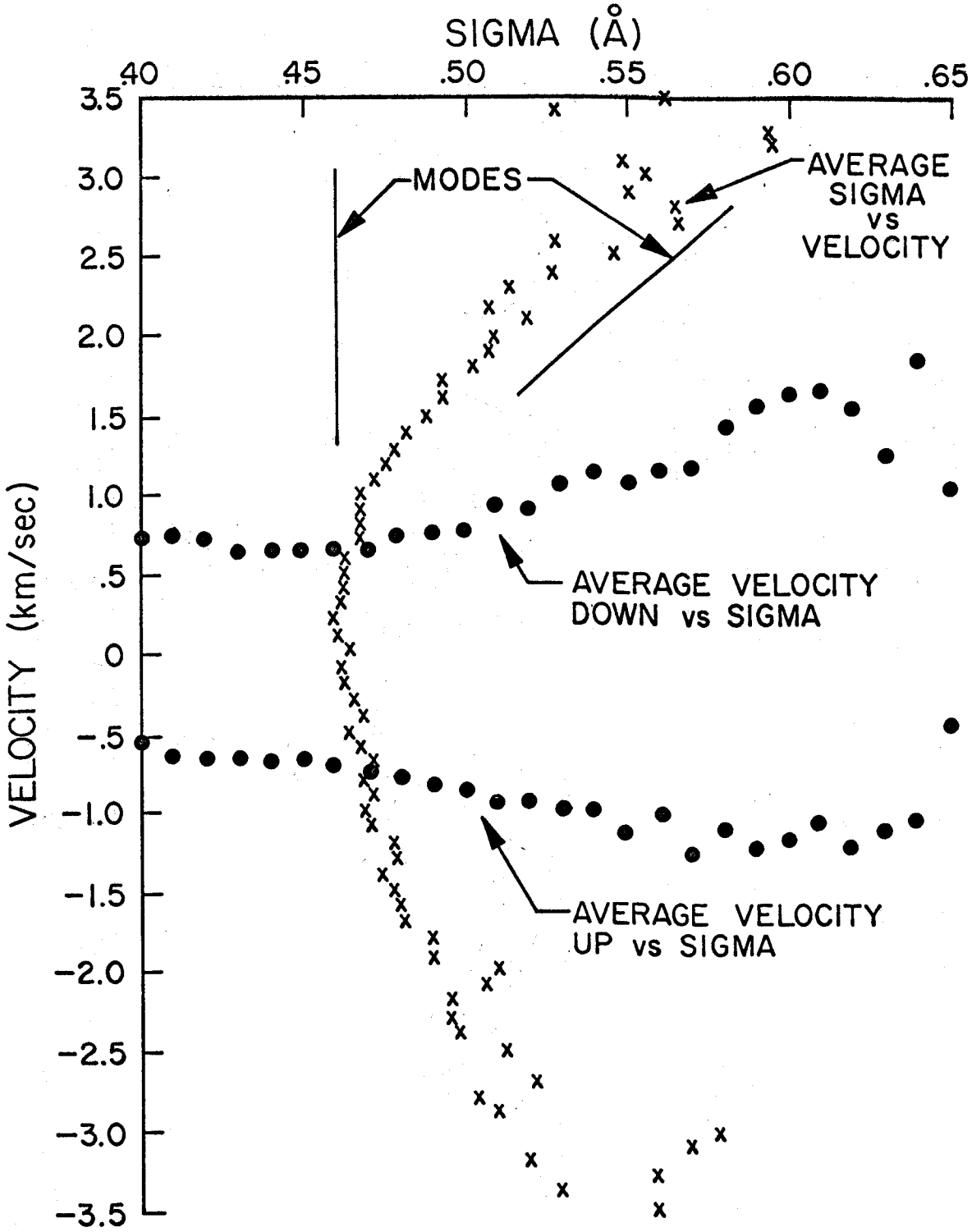
SIGMA (Å)
.40
.45
.50
.55
.60
.65
3.5
3.0
2.5
2.0
1.5
1.0
.5
0
-.5
-1.0
-1.5
-2.0
-2.5
-3.0
-3.5
VELOCITY (km/sec)
MODES
AVERAGE SIGMA vs VELOCITY
AVERAGE VELOCITY DOWN vs SIGMA
AVERAGE VELOCITY UP vs SIGMA

Figure 13

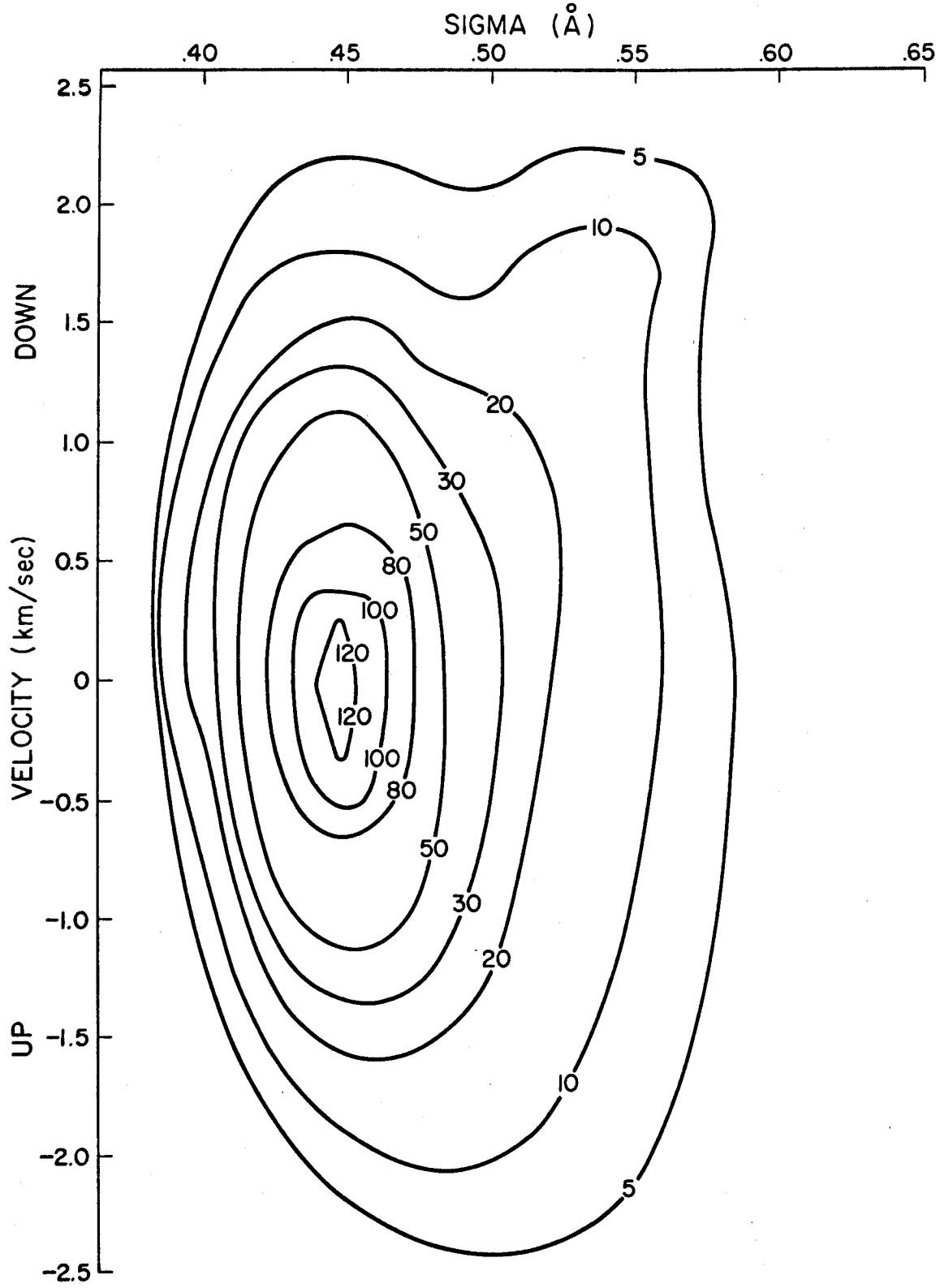
SIGMA (Å)
.40
.45
.50
.55
.60
.65
2.5
2.0
1.5
1.0
0.5
0
-0.5
-1.0
-1.5
-2.0
-2.5
DOWN
UP
VELOCITY (km/sec)
5
10
20
30
50
80
100
120
120
100
80
50
30
20
10
5

Figure 14

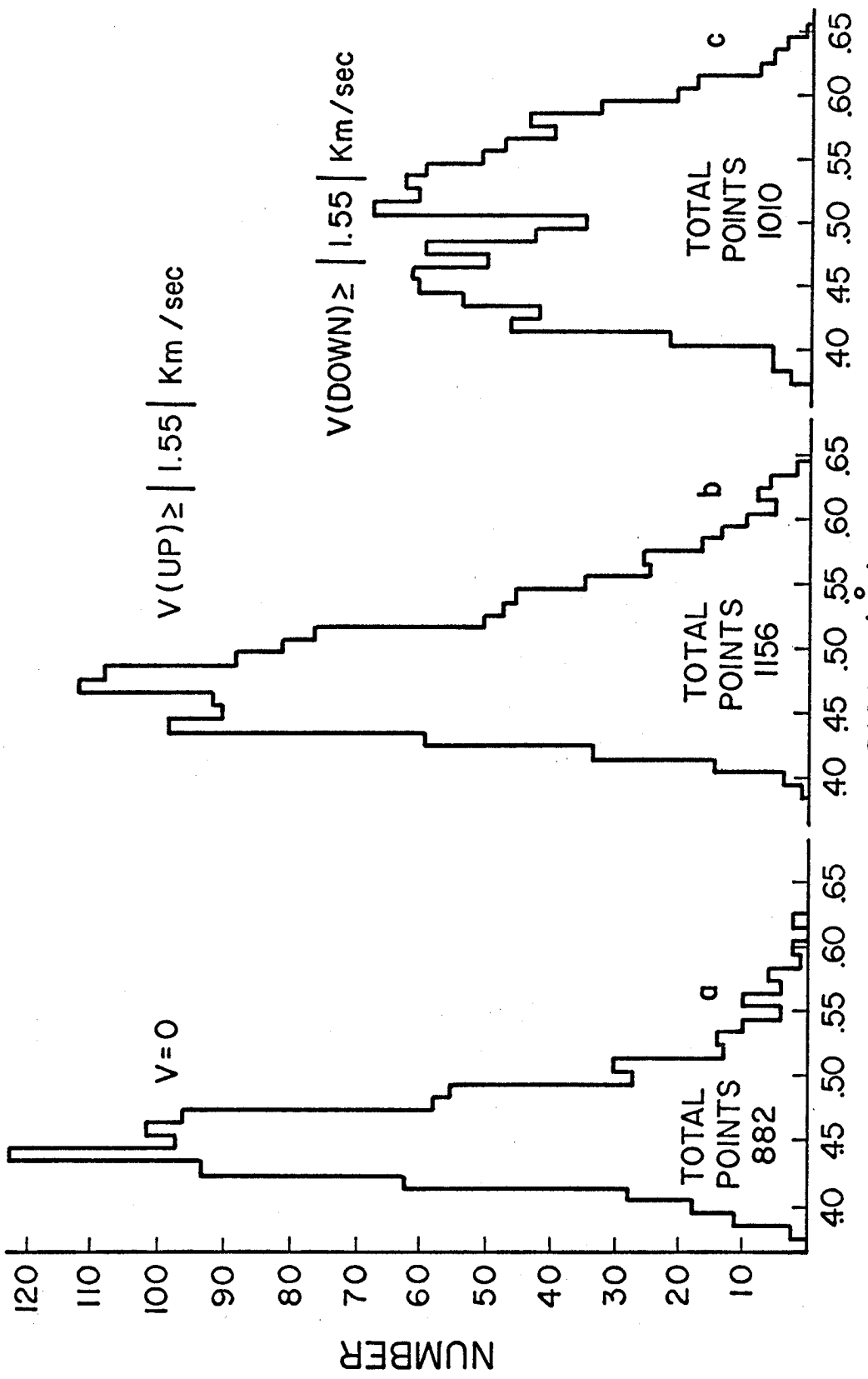
NUMBER
120
110
100
90
80
70
60
50
40
30
20
10
V=0
TOTAL POINTS 882
a
V(UP)≥ | 1.55 | Km/sec
TOTAL POINTS 1156
b
V(DOWN)≥ | 1.55 | Km/sec
TOTAL POINTS 1010
c
40 45 .50 .55 .60 .65
SIGMA (Å)

Figure 15

$$\sigma_v \text{ (down)} = .405 + .047 \, |V|$$

$$\sigma_v \text{(up)} \quad = .41 \quad + .040 \, |V| .$$

The modal sigma curve and the average sigma curve essentially coincide for upward velocities. This indicates that at least on the average the fast moving upward features are positively correlated with wide profiles. However, for downward velocities greater than 1.55 km/second the distributions of sigma are bimodal. Figure 15a shows the distribution of sigma for zero velocity; Figure 15b shows the sum of the sigma distributions for velocities greater than 1.55 km/second; and Fig. 15c the sum of the sigma distributions for velocities less than - 1.55 km/second. The bimodal nature of the sigma distributions for downward velocities is discussed further in the section on time correlation histograms.

4. Time Correlation Histograms.

The three-dimensional histogram was formed by sorting a set of sigma-velocity pairs for individual features on a number of single frames into an array of sigma-velocity bins. Since the sigma and velocity are known for corresponding points on all the frames, it was possible to form pairs for which the sigma member came from one frame and the velocity member came from a corresponding point on another frame taken either earlier or later in time. Because the number of frames was finite each shift of thirty seconds (one frame) resulted in the loss of 1081 sigma-velocity pairs that could be sorted to form a "time correlation" histogram. Time shifts of greater than 240 second

resulted in the loss of fifty percent or more of the possible pairs. Histograms with shifts of ± 30 to ± 240 seconds, in thirty second steps, were studied.

Figure 16 is an overlay of four schematic time correlation histograms and the three-dimensional histogram. The modal curves have not been shown on Fig. 16 to eliminate some confusion.

The reason for constructing the time correlation histograms was to learn about phase relations between velocity and profile width and to obtain estimates of lifetimes of the higher velocity features. For example, the bimodal distribution of sigma for downward velocities greater than 1.5 km/second could have been due to some downward velocity regions attaining higher than average velocity either before or after the profiles in those regions broadened. If the bimodal distributions were due to a phase effect, symmetric time shifts in opposite directions should cause two peaks of the sigma distribution calculated for the shifted histograms to change in relative height. Plots similar to Figs. 15b and 15c were constructed for shifts of ± 30, ± 60, ± 180, ± 240 seconds. None of the summed sigma distributions for upward velocities showed any bimodal structure, while all of the summed downward velocity sigma distributions were bimodal . Further, the relative heights of the two peaks of the down distributions remained the same for both positive and negative shifts in time. Hence, one can infer that there are at least two prominent types of downflow represented on the spectra, one characterized by higher than average velocity and higher than average sigma, and the other by higher than average velocity but average sigma. Note also that

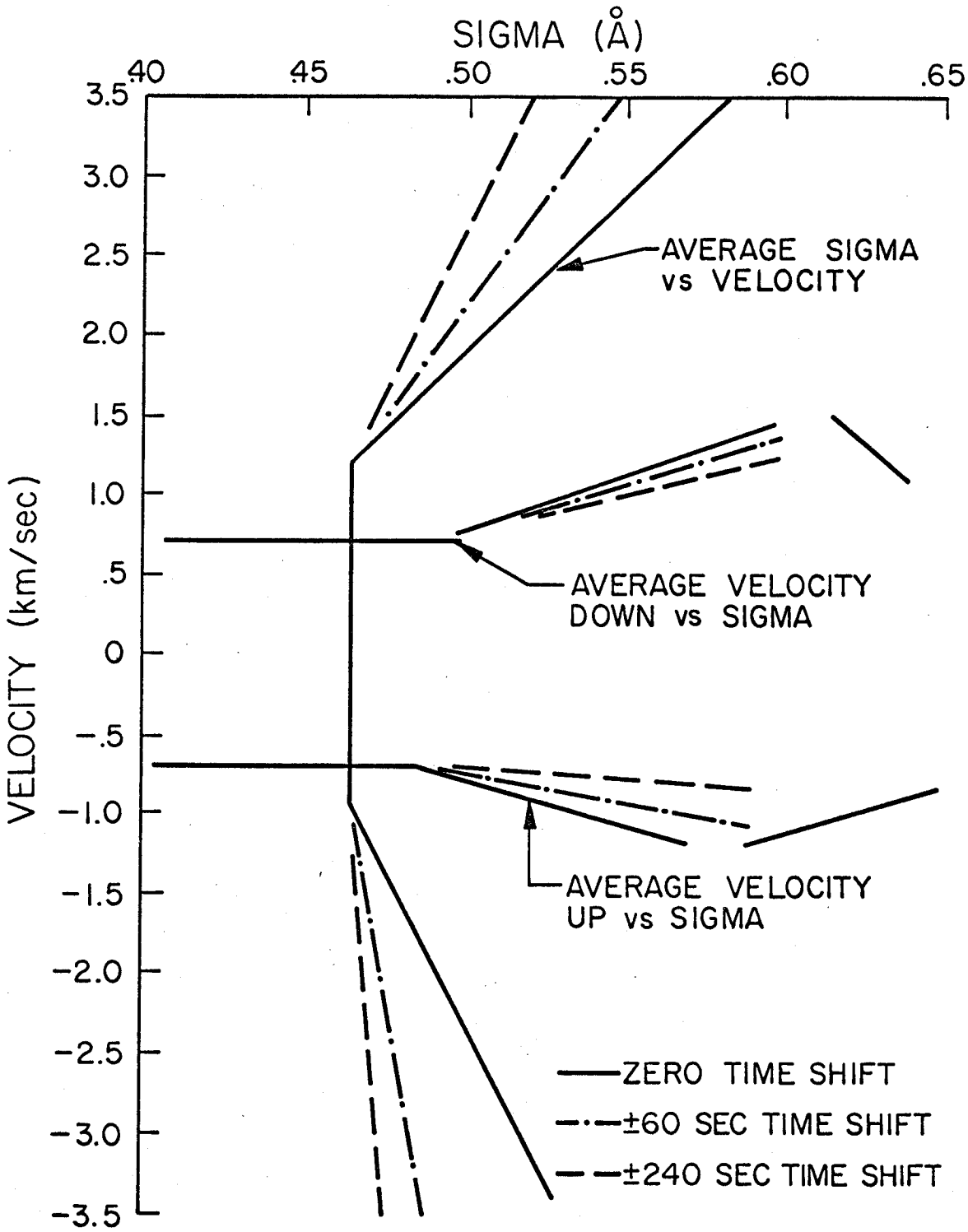
SIGMA (Å)
.40
.45
.50
.55
.60
.65
3.5
3.0
2.5
2.0
1.5
1.0
.5
0
-.5
-1.0
-1.5
-2.0
-2.5
-3.0
-3.5
VELOCITY (km/sec)
AVERAGE SIGMA vs VELOCITY
AVERAGE VELOCITY DOWN vs SIGMA
AVERAGE VELOCITY UP vs SIGMA
ZERO TIME SHIFT
±60 SEC TIME SHIFT
±240 SEC TIME SHIFT

Figure 16

Figure 12 shows that the total sigma distribution for downflow elements is somewhat different than the sigma distribution for upflow elements.

The average sigma versus velocity curves for time correlation histograms with symmetric time shifts were essentially the same. (On Fig. 16 they are shown as the same.) Since it has been shown that the bimodal distributions are not a phase effect, this implies that broadening and increased velocity tend to occur within thirty seconds of each other.

Some information on the lifetime of features can be obtained from the time correlation histograms. Since, when the sigma and velocity members of the pairs are taken from frames separated by times longer than the feature's lifetime, there should be no correlation between sigma and velocity. That half of the average sigma versus velocity curve corresponding to upward velocities becomes nearly parallel to the V-axis in ± 60 seconds. Also there are only five points on the original histogram ($\Delta t = 0$) on the low sigma side of a line connecting (.38Å, - 1.4 km/sec) and (.50Å, - 3.5 km/sec). (The region from - 1.4 to - 3.5 km/second contains 1469 points.) The rapid loss of correlation strongly suggests that there are not many upflow features that have a velocity lifetime much longer than 120 seconds. This is consistent with the lifetime measurement of Part III for upflow features.

With increasing time shifts the down velocity section of the average sigma versus velocity curve rotates much more slowly toward the V-axis than the up velocity section. At ± 240 seconds the down velocity

half still deviates considerably from the parallel. This suggests that the high sigma high speed downflow regions have lifetimes of at least 480 second and/or that sigma remains high in these downflow regions.

5. Averages along the Slit.

As was pointed out in the data reduction section, corresponding points on each frame have the same identification number. Therefore, it was possible to form the average over all twenty frames of, say, the velocity for corresponding points on the slit. In Fig. 17a and 17b are shown the average velocity and average sigma for all frames as a function of distance along the slit. Note that, in general, in regions where the average speed is high the average sigma is also high.

The spacing of the peaks of the average sigma plot is roughly 30×10^3 km. This suggests that the high sigma regions occur on the large cell boundaries.

6. Appearance of Shifted Profiles.

Using the data of the three-dimensional histogram it is possible to calculate whether the increase in profile width of the average feature of velocity V is sufficient to cause the feature to appear in absorption on both sides of the line at .7 Å from the core. In Fig. 18 are shown the plots of the percent increase in absorption from the mean of the average feature of velocity V through wavelength bands .1 Å wide centered at plus (% red) and minus (% violet) 0.7 Å from the core of Hα. It is clear from Fig. 18 that for speeds greater than 1.5 km/second the average feature appears as absorbing on both sides

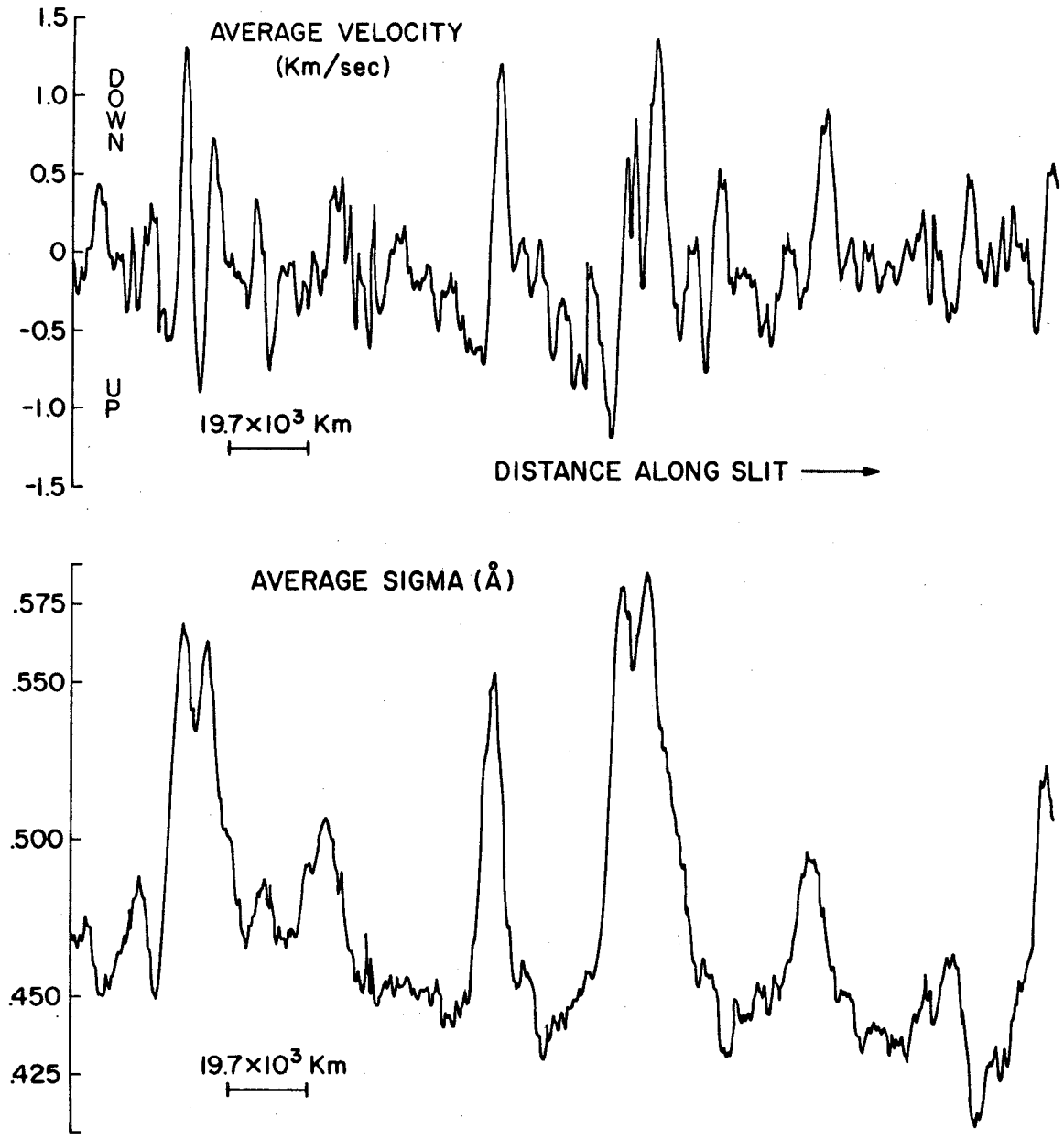
AVERAGE VELOCITY
(Km/sec)
1.5
1.0
0.5
0
-0.5
-1.0
-1.5
DOWN
UP
19.7×10³ Km
DISTANCE ALONG SLIT
AVERAGE SIGMA (Å)
.575
.550
.500
.450
.425
19.7×10³ Km

Figure 17

of the line.

The reason the calculation was carried out for bands centered at plus and minus 0.7 Å is that these wavelength bands are the ones generally used for the Hα wing movies. Thus, the measurements of the spectra yielded the same results that were obtained in Part II by comparison of Doppler and violet or red wing frames - high speed features are often visible in absorption on both wings of the line.

An extension of the calculations used in making Fig. 18 demonstrated that under some fairly broad assumptions the signal on the doppler frame is dependent only on the velocity and a correction function $f(\Delta\lambda_s)$, where $\Delta\lambda_s$ is the offset of the wing movies, and is independent of profile width.

The details of the above mentioned calculations are outlined below.

The least squares procedure fitted a gaussian to a set of four points. These points represented a set of relative intensities. To obtain an idea of the absolute intensity scale, the mean gaussian $G_m(\Delta\lambda)$ for the entire set of measurments was formed.

$$G_m(\Delta\lambda) = 1075. - 1003.1 \exp(-\frac{1}{2}(\Delta\lambda)^2/(.468)^2,$$

where 1003.1 was the mean central intensity and .468 the mean sigma. Properly normalized $G_m(\Delta\lambda)$ should agree with a mean Hα profile at $\mu = 1$ in the region the Hα profile is gaussian. Richard White's thesis[13] contained a mean Hα profile at $\mu = 1$. White's profile will be denoted as $H_m(\Delta\lambda)$.

When $G_m(\Delta\lambda)$ is normalized by

$$N = H_m(.3)/G_m(.3),$$

$NG_m(\Delta\lambda) \approx H_m(\Delta\lambda)$ to within 1.0 percent for $.3\text{Å} \leq \Delta\lambda \leq .62$ Å. It is convenient to define a correction function $f(\Delta\lambda)$ such that

$$f(\Delta\lambda) = H_m(\Delta\lambda)/G_m(\Delta\lambda).$$

In the range $.3\text{Å} \leq \Delta\lambda \leq .62\text{Å}$, $f(\Delta\lambda) \approx N$.

The gaussian profiles of velocity shifted features are of the form

$$G_v(\Delta\lambda) = 1075. - I_v \exp\left(- \frac{1}{2} (\Delta\lambda - v\lambda_0/c)^2/\sigma_v^2\right),$$

where I_v is the average central intensity for features with velocity V, σ_v is the average width of features of velocity V, λ_0 is the wavelength of Hα, and c is the velocity of light. If one assumes that the correction function for $G_v(\Delta\lambda)$ is approximately $f(\Delta\lambda)$, then the absorption of average features of velocity V through windows .1 Å wide centered at $\Delta\lambda = .7$ Å and $\Delta\lambda = -.7$ Å are

$$A_{red}(v) = \int_{.65}^{.75} f(\Delta\lambda - \frac{v\lambda_0}{c}) G_v(\Delta\lambda)\, d\Delta\lambda, \quad \text{and}$$

$$A_{violet}(v) = \int_{-.75}^{-.65} f(\Delta\lambda - \frac{v\lambda_0}{c}) G_v(\Delta\lambda)\, d\Delta\lambda.$$

The absorption of the mean profile through the same window is

$$A_{mean} = \int_{.65}^{.75} f(\Delta\lambda) G_m d\Delta\lambda.$$

Shown in Fig. 18 are

$$\%(v)_{red} = (A(v)_{red} - A_{mean})/(A_{mean}) \times 100$$

$$\%(v)_{violet} = (A(v)_{violet} - A_{mean})/(A_{mean}) \times 100.$$

The large scatter in Fig. 18 is due to scatter in σ_v.

The intensity of the average feature of velocity V seen on the Doppler frames is proportional to

$$D(v) = A_{red}(v) - A_{violet}(v).$$

If one denotes $v\lambda_0/c$ by Δ_v, and approximates integrals of the form

$$\int_{\alpha}^{\beta} f(\Delta\lambda - \Delta_v) G_v(\Delta\lambda)\, d\Delta\lambda$$

by

$$\left(\frac{\alpha+\beta}{2}\right) f\left(\frac{\alpha+\beta}{2} - \Delta_v\right) G_v\left(\frac{\alpha+\beta}{2}\right)$$

then it can be easily shown that

$$D(v) = .1\Big\{1075(f(.7 - \Delta_v) - f(-.7 - \Delta_v)) + I_v(f(.7 - \Delta_v) - f(-.7 - \Delta_v))\exp\left(\frac{.7^2 + \Delta_v^2}{2\sigma_v^2}\right)2\cosh(.7\Delta_v) + I_v(f(.7 - \Delta_v) - f(-.7 - \Delta_v))\exp\left(\frac{.7^2 + \Delta_v^2}{2\sigma_v^2}\right)2\sinh(.7\Delta_v)\Big\}.$$

Since $f(\Delta\lambda)$ is a slowly varying symmetric function, $[f(.70 - \Delta_v) - f(-.70 - \Delta_v)]$ is nearly zero, and $[f(.70 - \Delta_v) + f(-.70 - \Delta_v)]$ is nearly $2f(.7)$. Therefore,

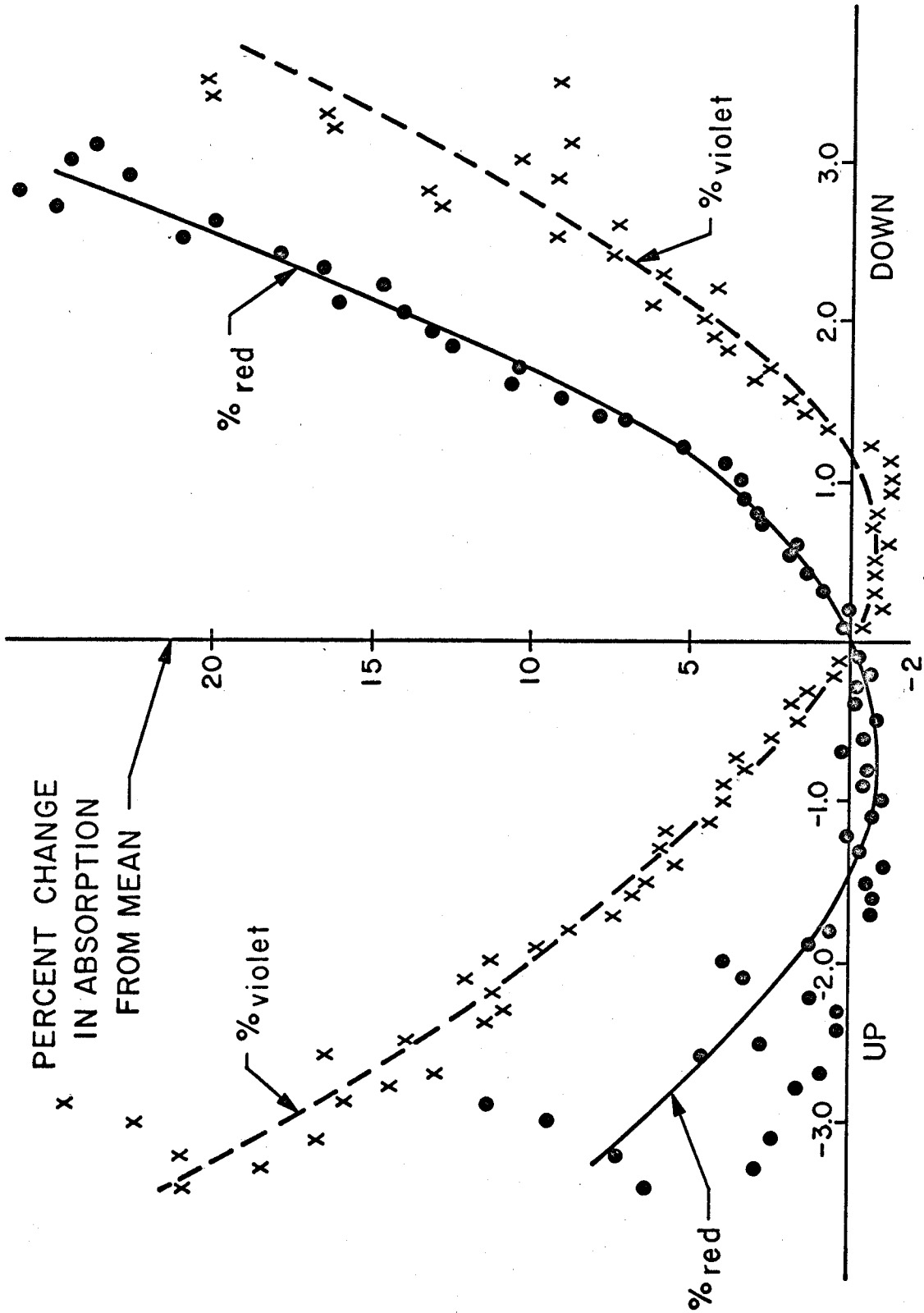
PERCENT CHANGE IN ABSORPTION FROM MEAN
20
15
10
5
-2
% violet
% red
% violet
% red
-1.0
-2.0
-3.0
1.0
2.0
3.0
UP
DOWN
VELOCITY (km/second)

Figure 18

$$D(v) \approx .1 \times I_v f(.7)\ 4 \sinh\left(\frac{.7\Delta_v}{\sigma^2}\right) \exp\left(-\frac{(.7^2 + \Delta_v^2)}{2\sigma^2}\right) \tag{10}$$

$$\approx C_0 C(\Delta_v, \sigma, .7)\ \Delta_v,$$

where C_0 is a constant and

$$C(\Delta_v, \sigma, .7) = \frac{1}{\sigma^2} \exp\left(-\frac{.7^2 + \Delta_v^2}{2\sigma^2}\right). \tag{11}$$

The only term in expression (10) dependent on σ is $C(\Delta_v, \sigma, .7)$. However, it can be demonstrated that for a window at .7 Å and velocities less than 20 km/sec, $C(\Delta_v, \sigma, .7)$ is independent of sigma for sigmas in the range $.38 \leq \sigma \leq .77$ Å.

Hence, one finds that the signal on the Doppler frame is dependent only on velocity, central intensity, and the correction function at the window wavelength to the extent that all profiles scale by a correction function. It may well be, of course, that $f(\Delta\lambda)$ is not the same for all features observed, and further $f(\Delta\lambda)$ may vary systematically with velocity and/or profile width. However, the properties of correction functions can be investigated by a program similar to that described in the data reduction section of this chapter, but using more than four scans and fitting by some other curve than a gaussian.

E. ACCURACY OF THE FITTING PROCEDURE

The least squares procedure used a set of four points to fit a gaussian, which is determined by three points. An error, the sum of the square of the difference between I measured and I calculated, was

calculated to gain an idea of the quality of the fit of the gaussians. The average error of the entire set of measurements was 5.6 ($\sum I_m^2 \approx 1.3 \times 10^5$), and no error exceeded twenty one. The size of the error was such that a sigma velocity pair sorted in to the three-dimensional histogram could go only into its "correct bin" or the correct bin's nearest neighbor. That is, a pair can vary only one bin from its correct position.

For $\Delta\lambda$'s greater than .6 Å individual profiles do differ from the gaussian shape, and the profiles may even be skewed. To investigate whether the estimate of the shift of the line center made by the gaussian differs from measurements of the shift made at greater than .6 Å, a series of one hundred tracings were made on the SPO spectra.

To measure the position of the line center a scale was marked so that scale divisions corresponded to .02 Å on the tracings. The dispersion on the traces was .2 Å/inch. The center of the line at any width could be found by sliding the scale parallel to the x-axis of the trace (dispersion direction) until the zero and the desired width both lay on the trace, and then simply marking the position of half the width. The centers of the profiles were found for widths of .8 Å (± .4 Å from the center), 1.2 Å, 1.6 Å, and 2.0 Å. In no case did the center measurements for a single profile differ by as much as .04 Å, which corresponds to 1.8 km/second, and the tracings went through some of the most shifted features seen on any frame. More importantly, for the sake of the three-dimensional histograms, when there was a shift of the center, the shifts always increased in magnitude with the widths. Hence, the velocities yielded by the gaussians were at worst systematically lower in magni-

tude than would have been measured at larger offsets.

Seeing effects tend to smear out all profiles, thus mixing to some extent each profile with its neighbors. Since high speed and broad features are relatively rare, seeing has a tendency to make the offsets and widths recorded somewhat smaller than they actually are.

The above arguments suggest that the numbers for the velocities and profile widths should be considered as lower limits on the apparent solar velocities and profile widths. However, the basic structure of the three-dimensional histograms, with which this part has been mainly concerned, should be relatively unaffected by either seeing or the fitting procedure.

PART VI SUMMARY - SUGGESTIONS - CONCLUSION

A. DISCUSSION AND SUMMARY

The properties of upflow and downflow features and the collective behavior of upflow and downflow features are summarized and discussed below.

1. Upflow

In Part III the average lifetime of a random sample of upflow areas was measured and found to be two or three minutes. In Part IV the decay of the correlation between speed and profile width time-shifted histograms implied that on the average upflow areas have a lifetime of about 120 seconds. Also in Part III, prominent upflow events were measured and found to have a lifetime of 113. seconds. These essentially independent measurements strongly suggest a single predominant upflow mechanism. This is not to say that there are not other upflow mechanisms, or that one cannot find occasional upflow features that last for more than a few minutes, but only that from 60 to 80 percent of the upflow features visible in the Hα wings further than .4 Å from the core are characterized by a lifetime of a few minutes.

Comparison of Doppler and wing movies showed (Part II) that upflow tended to occur in the fine elongated petals of the rosette structure seen in the wings. These violet wing absorbing regions were found to have lifetimes of about ten minutes (Part III).

During the comparison of Doppler and wing movies it was noted that upflow areas often appeared strongly in absorption in both wings. This broadening of the profiles of higher speed regions suggested by observation of the movies was confirmed by the data of the three-

dimensional histogram (Part V). The three-dimensional histogram demonstrated a positive correlation between profile width and higher speed regions. In Part V it was also shown that the increase in profile width was sufficient to cause an average upgoing feature to appear in absorption in both wings.

Individual areas in which upflow had occurred have been followed in time for somewhat longer than fifteen minutes (Part III). The downflow that occurs in these regions does not seem to change after a few minutes. Previously Beckers had reported a tendency for downflow to occur in some upflow regions about twelve minutes after the upflow had occurred. The results of Part III place an upper limit of 10 to 15 percent for the percentage of upflow features that are followed by downflow within five to fifteen minutes.

2. Downflow

The studies of downflow areas have not yielded a very clear cut picture. This is probably caused by the fact that downflow is intrinsically more complex than upflow. It may well be that there is a number of important downflow patterns, some related to the two minute lifetime upflow events, and others associated with the large cell convection.

The lifetime of random downflow regions measured in Part III was six to nine minutes. This measurement was made somewhat ambiguous by the presence of downflow features that persisted for times longer than fifteen minutes. This long-lived component represented approximately 20 percent of the downflow areas. From the appearance on a Doppler frame there was no way to distinguish a downflow feature that dis-

appeared in thirty seconds from others that lasted the entire length of a movie of forty minutes.

By comparing Doppler and wing movies (Part II) it was observed that downflow tended to occur in the central regions of the rosette structure. The lifetime of the red wing absorbing features was about ten minutes (Part III). However, about 20 percent of the red wing absorbing features were observed to last 15 minutes or more and a few of them were followed the length of an entire movie.

The time-correlation (Part V) histograms showed that the correlation between speed and profile width took longer than six minutes to decay.

The comparison of Doppler and wing movies showed that many downflow areas appeared in absorption on both wings of Hα, just as had been noted with upflow areas. However, the data of the three-dimensional histogram showed that there were at least two types of higher speed downflow regions, one characterised by wider than average profiles and the other by average width profiles.

Perhaps if the series of spectra used for the analysis in Part V had been taken in conjunction with spectroheliograms upon which the location of the spectrum was marked, it would have been possible to identify and classify different types of downflow features, but at present I can only suggest that a serious attempt be made to obtain such pairs of spectra and spectroheliograms. (In another section of this part a suggestion is made for how this might be accomplished.)

3. Collective Behavior of the Up and Downflow

As noted in Part II one of the most noticeable characteristics of

the Doppler movies was the fluctuation of downflow in regions corresponding to the network seen in the wings. The total downflow area in 30×10^3 km square regions was found to fluctuate as a function of time with a period of 550 ± 25 seconds (Part IV). The total upflow as a function of time for the same set of regions was also found to fluctuate with the same period.

Cross-correlation of the plots of upflow and downflow versus time indicated that the relation between upflow and downflow varied randomly from region to region.

At present it is not known over how large an area the fluctuation in total upflow or downflow can be observed.

B. OTHER OBSERVATIONS

The dual camera has been used for observations in lines other than Hα. Movies have been taken in Hβ (λ4860), Na (λ5896), CaI (λ6103), CaII(K) (λ3933), and CaII (λ8542). The CaI (λ6103) movies have been reduced to form Zeeman movies. Only a few observations were made in CaI (λ6103). CaII (λ3933), and Na (λ5896) represent only exposure and film tests. A number of observations were made in Hβ but, unfortunately, the quality of the seeing in the Hβ movies left much to be desired. During the 1965 observing season a series of observations was made in CaII (λ8542). These have not yet been cancelled. Also during 1965, runs were made in Hα using Kodak 2475 film. These tests indicated that Hα movies at .7 Å can be taken at frame rates of 5 per minute at the sacrifice of some contrast.

Howard and Harvey[11] have reported fluctuating transverse motions

in the Hα chromosphere which are more visible on the violet than the red wing, and have a period of about 30 seconds. Similar observations have been made by Beckers [14] and Zirin[15]. My Hα wing movies also show the same effect. Further similar motions are also visible in Hβ and CaII (λ8542).

C. SUGGESTIONS FOR FUTURE OBSERVATIONS

After several years of operation of the dual camera and spectroheliograph, I have a few suggestions for the improvement of the methods for obtaining and reducing data. These are listed below.

1. The statistical study of spectra described in Part V would have been much more valuable if one had had a simultaneous series of photographs of Hα upon which the location of the spectrum was marked. It is my opinion that a serious attempt should be made to obtain such a series of spectra and spectroheliograms. At Mount Wilson this could be done by coordinated experiments at the 60 foot and 150 foot tower telescopes, the 60 foot tower taking spectroheliograms and the 150 foot tower taking high dispersion spectra. Another method of obtaining the data would be to modify the shutter on the beam splitter and the exit slit of the SHG, so that the dual camera could take both the spectrum and the spectroheliograms.

The modifications required for the beam splitter would be merely to install separate shutters for the two output beams. The exit slit modification would be more complex. It would require either a new exit assembly that covered only one of the images, or a modification of the present exit slit assembly so that one half of the slit could be

removed.

With the above modifications the dual camera and SHG could be operated as follows. A traverse would be started, and the shutter corresponding to the partial exit slit (image shutter) would remain closed. This action would cause a normal spectroheliogram to be formed on the film in one of the camera's transport units. Near the middle of the traverse the SHG would be stopped, the image shutter closed, and the spectrum shutter opened momentarily. Then the SHG would be restarted on its traverse, and the image shutter reopened. Since there would be no exit slit for the beam controlled by the spectrum shutter, a spectrum would be exposed on the film in the other transport unit. Also a dark line would be made at the location of the spectrum on the spectroheliogram.

With the modifications suggested the dual camera and SHG could take simultaneous movies in any line desired.

2. It was mentioned in Part II that it was possible to make movies sensitive to the presence of horizontal motions. Such lateral displacement movies would be made by canceling a movie with a contact of itself. But instead of subtracting frame i from frame i of the contact, frame i would be subtracted from frame i + s of the contact.

Lateral displacement movies will require an improvement in the telescope guiding. Further since it would be desirable to study several values of s for each given movie, it will also be necessary to construct an automatic cancellation machine before lateral displacement movies become practical.

3. The autocorrelations studies described in Part IV involved a large amount of labor in making maps of portions of the projection screen, measuring areas on the maps, and then punching cards so that the computer could handle the data. Unfortunately, the processing carried out in Part IV is necessary to reduce the tremendous amount of data on movie frames to a form that is convenient for analysis

Since the regions of interest on the film are approximately .5 mm square and each frame is 50 mm by 20 mm, each movie frame carried approximately 4×10^5 film density information locations. Normally the range of film density spans two decades. This means that even if a digitizing microphotometer were available for the recording of the data on the movies, each three movie frames would require a roll of low density tape.

The necessary preprocessing operations could be considerably simplified by means of a projection screen upon which a number of photosensitive cells would be placed. The cells could be placed at locations of interest, and their output could be fed directly to a digitizer, thus eliminating tedious measurements and card punching.

Sufficiently sensitive inexpensive small phototransistors are now available. These have adequate output to drive a digital voltmeter. The construction of a projection screen with 10 to 20 of these transistors would allow for much more rapid study of Zeeman and Doppler movies.

D. CONCLUSIONS

This thesis has demonstrated that Doppler movies are possible, and that they represent a useful research tool. The study of the Doppler

movies has led to the discovery of collective behavior of both upflow and downflow on a scale an order of magnitude larger than individual features themselves. Further a good deal of information has been obtained about the characteristics of the small scale upflow and downflow features.

In the recent literature one finds a good deal of discussion of spicules as observed on the disk. In this thesis I have not attempted to identify the various upflow and downflow patterns observed as those corresponding to spicules. I do not think it would serve any useful purpose to add confusion to the field by naming certain flow patterns as corresponding to spicules of type A, B, C etc. Rather I would prefer to let my observations stand as an incentive for future study.

APPENDIX I DESIGN CONSIDERATIONS

There were two basic requirements on the design of the camera system. One, that the beam splitter images had to be photographed in precise registration with respect to the film's sprocket holes, in order that the cancellation operation could be performed with respect to the sprocket holes. Two, that any modification of the equipment in the 60 foot tower for the camera system would not affect the other users of the telescope. Besides these two basic requirements it was always kept in mind that the camera would be operated at 5 a.m. and therefore should be as simple as possible to operate.

The design layout of the camera was determined by the optical properties of the telescope and spectroheliograph, and the width range of commercially available films.

The magnification of the telescope lenses, and the spectrograph are a function of wavelength. This causes the separation of corresponding points of the two beam splitter images to vary with wavelength. If both images are recorded on a single film, considerable complications are introduced in the cancellation procedure to separate the images. Separation by either physical slitting or optical image slicing is impractical because of cost. More importantly, however, the separated films would be only half as wide as the original film, and as the width of the film decreases the accuracy of the alignment during the cancellation operation must correspondingly increase. Because there are practical limitations on film width, it was decided that the camera would use two separate films, thus requiring two

separate transport units. To correct for the variation in the separation of the images, it was decided to make one of the transport units movable with respect to the other.

As mentioned above the larger the film used for the original movie, the easier the cancellation operation will be. Therefore, as large a film size as possible was desired. Eastman Kodak will coat any emulsion on any film base, and slit and perforate to order. Unfortunately, the minimum order for a special film involves the purchase of between five to ten thousand dollars worth of that single film. Therefore, it was decided to only consider the use of films available from stock.

The widest perforated film available in a range of emulsions suitable for the spectral ranges the camera system could be expected to be used in was 70 mm. The choice of 70 mm film did involve some compromise as the best emulsion for a given task is not always available in 70 mm. In fact, the Linagraph Shellburst used almost exclusively for the movies discussed in this thesis was not the film of choice; Spectroscopic Emulsion II-F would have been superior.

However, the problem of a limited choice range of emulsions is decreasing and will continue to decrease as the trend of government users to 70 mm camera equipment increases. Also at present there exists a strong possibility that special "non stock" emulsions can be obtained by calling Eastman Kodak Special Sensitization Divison, Rochester, New York, and requesting information about the location of users of the particular non stock emulsion. Because of the minimum order requirements the user will often be willing to

part with a few rolls of film. Further, the Special Sensitization Division often saves a limited number of non stock emulsion films.

It cannot be emphasized too strongly that one must call the Special Sensitization Division in Rochester, New York.

Since 70 mm film is almost as wide as the beam splitter image, it was decided not to use relay optics, but to place the film plane of the camera as close as possible to the exit slit of the spectroheliograph. The elimination of relay optics removes the possibility of image degradation by the extra optics. Also with the film plane immediately above the exit slit, vibrations caused by the transport units' motors are more easily damped than with a relay system which necessarily involves a lever arm between the film plane and exit slit.

Thus, the camera configuration was determined by the requirement that the separation of the two recorded images had to vary coupled with the fact that 70 mm film is the widest suitable commercially available film.

The basic requirement of precise location of the images with respect to the sprocket holes was rather easily satisfied, since there exists a large commercial market for high precision camera equipment, and almost all the sources of supply of that market are located in the Los Angeles area. Professional motion picture cameras typically locate the sprocket holes to ± .0001 inch. Therefore, all that was required was to find an advance mechanism that would fit into the camera box.

Basically all precision cameras use one of two types of transports-pin register or geneva. Pin register units have the capability of operational frame rates of 250 to 300 frames per second, and are generally bulkier and more expensive than genevas. Genevas usually are limited to frame rates of 24 frames per second. They are the standard film transport found in professional projection equipment.

Since the dual camera system could well afford to delay for a second between frames, the geneva's frame rate limitation was not serious. A geneva from an Automax G-2 was used in the dual camera. With the unit installed in the camera the leading edges of the sprocket teeth returned to the same position to within .0008 inches total indicator reading. The leading edges of the sprocket holes are held against the leading edge of the sprocket teeth by means of a tensioning unit inside the rear sprocket. (For details of the adjustment of the rear sprocket tension, see Appendix II.)
The film is located laterally by $4\frac{1}{2}$ inch long rails separated by .0005 inches more than the film width.

In use, the camera motors, which are mounted on vibration dampers, are operated only during the time the shutter on the beam splitter is closed, so that there are no problems caused by motor vibration during the exposures.

APPENDIX II DUAL 70 mm CAMERA

A. INTRODUCTION

The purpose of the dual camera is to precisely advance film on a signal from the control system. All operations of the camera are controlled by the camera control system which is in Appendix III.

The dual camera is basically two 70 mm film transport units that are coupled together and mounted on a base the size of an 8 x 10 plate holder (see Figures A1 through A5). Because the main sprockets are connected together only one film advance mechanism is necessary for the two units. The transport containing the film advance mechanism is called the "drive" unit; the other is called the "slave". Externally the drive box is easily distinguished by the film take-up motor mounted on top of it, and the electric clutch in the center of the transport's door.

The drive box is attached to the camera base plate. The slave unit, however, is not fixed to the base plate. It is movable in a direction perpendicular to the long dimension of the boxes, by means of two lead screw mechanisms on the front and rear sides of the slave unit. This motion allows the center-to-center distance of the transport units to be changed.

B. OPERATION

Before the camera can be used, the dark slide guides and plate holder cover must be removed from the plate holder assembly of the SHG. The guides are mounted on the rear of the plate holder assembly and are removed by unscrewing four screws - two in each guide.

The plate holder cover is removed by pushing the cover to the operator's left and lifting it off its hinges.

After the guides and the plate holder cover are off, the camera can be set in the position normally occupied by the plate holder. In position and with the two cables to the control system connected, the camera is ready to use. All that remains is to open the dark slides.

C. LOADING AND UNLOADING THE CAMERA

The dual camera was designed with the knowledge that a darkroom would always be available for loading purposes. For this reason no attempt was made to design the camera for loading in a lighted area. Hence, the operations of insertion and removal of film must be carried out in the darkroom. In most cases the film used will be a high speed panchromatic type that does not allow the use of safelights.

Since a large portion of the loading and unloading procedure must be carried out in total darkness, a good deal of care has gone into designing the camera so that the loading can be performed in as simple and foolproof a manner as possible. The camera doors are made so that they will not close unless all interior parts are in their proper operating position and locked in place. An auxiliary film advance mechanism allows the quick advancement of the film for easier threading in the loading procedures.

Because of the ease with which the camera's interior parts can be misaligned or damaged by careless handling, it is suggested

that the new operator first practice the loading and unloading procedures in a well-lighted area. Ordinarily, the camera is loaded on the bench in the 60 foot solar tower, but any area large enough to support the camera and allow it to rotate 180^{o} for access to both transport units will suffice. With some experience the entire loading operation can be carried out in about five minutes.

1. Loading Procedures

The operating knob for the auxiliary fast film advance mechanism is not a permanent part of the camera. It is a separate part that must be taken to the darkroom for the loading procedure. The knob is stored in the spare parts supply box for the camera system. Besides the knob for the fast film advance the loading area should contain scissors, two 70 mm number 10 spools, two foam plastic pressure washers, two spool retaining screws, two rolls of Scotch "Magic Mending Tape" and the film to be used in the camera. Good scissors are extremely important. The Estar (Mylar) base film often used will not rip, and must be cut in case the film becomes tangled during the loading operation. Two rolls of tape are suggested because of the high probability of the tape sticking to the roll and the low probability of getting it unstuck in the dark.

The camera should be placed on the loading area with the rubber belt facing the operator, and the following procedures should be performed in the order listed.

Procedures (1) through (8) and (17) can be carried out in the light, (9) through (16) require total darkness.

The location of many of the parts of the camera is shown in Fig. A5.

(1) Removal of the drive unit door.

Before the door can be opened, the rubber belt from the main motor pulley to the pulley on the electric clutch must be removed. This is done by grasping the belt and slipping it off the larger pulley. Then the blue Amphenol connector on the end of the electric clutch cable should be disconnected from the top of the drive unit. The similar connector on the take-up motor cable need not be disconnected.

The door can now be opened by loosening the brass captive screw at the top center of the door. The door is unfastened as soon as the screw turns freely. It is not necessary (or desirable) for the captive screw to be removed. The door is removed by pulling gently on the captive screw until the top of the door moves about a quarter inch away from the top of the camera box. This frees the light baffle on the inside of the door. The door can then be lifted up and off.

(2) Rotation of the clutch plate assembly.

The clutch plate is the bright metal disk in the center of the drive unit. (The clutch plate is not shown in Fig. A5.) Immediately behind the clutch plate is the clutch backing plate. The backing plate has two ears which can be easily grasped by the thumb and forefinger. The lower ear covers the input shaft of the auxiliary film advance mechanism. The clutch backing plate should be pulled outward about half

an inch. In the out position the entire clutch assembly is disengaged from the film advance mechanism. With the assembly pulled out half an inch, the two steel dowel pins which position it in the clutch assembly mount will be free. The freed assembly should then be rotated about five degrees in the clockwise sense. After the rotation the assembly should be pushed gently forward, and rotated. The rotation should be continued until the dowel pins re-engage in the mount. In the rotated position the assembly will be a quarter inch from the mount.

The rapid advance input shaft is now uncovered.

(3) Rotation of the drive unit rear sprocket.

The rear sprocket shaft is positioned and supported at its outboard end by an L shaped arm. The arm pivots on a stainless steel pin. The pin extends through a bearing mounted on the side of the transport box. The end of the pin is slightly larger than the diameter of the bearing. The pin should be pushed forward until it is stopped by the bearing. The arm is then free of the sprocket shaft, and can be rotated 90^{o} in a counterclockwise direction. With the arm in the rotated position the rear sprocket is ready to be rotated.

The rear sprocket is rotated by pushing the drive unit rear sprocket lever downward until a stop is felt. If the slave unit lever is mistakenly operated, the lever mechanism may jam, since the slave rear sprocket is still locked in

position.

In the rotated position the rear sprocket is about an eighth inch from the pressure plate. This spacing allows the film to be easily slipped under the rear sprocket.

(4) Rotation of the drive unit main sprocket pressure rollers.

The main sprocket pressure rollers are rotated into their loading position by pushing the roller assembly away from the main sprocket. The roller assembly will snap into the loading position.

(5) Removal of the slave unit door.

The camera should be rotated 180^{o} to allow access to the slave unit. The slave door is opened and removed in the same manner as the drive door (procedure (1)).

(6) Rotation of the slave unit rear sprocket.

The slave rear sprocket is rotated in the same manner as the drive rear sprocket (procedure (3)). Caution should be exercised that the slave rear sprocket lever is pushed. Further movement of the drive lever may cause it to disengage from the sprocket shaft.

(7) Rotation of the slave main sprocket pressure rollers.

The slave pressure rollers are positioned in the same manner as the drive unit rollers (procedure (4)).

(8) Installation of the take-up spools.

A 70 mm number 10 spool should be placed on the slave unit take-up shaft with a square hole side toward the back wall of the unit. When the spool is on the shaft it should be

rotated to check that the square hole has engaged the square end of the shaft. A spool retaining screw is not used on the take-up shaft.

The camera should be rotated 180°, and the take-up spool placed on the drive unit take-up shaft.

Some number 10 spools have two square holes, while others have one square and one round hole. Either type may be used as take-up spools. But the square-square type offer the advantage of being foolproof.

(9) Insertion of the film in the drive unit.

With the lights out and the darkroom door closed one of the film cans should be opened. If the end of the film is not square with the length, it should be trimmed with the scissors. The film spool should be placed on the feed shaft so that when the film is unwound the spool rotates clockwise. (The film used in the camera must be wound emulsion side in.) A foam plastic washer should be placed on the shaft, and the spool secured with a spool retaining screw. The retaining screw should be tightened until it is snug.

Approximately six inches of film should be unwound. Then the film should be slipped under the rear sprocket. Next the film must go under the pressure plate. To get the film under the pressure plate, the pressure plate locating rod must be pushed inward with the forefinger of the right hand at a point just above the locating rod bearing. With the pressure plate held in the tilted position the film can be slipped under the

pressure plate with the left hand. The right hand can then be removed, and the pressure plate will fall back into place. It is only necessary that a short length of film be under the pressure plate.

The rear sprocket lever should then be pulled upward until the rear sprocket stops in the operating position. The sprocket shaft support arm should be rotated 90^{o} clockwise, and pushed inward to secure the rear sprocket.

The rear sprocket should be rotated clockwise with the right hand until some resistance is felt. The end of the film should then be butting against the teeth of the main sprocket. The operator should check this condition by sliding a finger of his left hand under the main sprocket.

If the film is not up against the main sprocket, the pressure plate should be jiggled in the case the edge of the film is caught under the pressure plate. The rear sprocket should be rotated 90^{o} counterclockwise, and then clockwise until resistance is felt. If the film is still not against the main sprocket, procedures (3) and (9) should be repeated.

(10) Engagement of the film by the drive unit main sprocket.

The square hole in the end of the film advance knob should be placed over the end of the square shaft uncovered by the rotation of the clutch assembly. Rotation of the knob in a clockwise sense through four revolutions will engage the film and advance it above the top of the pressure rollers.

The pressure roller assembly can then be flipped down against the drive sprocket.

The film advance knob should not be removed at this point.

(11) Insertion of the film in the slave unit.

The camera should be rotated 180^{o} to allow access to the slave unit.

The procedure for inserting the film in the slave unit is the same as in the drive unit. However, there is more room in the slave due to the absence of a film advance mechanism. Hence, the insertion operation should be somewhat easier.

(12) Engagement of the film by the slave unit rear sprocket.

The film advance knob should be turned until the film reaches the take-up spool - about ten revolutions.

The slave pressure rollers can be flipped down, and the film advance knob removed from the drive unit.

(13) Attachment of the film to the slave unit take-up spool.

The take-up spool rotates in the clockwise direction. The end of the film should be taped with "Magic Mending Tape" to the spool so that the film is wound emulsion side in.

(14) Replacement of the slave unit door.

The door is replaced by a reversal of the removal procedure. If the door does not close easily, the position of the rear sprocket arm, and the pressure roller assembly should be checked.

(15) Attachment of the film to the drive spool.

The film should be taped to the take-up spool in a manner

similar to that used in the slave unit. However, in the case of the drive unit the clutch assembly mount makes the procedure considerably more difficult.

(16) Replacement of the drive unit door.

Before the drive unit door can be replaced the clutch assembly must be rotated back into its operating position. This can be accomplished by reversing the rotation procedure (procedure (2)). If, after the assembly has been placed back in the original position, it does not set flush against the assembly mount, the clutch plate should be rotated manually until the assembly snaps into place.

With the clutch assembly in its proper position the door can be replaced by a reversal of the removal procedure. If the door does not close, the rear sprocket, the pressure roller assembly, and the clutch plate should be checked.

(17) Attachment of the vee belt and clutch cable.

At this point the lights may be turned on.

The vee belt is reinstalled by placing it on the smaller pulley and slipping it over the larger one. The electric clutch cable connector should be plugged into the connector in the top of the unit.

The loading procedures are now completed.

2. Unloading Procedures

The unloading procedure followed will depend on the amount of film remaining in the camera. If there is sufficient film for at least another "run" the "middle of the roll" procedure should be performed.

If there is not enough film the "end of the roll" procedure should be carried out.

a) Middle of the Roll Procedure

The camera should be placed on the darkroom bench with the vee belt facing the operator. The film advance knob, scissors, two rolls of "Magic Mending" tape, two rolls of photographic tape, two empty 70 mm film cans, two empty number 10 spools, and a pencil should be in the darkroom. The empty spools should be placed on the table with the square hole side up.

After removing the vee belt and the electric clutch connector, the darkroom lights must be turned off. Procedures (1), (2), and (5) should be performed, and the film advance knob placed on the rapid advance input shaft.

Using the scissors the drive unit film should be cut off just before the take-up spool. Immediately after removing the exposed film from the camera, the date and "drive unit" should be written on it. A step wedge should be exposed and the film placed in a can and sealed with the photographic tape. In a similar manner the film should be removed from the slave unit, marked, and sealed in the remaining film can.

Procedures (8), (13), (14), (15), and (16) should be performed, the lights turned on, and the vee belt and cable connector reinstalled.

b) End of Roll Procedure

For the end of the roll procedure the film advance knob, scissors, two rolls of photographic tape, four empty film cans, and a

pencil should be taken into the darkroom.

After removing the vee belt and the clutch connector, the darkroom lights should be turned off. Procedures (1), (2), and (3) performed, and the film advance knob placed on the auxiliary input shaft.

Using the scissors the film in both units should be cut off just behind the rear sprockett. Then the advance knob should be rotated clockwise until the ends of the films are free of their respective main sprockets. The exposed films should then be marked, step-wedged, and sealed in film cans.

The spool retaining screws can then be undone, and the spools with the remaining unexposed film removed and sealed.

The lights should be turned on, and procedures (14), (16), and (17) performed.

D. MAINTENANCE

The 70 mm camera has operated for two summer observing seasons with the loss of less than a quarter of a single mornings run due to an equipment failure. The camera control system has never caused a loss of observing time. The single breakdown was caused by the main camera motor stopping and over-heating during breakfast. The original synchronous motor was replaced by an induction motor that has operated perfectly for more than a year.

The camera's ball bearings should be oiled at the beginning and end of each years observing season. Ball bearings are used on the take-up shaft, take-up motor, rear sprocket shaft, geneva mechanism,

and the electric clutch.

E. ADJUSTMENTS

Under normal circumstances adjustments of the camera system will not have to be made. However, the rear sprocket tension and the center-to-center distance of the transport units can be varied.

The rear sprocket has a small friction clutch built into it. By moving the clutch pressure plate on the sprocket shaft the drag on the rear sprocket can be varied. The pressure plate is held in position by an allen set screw. A small hole in the rear sprocket located about an eighth inch from the outside sprocket teeth allows access to the set screw.

The center-to-center distance of the two transports can be varied to compensate for the change in the center-to-center distance of the images that result from changing the operating wavelength. The value of this adjustment is somewhat mitigated by adjustments in the film cancellation machine.

Before the adjustment can be made the coupling between the two main sprockets must be loosened. To gain access to the set screw that locks the coupling together, an access screw in the coupling light shield must be removed. The coupling light shield is the tube between the two transport units along the axis of the main sprockets. The access screw is a bright stainless steel allen cap screw located in the end of the tube nearest the drive unit. The screw is easily seen by looking between the two transport units from the main motor end of the camera. The access screw is removed by means of a special extension

allen wrench. This tool is a quarter inch diameter aluminum rod six inches long with an allen wrench pressed in each end. The larger of the two allen wrenches fits the access screw; the smaller fits the set screw. The tool is kept in the camera parts box.

A half turn of the set screw is sufficient to loosen the coupling. Under no circumstances should the set screw be removed. Many, many unhappy hours will be spent if the set screw falls inside the coupling light shield.

After the coupling is loose, the cap screws that clamp the slave unit to the camera base should be loosened. The slave unit can then be moved by turning the knurled knob on the lead screw assembly located just above the rear sprocket levers.

The camera is put back into operating condition by reclamping the slave unit, tightening the set screw, and replacing the access cap screw in the coupling light shield.

F. MINOR REPAIRS

Several minor repairs have been necessary during the two observing seasons, but they have resulted in the loss of only five to ten minutes of observing time. A list of these repairs together with some other probable minor repairs, and the methods for effecting the repairs are listed below.

1. Replacement of the dark slides .

The dark slides used on the camera are marked with a white line. The entire aperture is uncovered when the white line is visible. If the line is ignored, the dark slides may be pulled out of their

guides. When a dark slide is pulled out too far, it cannot be re-inserted normally. Attempts to force a slide inward will result in damage to the dark slide guides.

No loss of observing time should result from pulling a slide out too far. This is because the dark slides are only opened when the camera is on the SHG and ready to run. However, at the end of the run the dark slide will not close. To prevent ruining of the last of the morning's pictures an extra 15 frames should be advanced before the camera is removed from the SHG. The camera should be taken to the dark room and the "end of the roll" unloading procedure performed.

After removing the film, the camera should be turned on its side to gain access to the underside of the base plate. Under each dark slide is a panel secured by eight flat head screws. The panel under the dark slide being reinstalled should be removed. With the panel off, the dark slide can easily be reinserted into its guides. The panel should then be replaced.

2. Rubber take-up belts.

The rubber belts between the pulleys on camera take-up shafts and the pulleys on the distribution shafts of the camera are neoprene O-rings. If a belt breaks it can be replaced by removing the two screws on the self-aligning bearing mount of the concerned distribution shaft and slipping a new belt on the shaft. As soon as the new belt is on the shaft the bearing mount can be reinstalled. The belt should then be slipped on the take-up shaft pulley. A long rod (one of the extension allen wrenches will do) is helpful in guiding the belt over the take-up pulley. After the belt is one the take-up pulley, it should be

slipped over the distribution shaft pulley.

3. Bead chain belts.

Under normal circumstances a spare bead chain belt will be kept on each shaft to use in the case of breakage. If the chain breaks, the spare belt can be quickly slipped in place. If there is not a spare belt on the shaft, a new one can be made up. It is not necessary to remove a bearing mount as the bead belt can be constructed on the shaft. Parts and a special tool for making bead chain belts are kept in the parts box.

No observing time should be lost from a belt breaking as ample warning of an impending break will be given by the characteristic sound of the bead chain slipping on its pulley.

4. Take-up pulley.

If a take-up pulley begins to slip on its shaft, its set screw must be tightened. The set screws are located inside the pulleys, and the pulley belt must be slipped off to gain access to them. An allen wrench on the end of an aluminum rod allows the set screws to be tightened easily.

Figure A1 Dual camera installed on SHG and connected to the camera control system.

Figure A2 A view of the camera showing the main motor. Note the spare bead belt. The drive unit dark slide is open.

Figure A3 A view of the camera showing the rear sprocket levers. The knurled knob above the rear sprocket levers moves the slave transport.

Figure A4 A view of the slave unit with the pressure plate removed. The (slave unit) dark slide is half way open.

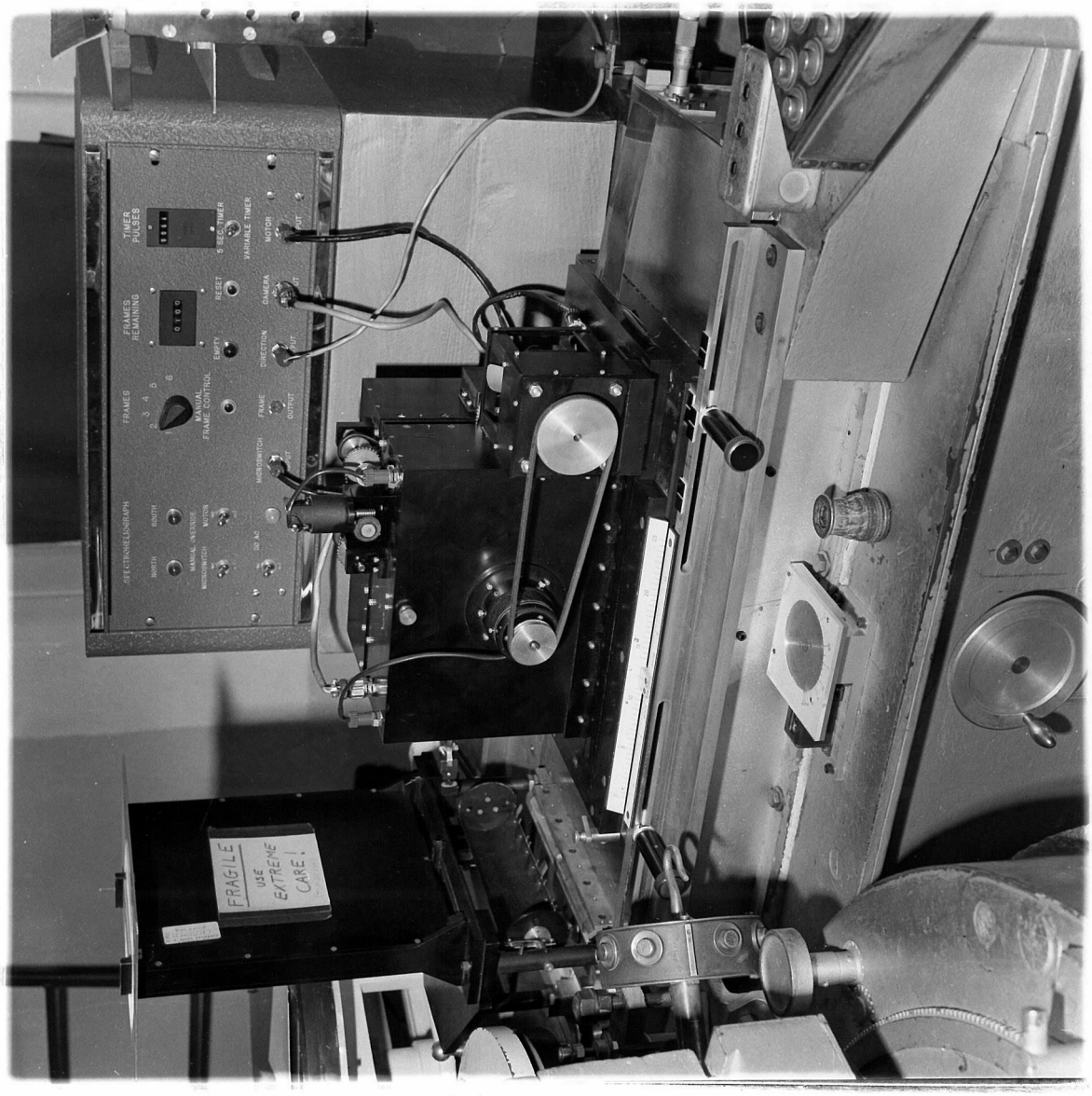

Figure A1

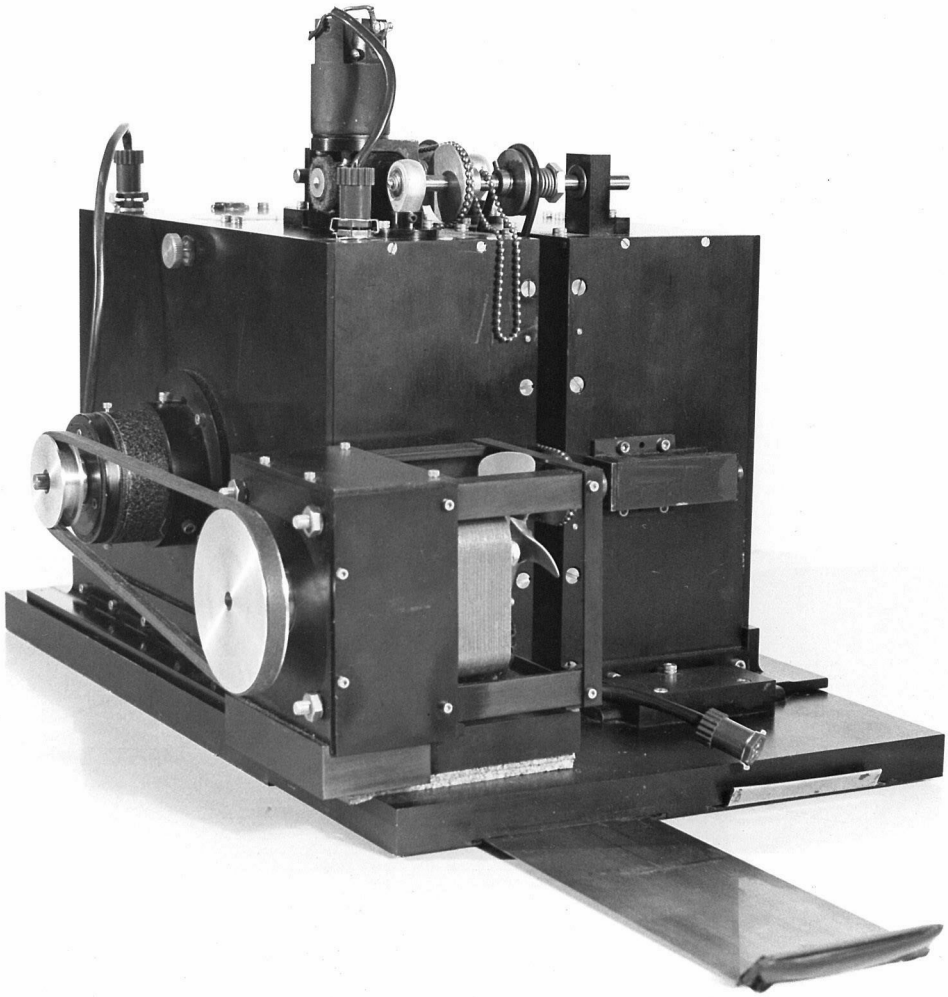

Figure A2

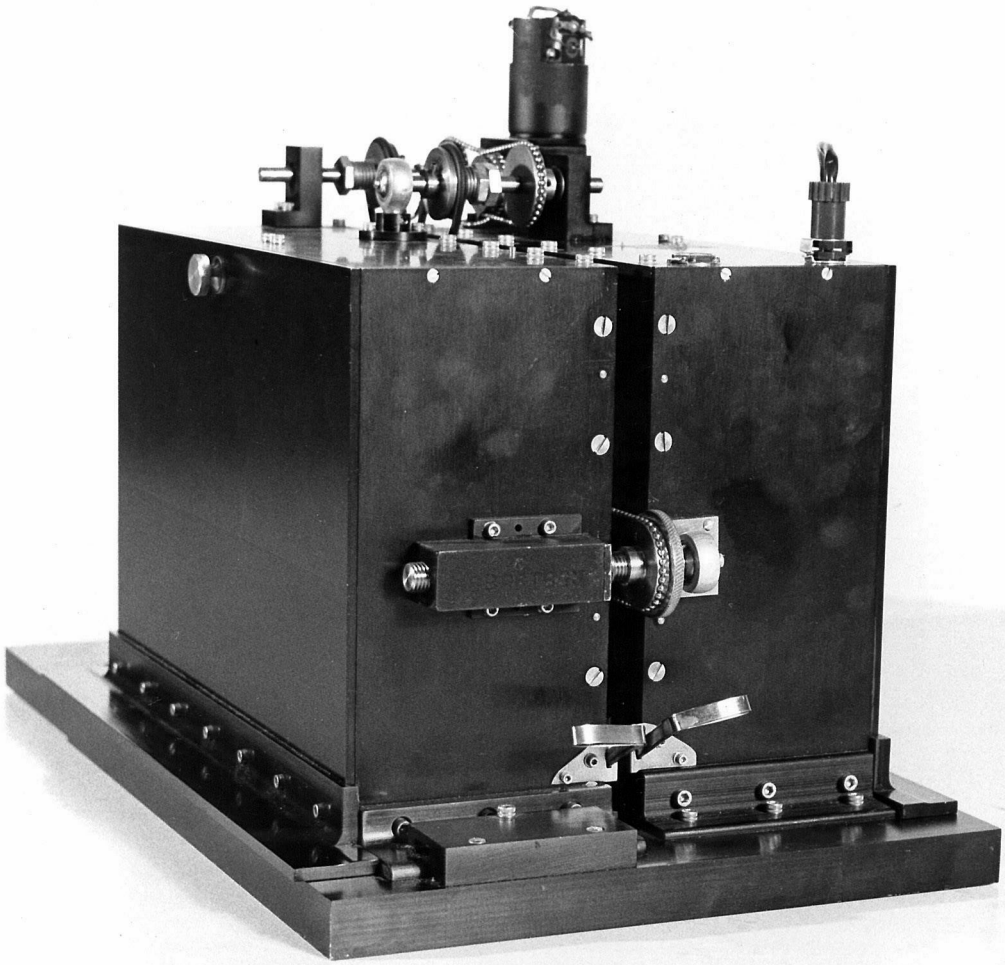

Figure A3

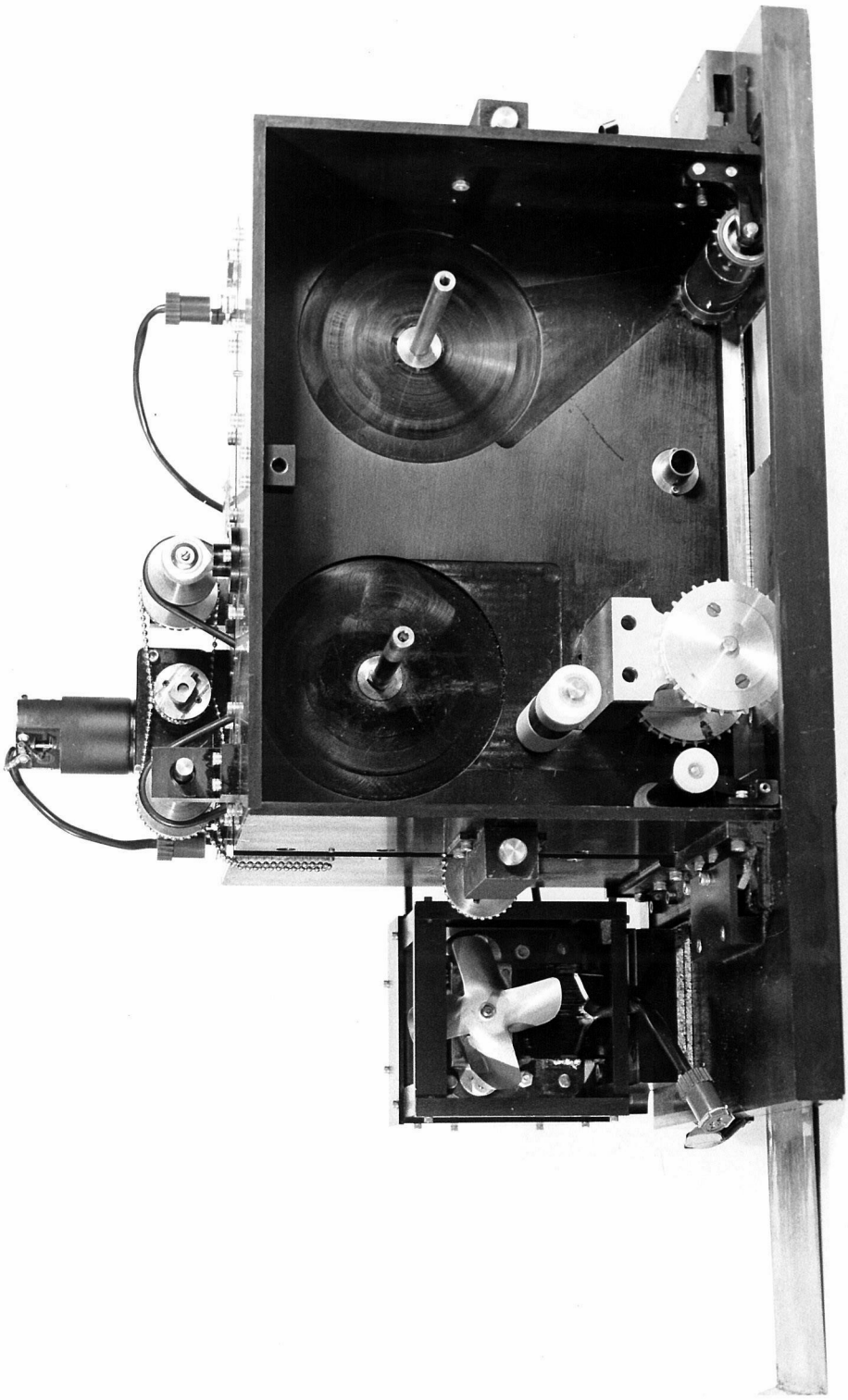

Figure A4

Figure A5 70 mm Camera Side View of Drive Unit

The drive unit is shown ready for loading. Procedures (2), (3), and (4) have been performed.

The clutch plate assembly has been removed to show the interior more clearly.

a) Clutch Assembly Mount
b) Rapid Advance Input Shaft
c) Main Sprocket
d) Rear Sprocket
e) Rear Sprocket Support Arm
f) Feed Spool Shaft
g) Take-up Spool Shaft
h) Main Sprocket Pressure Rollers
i) Main Motor Pulley
j) Main Motor Cage
k) Amphenol Connector for Electric Clutch
l) Camera Output Connector
m) Take-up Motor
n) Connector of Take-up Motor
o) Pressure Plate Locating Rod
p) Pressure Plate Locating Rod Bearing
q) Pressure Plate
r) Guide Roller

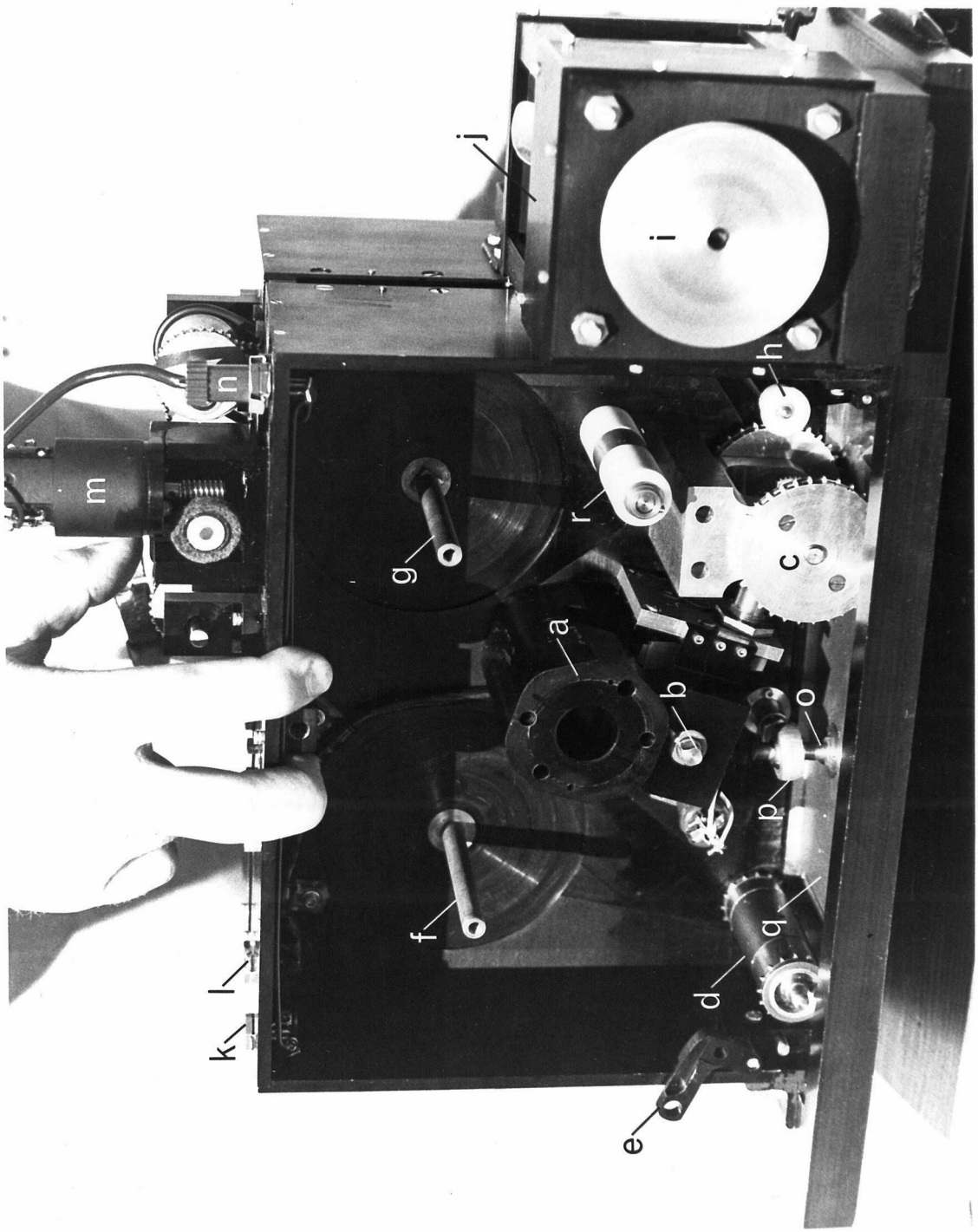

Figure A5

APPENDIX III CAMERA CONTROL SYSTEM

A. INTRODUCTION

The purpose of the camera control system is to automatically advance the dual camera a selected number of frames and then reverse the SHG on an integral multiple of a selected time interval. In use the operator need only adjust the SHG brightness control to that indicated by the brightness meter. The control system will automatically start the SHG on an integral multiple of the selected time base regardless of brightness setting.

B. OPERATION AND DESCRIPTION OF THE CONTROLS

The following is a brief description of the function of the controls and displays on the control system front panel (see Figs. A6 and A7). In order for the controls to operate as described the cable from the SHG and the cables to the dual camera must be connected, and the SHG motor control must be on.

Off-On Switch is a toggle switch which turns on (up position) the power for the control system.

On Indicator Light is an orange neon lamp which goes on shortly after the control system is turned on.

Microswitch Manual Override switch is a toggle switch which must be in the up position for the control system to operate automatically. When the switch is in the down position the SHG drive can be operated manually by the normal button control. The switch must be in the down position when frames are advanced manually.

Microswitch Indicator Lamps are yellow neon lamps. One of the lamps goes on when the North-microswitch of the SHG is closed, the other when the SHG South-microswitch is closed.

Motor Override Switch is a toggle switch which must be in the up position for film to be advanced automatically. In the down position the main camera motor will run continuously. When the switch is in the down position 110 Vac is across the cable to the main camera motor. Therefore, the cable to the main camera motor should not be removed when the switch is down because of the high probability of shorting the cable connector on the metal camera body or fingers.

Manual Frame Advance Button is a push button switch which operates the camera film advance mechanism if the motor override and microswitch override switches are in the down position.

The camera advance circuit requires only a momentary pulse. Therefore, it is unnecessary to hold the advance button down throughout the entire film advance cycle. No harm is caused by prolonged depression of the button, but only one frame will be advanced regardless of the duration the button is depressed. Depressing the button during the advance cycle has no effect.

Frame Selector Switch is a six position rotary switch. At the end of each traverse of the SHG the camera will advance the number of four sprocket hole frames indicated by the frame selector, if the microswitch and motor override switches are in the up position.

The number of frames to be advanced can be changed at any time, except when either the North or South microswitch indicator light is on.

Frames Remaining Counter is a resettable subtracting counter. The number in the counter register decreases by one each time a frame is advanced by the camera. When the number in the register reaches zero the control system ceases to operate and the red empty light under the counter goes on.

The counter can be set to any number less than 10,000 by raising the front cover and setting the counter dials to the desired number. The number in the dials can be changed at any time, except when either the North or South microswitch light is on.

Empty Indicator Lamp is a red neon lamp which goes on when the frames remaining counter reaches zero. When this lamp is on the control system will not operate.

Reset Button is a push button switch. When the red empty light is on and after the frames remaining counter has been set to a number other than zero, depression of the reset button will allow the control system to again operate automatically. If the frames remaining counter is allowed to remain at zero, depression of the reset button will not cause automatic operation to resume.

Depression of the reset button when the empty light is off will cause the light to go on. This situation is remedied by again pushing the reset button.

Timer Switch is a toggle switch which selects one of the two pulse timers that operate the timer pulse counter and gate the SHG reversal. The up position usually selects a timer that gives a pulse every five seconds.

The timers chosen by the selector switch are an Industrial

Timer CM-1 (up position) and CM-5 (down position). The duration between pulses on both of the timers can be changed by replacing the gear rack in the timer. CM-1 has an interval range between four and ninety seconds, and CM-5 has a range between two and eighteen minutes. The gear racks available and the times they yield can be found in the Industrial Timer Catalog. A number of gear racks are included in the parts supply for the control system. The pulse interval yielded by each of the racks for the timers in the control system is noted on the racks.

Timer Pulse Counter is an electrically reset Sedeco adding counter. It counts the pulses from the selected timer during the traverse of the SHG and film advance cycle. The next timer pulse after the film advance cycle is completed resets the counter to zero and starts the SHG traverse. Thus, the time between frames is the maximum number that appears on the timer pulse counter plus one multiplied by the interval between timer pulses.

C. LOGICAL STRUCTURE

The camera control system circuit contains five basic sections that perform logical operations depending on the status of the SHG and the dual camera. These are: Status of the SHG, Camera Advance Pulse, Camera Advance, Frames Remaining, and SHG Reversal. An outline of the logical structure follows:

Status of the SHG

If the North (or South) indicator lamp is on, then (1) power is connected to the Camera Advance Pulse section and (2) the SHG

reversal circuit is completed, but not powered. When a pulse from the SHG reversal section is received the SHG is started going South (or North).

Camera Advance Pulse

If (1) the North or South indicator lamp is on and (2) the frame selector switch is at N, then (1) N pulses go to the camera advance section and (2) the N + first pulse goes to the SHG reversal section.

Camera Advance

If (1) there is a pulse from the Camera Advance Pulse section and (2) the main camera motor is in the automatic mode and (3) the previous frame was fully advanced, then(1) a single frame is advanced and (2) after the frame is advanced a correlation pulse goes to the frames remaining section.

Frames Remaining

If there is a correlation pulse from the camera advance section then one is subtracted from the number in the counter.

If (1) there is a correlation pulse from the camera advance section and (2) the counter is at 1, then the power to the Status of the SHG section is disconnected, and automatic operation ceases.

SHG Reversal

If (1) there is an SHG pulse from the Camera Advance Pulse section and (2) a timer pulse after the SHG pulse, then (1) an SHG traverse is started and (2) the timer pulse counter resets to zero.

If there is a timer pulse before the SHG pulse, then the timer pulse counter is advanced one.

D. MAINTENANCE

Occasionally, the contacts on the motor operated rotary switch should be cleaned. No other maintenance has been necessary in the two summers of operation.

Figure A6 A view of the control system front panel

Figure A7 A view of interior of the camera control system. The Industrial Timer CM-5 is closest to the rear of the chassis.


SPECTROHELIOGRAPH
NORTH
SOUTH
MANUAL OVERRIDE
MICROSWITCH
MOTOR
110 AC
FRAMES
1
2
3
4
5
6
MANUAL
FRAME CONTROL
MICROSWITCH
INPUT
FRAME
OUTPUT
EMPTY
FRAMES
REMAINING
0 T 3 7
DIRECTION
OUTPUT
RESET
CAMERA
OUTPUT
TIMER
PULSES
0 0 0 2
5 SEC. TIMER
VARIABLE TIMER
MOTOR
OUTPUT

Figure A6

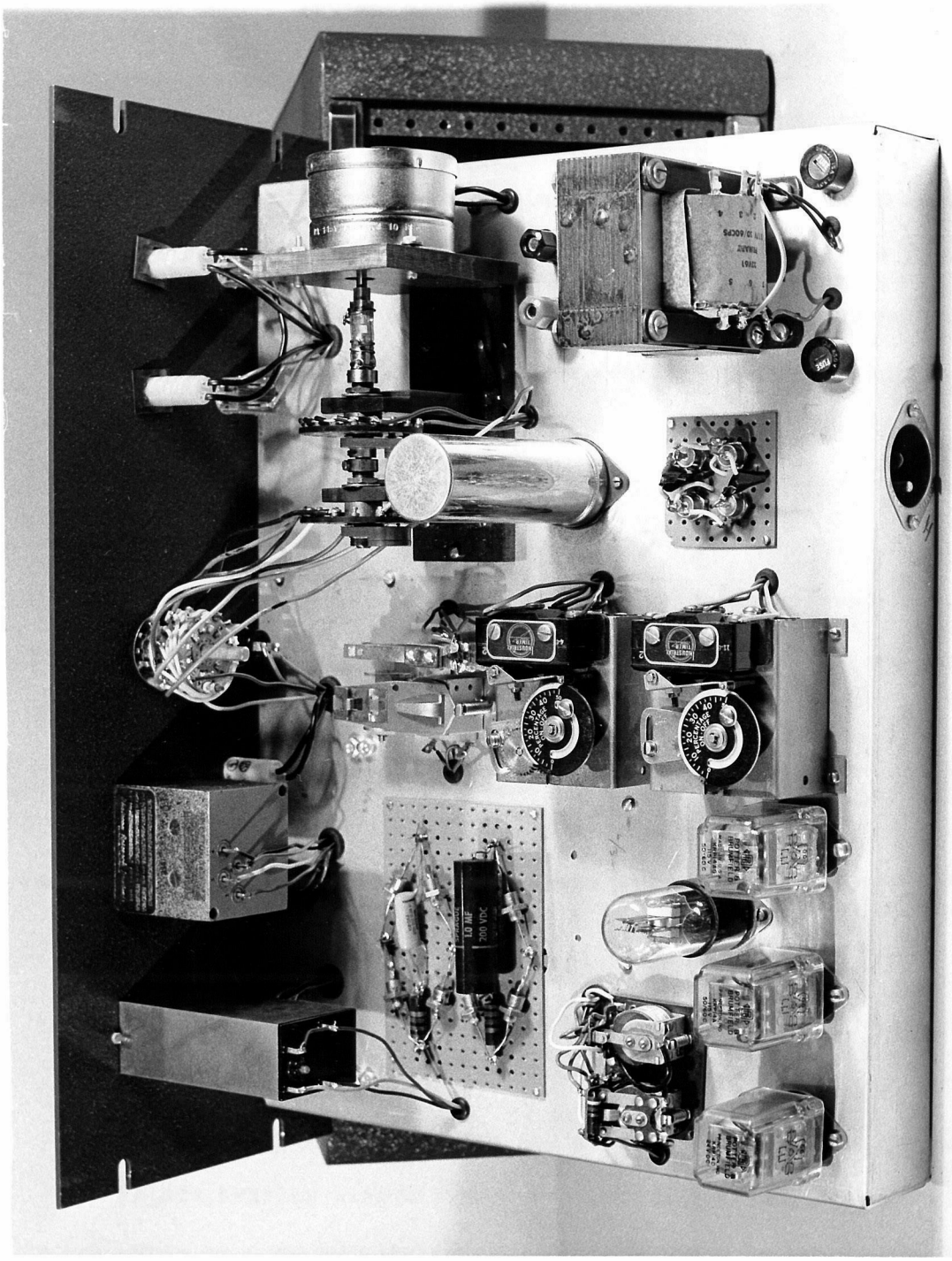

Figure A7

APPENDIX IV CONTACT PRINTER

A. INTRODUCTION

At present no commercial film processing corporation is set up to produce unit gamma contact prints of black and white 70 mm film. Hence, the unit gamma contact prints of the 70 mm movies must be produced in the laboratory. With a few simple nonpermanent modifications the dual camera system can be used to produce satisfactory contact prints.

B. SET-UP

A darkroom is required for the copying procedures. The set-up of all the cancellation equipment, except the camera control, is shown in Fig. A8. The control system can be placed in any convenient location.

The camera output and motor output cables should be connected. A special cable with a push button switch on the end should be plugged into the microswitch input of the control system.

C. LOADING

(1) Installation of the glass aperture plate.

Camera loading (CL) procedures (CL1), (CL2), (CL3) and (CL4) should be performed. Then the pressure plate and pressure plate bearing assembly must be removed from the camera unit. This is done by tilting the pressure plate in the manner suggested in camera loading procedure (CL9), and pulling gently outward on the pressure plate bearing until the bearing is free of its mount.

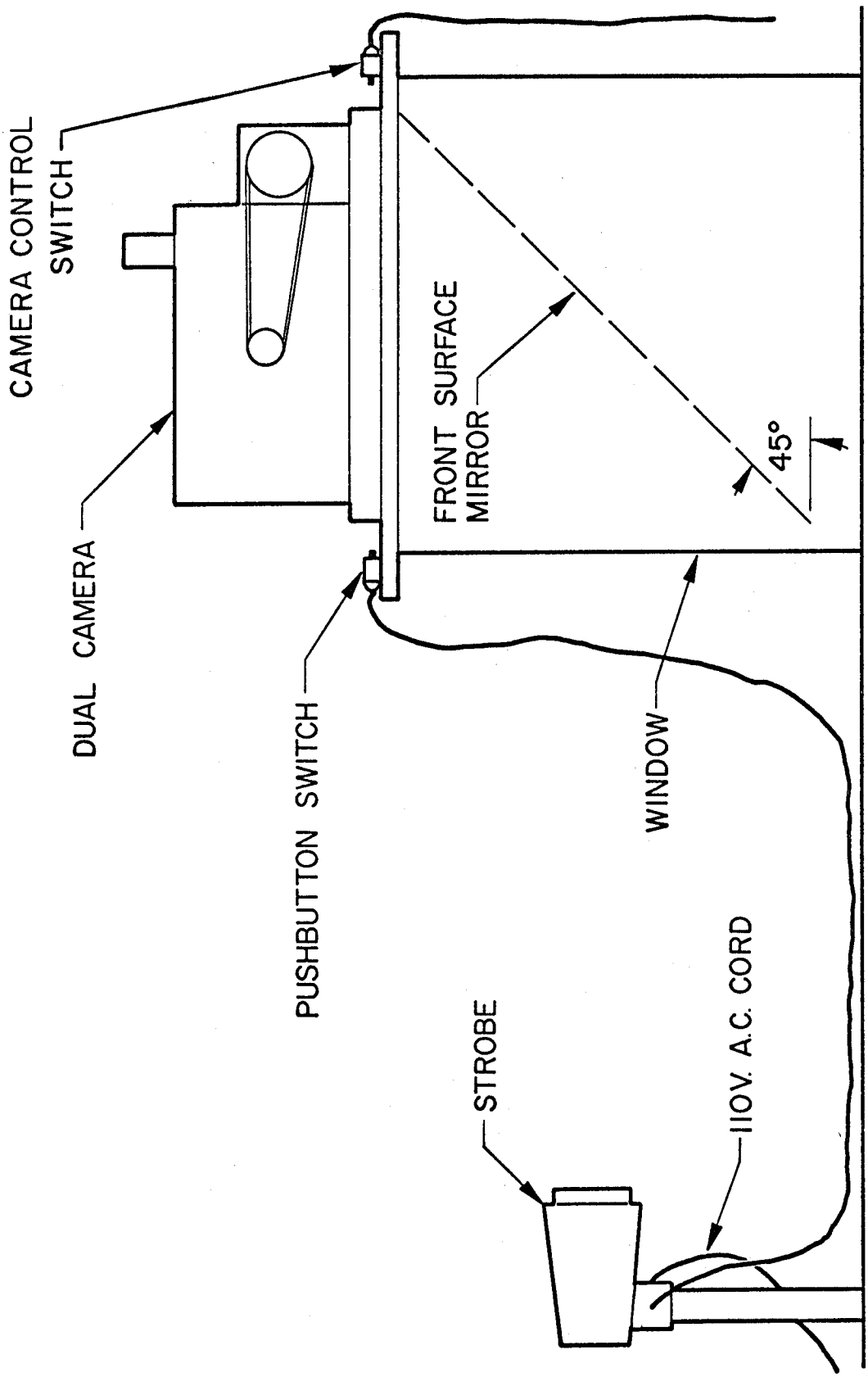
CAMERA CONTROL SWITCH
DUAL CAMERA
PUSHBUTTON SWITCH
FRONT SURFACE MIRROR
45°
WINDOW
STROBE
110V. A.C. CORD

Figure A8

The dark slide of the drive unit should be pulled open, and the glass aperture plate placed in the aperture. The pressure plate should not be replaced at this time.

(2) Loading of the film to be copied.

The film to be copied should be loaded so that film passes under the pressure plate emulsion side up. Since the film is wound emulsion side in, the feed spool should unwind counter-clockwise.

Camera loading procedures (C13), (CL4), (CL9), and (CL10) should be carried out. Since the pressure plate is not installed, (CL9) will be somewhat simplified. After the film is engaged by the main sprockets the film should be advanced by rotating the rapid advance knob clockwise until the first movie frame is on the aperture plate. If a section of the frame falls on the edge of the aperture, the operator should rotate the fast advance knob counterclockwise until the film is again free of the main sprockets. The film should then be re-engaged so that the aperture plate does not intersect the first frame. The pressure plate should now be reinstalled.

(3) Loading the Copy Film.

The camera control frame selector switch should be turned to six, and all the toggle switches on the control panel should be placed in the up position.

At this point the darkroom lights must be turned off, and must remain off until the entire movie is copied.

A length of the copy film slightly longer than the film to

be copied should be unwound from a supply spool. The film must not be spooled, but loosely wound emulsion side in.

The loose roll of film should be placed in the camera between the feed spool and the clutch assembly mount. Properly inserted the film will unwind clockwise.

Camera loading procedures (CL9) and (CL10) should be performed.

If the copy film had been loaded correctly, under the pressure plate the emulsions of the copy film and the original negative will be in contact.

The copy film should be taped to the original negative, and the negative should be taped to the take-up spool. Then camera loading procedures (CL16) and (CL17) should be performed, but the room lights should not be turned on.

D. OPERATION

To expose the copy film the push button connected to the strobe should be actuated. Then the push button connected to the camera control system should be depressed. The above cycle should be repeated until the entire move is copied. After the copying operation is complete the take-up spool should be removed and sealed in a film can.

Because of possible variations in the film, the distance of the strobe from the film plane (light intensity), developer, and temperature, it is strongly suggested that a contact print be developed immediately after exposure. If unity gamma is not achieved, another copy can be easily made with an appropriate adjustment in light intensity and/or development.

APPENDIX V CANCELLATION MACHINE

A. INTRODUCTION

The purpose of the cancellation machine is to form a 35 mm doppler movie from a 70 mm movie taken in one wing of a spectral line and a unity gamma contact print of the simultaneous 70 mm movie taken in the other wing of the line. The apparatus is also used for making 35 mm reduction prints from single 70 mm movies taken in the wings.

Basically the cancellation machine consists of a Bell and Howell Eymo 35 mm motion picture camera mounted over a combination light box and film alignment jig (see Figs. A9 through A12). The device is manually advanced and forms either the doppler or wing 35 mm movie frame by frame.

Rather than discussing the methods by which the two films are held in their jigs and aligned with respect to each other and the 35 mm camera, the set-up, loading, and operation of the machine will be described. Use of the apparatus will do much to explain the alignment methods.

B. SET-UP

The cancellation machine and the necessary accessory equipment for its use is kept in 19 Bridge.

The following procedures should be carried out in the order listed. The location of many of the parts mentioned below is shown in Figs. A9 and A10.

(1) Hook-up of the Machine.

The Sorensen voltage regulator should be turned on and

allowed to warm up. The Variac should be plugged into the regulated 110 vac. The on-off switch of the Variac should be off. The plug from the light box assembly should be plugged into the Variac. The two leads from the shutter timer should be connected to the two screw terminals on the Eymo, and the shutter timer plugged into the regulated 110 vac. Attaching an air hose to the quarter inch pipe nipple on the back of the light box completes the hook-up.

(2) Preparing the 35 mm Camera.

The cancellation machine data book should be consulted to find out if the Eymo is loaded. If the camera is not loaded, it should be wound and loaded with a 150 foot roll of 35 mm Kodak Linagraph Shellburst (Estar) SP 417. If loading the Eymo is not obvious, an operating manual should be consulted. When new film is loaded an entry should be made in the data book.

C. LOADING

1. Loading the Lower Film.

If a rubber band is connected to the pressure control lever of the rear pressure plate, it should be removed from the lever. The lever can then be raised, and the rear pressure plate removed. The screws on the three springs holding down the center pressure plate should be loosened, and rotated to free the pressure plate. The center pressure plate should be removed carefully so as not to damage the teeth of the upper main sprocket. When both pressure plates are out, the aperture plate and both pressure plates should be cleaned with a mild

glass cleaner.

Note that the bottom of the center pressure plate and the section of the light box aperture plate upon which the rear pressure plate rests has a pattern of epoxy bosses the shape of sprocket holes on them. These bosses hold the two films in position.

The original film is normally loaded on the lower sprockets. The film should be threaded as shown in Fig. A10. The film should pass under the center pressure plate emulsion side up.

After the lower film is threaded the rear and center pressure plates should be replaced, and the center pressure plate springs rotated into their operating position, and their locating screws re-tightened. Then a rubber band should be looped over the protruding screw on the front of the light box and stretched onto the end of the pressure control lever.

2. Focusing.

The focusing operation should be performed at this time, if necessary. Ordinarily the focus will not change once it is set. In general, it only need be checked after the cancellation machine has not been used for some time.

The procedures below should be carried out in the order listed. Figure A11 shows the Eymo and light box in focusing position.

(1) Movement of the light box and camera lens mount to the focusing position.

If the camera lens is positioned over the center of the center pressure plate, the knob in the center of the turret lens assembly should be pulled downward until the assembly

will turn. The assembly should then be rotated 120° counterclockwise and allowed to slip back up into position. If the lens is neither over the center pressure plate or 120° counterclockwise from the pressure plate, it should be rotated 120° clockwise. Then the clamp on the front of the light box should be removed, and the light box slid forward until the center of the pressure plate is under the camera lens. The rectangular aluminum spacer plate should be placed between the light box and the L shaped locating frame. The light box should be pushed firmly against the spacer plate and the long arm of the locating frame.

(2) Focusing the Camera.

The air supply and the Variac should be turned on. While pressing upward on the pressure control lever, the lower main sprocket knob should be turned until the first movie frame is under the lens. If the main sprocket knob resists turning the film should be tapped from below just after it passes over the lower rear sprocket. Now the first movie frame should be visible through the eyepiece of the Eymo's reflex viewfinder. The brightness of the image can be adjusted by the Variac. The lens opening should be at f 2.0.

Focusing is performed by moving the lens up or down in its mount. It should not be necessary to change the position of the camera to focus. However, if the image cannot be focused without moving the camera, the camera can be moved

by pushing upward on the camera mount lock knob. Under no circumstances should the lock knob be released unless the operator's other hand is under the camera and holding it firmly. If a hand is not under the camera when the mount is unlocked, the camera will rapidly slide downward until it crashes into the stop at the end of the mount.

(3) Alignment of the light box.

If after focusing the image, the frame is not centered in the view finder, the screws on the L shaped frame should be loosened and the light box moved until the frame is centered. The screws can then be tightened.

(4) Returning the camera to the operation position.

The air supply and the Variac should be turned off.

The camera and light box are returned to their operating positions by reversing procedure (1).

3. Loading the Upper Film.

If a doppler movie is to be made, the unity gamma contact should be loaded on the upper film assembly as shown in Fig. A12. The film should pass under the center pressure plate emulsion side down. When both films are correctly loaded their emulsions will be in contact under the center pressure plate.

D. OPERATION

The cancellation machine can, as mentioned earlier, be used to produce either 35 mm doppler movies or 35 mm copies of wing movies. The operating procedures listed below are for making doppler movies. Wing

copies are produced by a similar method in which the upper film is not used. Hence, the procedures listed below can be used to make wing copies by neglecting the operations involving the upper film.

(1) Centering the first frame of the lower film.

The lower film should be advanced until the first movie frame is under the center pressure plate. This is done by pushing upward on the pressure control lever and turning the knob on the lower main sprocket clockwise. If the main sprocket knob resists turning, the lower film should be tapped from below just after it passes the rear sprocket. The operator will notice that as the lower film's sprocket holes pass over the bosses on the light box aperture plate the resistance of the main sprocket knob to turning will increase. This is a normal condition.

With the film centered below the center pressure plate the lower main sprocket should be slowly rotated clockwise until the sprocket holes engage the epoxy bosses in the aperture plate. During the rotation the pressure plate lever should not be pushed up. The operator should be able to feel when the sprocket holes engage the epoxy bases. However, the engagement can be checked by looking through the rear pressure plate.

(2) Centering the First Frame of the Upper Film .

The upper main sprocket knob should be rotated counterclockwise until the first movie frame is centered under the center pressure plate. If the knob resists turning freely, the

upper film should be tapped lightly from above just before it passes under the center aperture plate. With the first frame below the center pressure plate, and pressing gently on the metal frame of the center pressure plate, the upper main sprocket knob should be rotated until the upper film's sprockets engage in the epoxy bosses on the pressure plate. This condition can be checked by looking through the center pressure plate.

(3) Alignment of the Upper and Lower Films.

Usually the first frames on the 70 mm films are taken in the center of the line. Thus, aligning the upper and lower films produces a uniform gray field.

The two films are aligned by loosening the two cap screws that hold the center pressure plate locating frame in position and moving the center pressure plate until a uniform gray field results. The gray field can be quickly and easily obtained. However, retightening of the cap screws to lock the locating frame in the desired position will almost always destroy the alignment. In fact, a new operator may get the feeling that it is impossible to tighten the cap screws without destroying the alignment. However, with sufficient practice and patience the operation can be mastered.

(4) Exposure Settings.

The data book should be consulted for the settings of the shutter timer, the camera lens opening, and the light meter. The settings will vary depending on whether a doppler or

wing movie is being made. The various settings should be made, checked, and recorded in the data book.

The exposure meter used is a Sekonic Micro Leader L-98. The meter's operating manual should be read before it is used. Before each use the battery in the meter should be checked by the method outlined in the manual.

The window of the exposure meter should be placed over the center of the center pressure plate and the Variac adjusted until meter reads the value obtained from the data book. The exposure for the first frame is then set. The meter should be set again on the first frame with a doppler signal, and then periodically during the reduction.

(5) Exposure of the First Frame.

A frame is exposed by pushing the toggle switch on the cable from the shutter timer to the down position. After the exposure the switch must be returned to the "up" position for at least five seconds before the next exposure is made. This must be done to insure the proper charging of the capacitors in the shutter timer.

(6) Advancing the film to the next frame.

Normally the frames taken by the 70 mm camera are either four or eight sprocket holes long. Hence, both the upper and lower films must be advanced either four or eight sprocket holes to take each successive frame. The camera is capable of producing frames longer than eight sprocket holes long, but this cancellation machine is not capable

of reducing them.

The lower film should be advanced slightly more than three (or seven sprocket) holes by the method discussed in procedure (1). Then the pressure lever should be released, and the lower main sprocket knob rotated clockwise until the bosses on the aperture plate engage the sprocket holes in the lower film.

The upper film should be advanced slightly more than three (seven) by the method discussed in procedure (2). Then pressing lightly on the metal frame of the center pressure plate, the upper main sprocket knob should be rotated counter-clockwise until the bosses on the center plate engage the sprocket holes in the upper film.

The center pressure plate should be pressed firmly against its locating frame, and the shutter timer switch thrown. Procedure (6) should be repeated until the 70 mm movie is reduced.

(7) Removal of the 35 mm film.

Since the capacity of the developing reels is 31.7 feet, no more than thirty one feet of exposed film should be allowed to accumulate in the Eymo. Often the camera will have to be unloaded before thirty one feet have been taken, as the film should not be removed in the middle of a reduction run.

After removing the film from the Eymo, it should be sealed

in a 35 mm film can. The can should be marked with the date of reduction, the date and type of the original film and the type of reduction procedure performed. The remaining footage in the camera and the date of removal should be recorded in the data book.

Although the operations described above appear rather involved, and although initial attempts to operate the cancellation machine will be rather time consuming for the new operator, with some practice a two hundred frame doppler movie can be made in about one hour. Two hundred frame long wing movies can be made in about ten minutes.

E. MAINTENANCE

Other than replacing the rubber band on the control lever occasionally, the cancellation machine should beed no general maintenance. All the bearings are either oil-less bronze or teflon and the bulbs in the light box have a 5000 hour lifetime.

The epoxy bosses on the aperture plate and the center pressure plate have not worn appreciably in two years of service, but in time they will have to be recast. Also there exists the possibility that a film may be used that has a development shrink that is sufficiently large that the epoxy bosses are no longer spaced correctly for the film. The film shrinking effects are less likely to be serious if Mylar base films are used instead of acetate. However, even with Mylar base films the epoxy bosses must be cast from a piece of developed film. If the bosses are cast from undeveloped film, the developed films will not fit the bosses properly.

Figure A9 Cancellation Machine and Accessory Equipment

The apparatus is shown ready to be loaded with film.

(a) Eymo camera
(b) Release Knob of Camera Mount
(c) Camera Mount
(d) Take-up Assembly
(e) Supply Assembly
(f) Electric Timer
(g) Spring Winder for Eymo
(h) Variac
(i) Shutter Release Switch
(j) Camera Support Arm
(k) Screw Terminals.

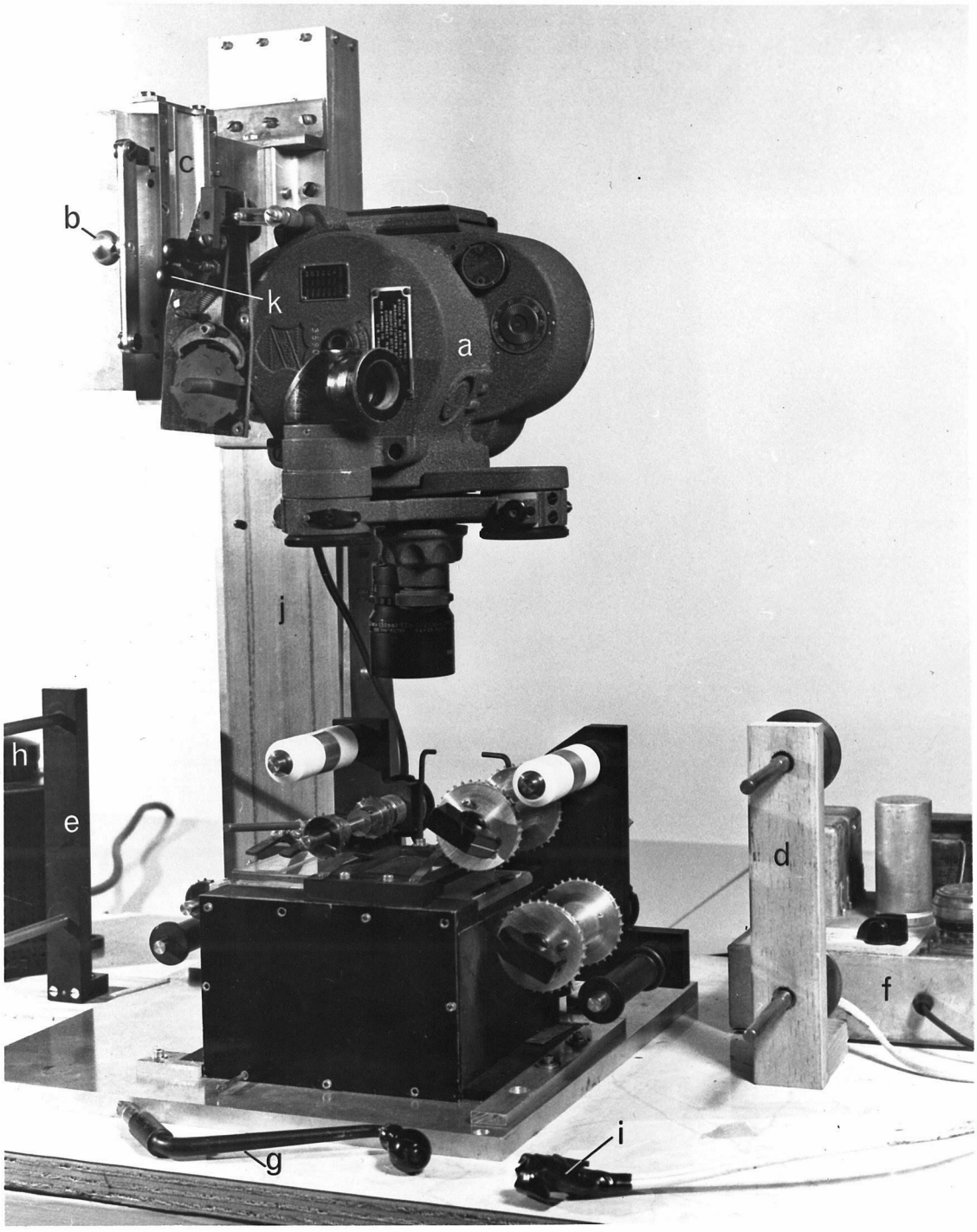

Figure A9

Figure A10 Light Box of Cancellation Machine

The light box is shown with lower film installed.

(a) Upper Guide Roller
(b) Upper Main Sprocket
(c) Upper Rear Sprocket
(d) Upper Guide Roller
(e) Lower Guide Roller
(f) Lower Main Sprocket
(g) Lower Rear Sprocket
(h) Lower Guide Roller
(i) Center Pressure Plate
(j,k,l) Center Pressure Plate Springs
(m) Adjusting Screw Center Pressure Plate Location Frame
(n) Rear Pressure Plate
(o) Rear Pressure Plate Pressure Control Arm
(p) Clamp
(q) Locating Frame
(r) Lower Attachment Point for Pressure Control Arm Rubber Band.

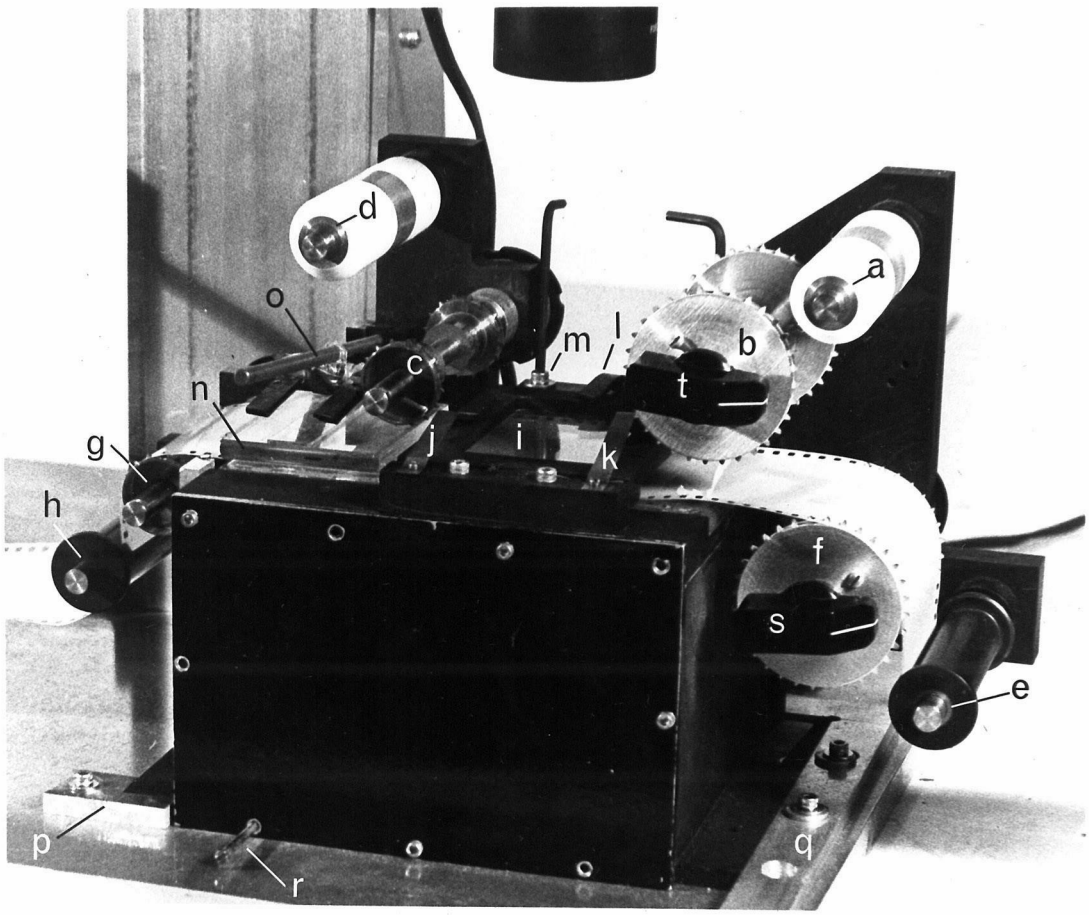

Figure A 10

Figure A11 Cancellation Machine in Focusing Position

Note that the lens turret has been rotated 120^{o} from its normal position, and that the cancellation box is slid forward.

Figure A12 Light Box of Cancellation Machine

The light box is shown with both upper and lower films loaded.

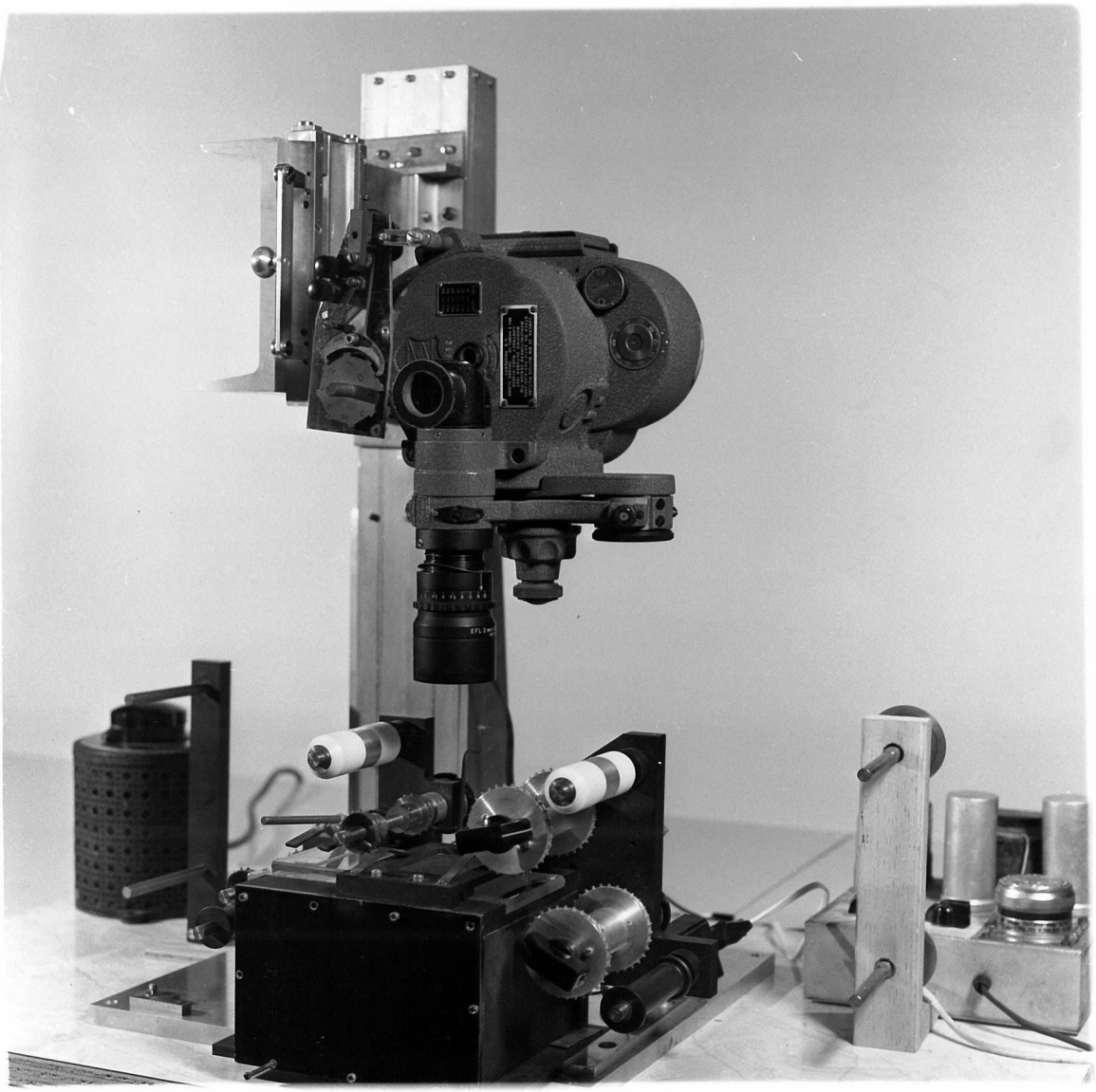

Figure A11

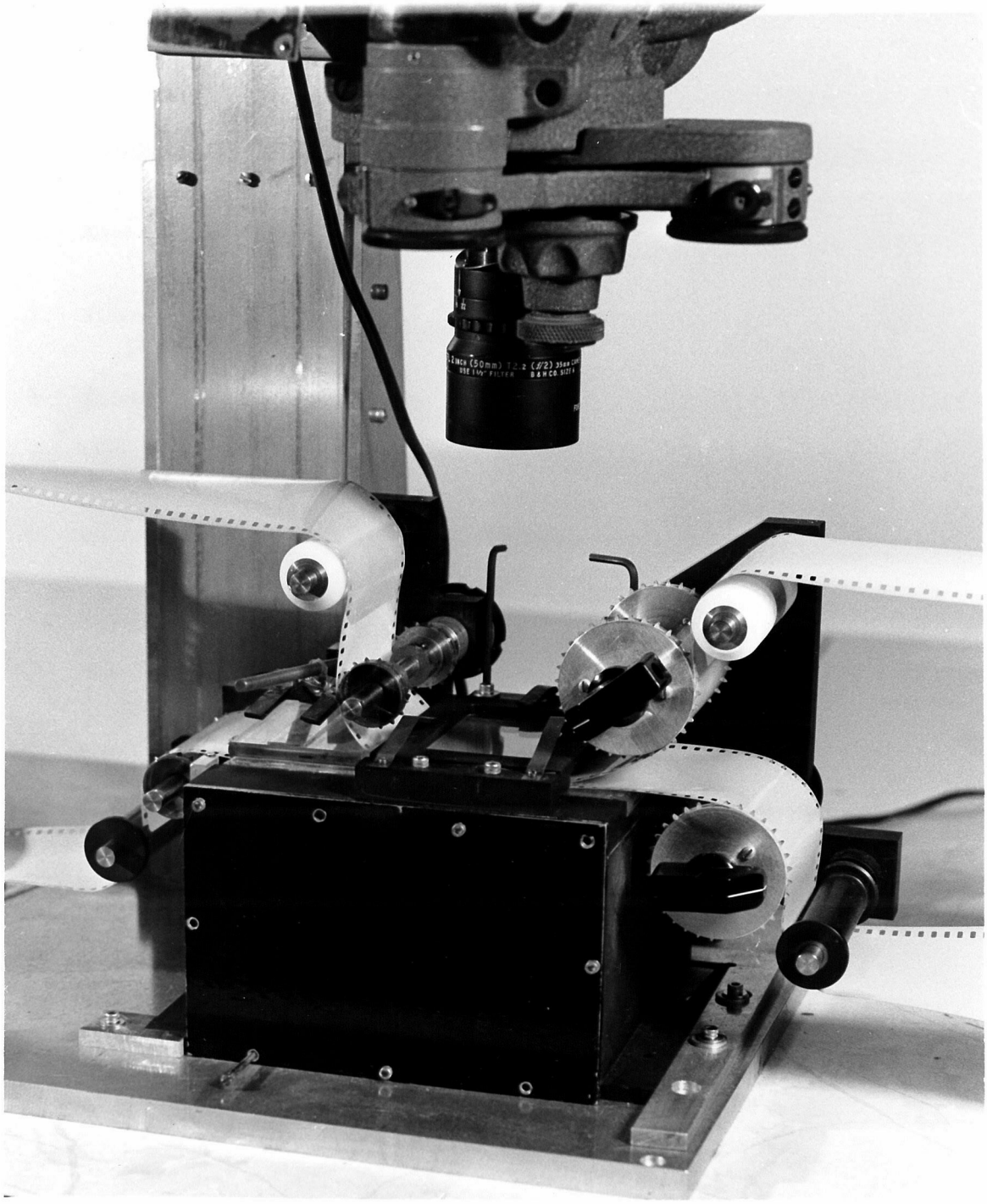

Figure A12

REFERENCES

1. Leighton, R.B., Ap. J., 130, 336-380 (1959).

2. Leighton, R.B., Nuovo Cimento (Supp.) 22, 321-325 (1961).

3. Leighton, R.B., Noyes, R.W., and Simon, G.W., Ap. J., 135, 474-499 (1962).

4. Noyes, R.W., Ph.D. Thesis, California Institute of Technology, (1963).

5. Simon, G.W., Ph.D. Thesis, California Institute of Technology, (1964).

6. Simon, G.W., and Leighton, R.B., Ap. J., 140, 1120-1147 (1964).

7. Sheely Jr., N.R., Ph.D. Thesis, California Institute of Technology (1965).

8. Beckers, J.M., Ph.D. Thesis, University of Utrecht (Netherlands), (1964).

9. Cragg, T., Howard, R., and Zirin, H., Ap. J., 138, 658 (1963).

10. Bhavilai, R., Monthly notices of the Royal Astronomical Society, 130, 411-422 (1965).

11. Howard, R., and Harvey, J.W., Ap.J., 139, 1328-1335 (1964).

12. Blackman, R.B., and Tukey, J.W., The Measurement of Power Spectra, 14-37, (New York, Dover Publications, 1959).

13. White, D.R., Ph.D. Thesis, University of Colorado (1962).

14. Beckers, J.M., Private Communication, December 1965.

15. Zirin, H., Private Communication, May 1965.